Received: 2 October 2017
IOTC-2017-WPTT19-31

Updated CPUE standardizations for bigeye and yellowfin tuna caught by Taiwanese longline fishery in the Indian Ocean using generalized linear model

Yu-Min Yeh[1], Simon Hoyle[2] and Shu-Ting Chang[3]

[1]Department of Tourism Management and Master Program of Leisure Environment Management, Nanhua University, 55, Sec. 1, Nanhu Rd. Chung Keng Li, Dalin, Chiayi 62248, Taiwan

[2]IOTC consultant, New Zealand. Email: simon.hoyle@gmail.com.

[3]Overseas Fisheries Development Council il of the Republic of China, 3F, No, 14, Wenzhou St., Da'an Dist., Taipei 106, Taiwan (R.O.C.)

Abstract

Updated Taiwanese longline fishery data to 1979-2016 were used in this analysis. We used cluster analysis to classify longline sets into groups based on the species composition of the catch, to understand whether cluster analysis could identify distinct fishing strategies. Bigeye and yellowfin tuna CPUE were then standardized. All analyses were based on the approaches used by the collaborative workshop of longline data and CPUE standardization for bigeye and yellowfin tuna held in June 2017 in Taipei and in July 2017 in Busan.

Introduction

The Working Party on Tropical Tunas (WPTT) and the Scientific Committee of the Indian Ocean Tuna Commission (IOTC) have noted that the CPUE trends from longline fisheries for bigeye tuna in the Indian Ocean differ considerably between Taiwan and Japan (Anonymous 2013a). Much effort has been devoted to dealing with this issue from various point of views, considering data quality, data management systems, analytical methods, etc. (Anonymous, 1998; OFDC, 2013; Hoyle S., 2014; Okamoto H., 2014; Yeh, 2014). In June and July of 2017, several collaborative studies were conducted between national scientists with expertise in Japanese, Taiwanese, Korean fleets, Seychelles longline fleets, an IOTC scientist, and an independent scientist, Dr. Simon Hoyle. The workshops addressed Terms of Reference covering several important and longstanding issues related to the bigeye and yellowfin tuna CPUE indices in the Indian Ocean. Data from the Seychelles longline fleet were considered at this meeting for the first time, as a valuable source of independent information.

In this analysis, a framework analysis suggested by the collaborative study was conducted using updated Taiwanese operational data.

Materials and methods

In this analysis, operational catch and effort data with 1 degree by 1 degree resolution from the logbooks of Taiwanese longline fishery from 1979-2016 were used, as provided by Overseas Fisheries Development Council (OFDC). From 2013, the Taiwanese Fisheries Agency has supported the Taiwanese pelagic longline fishery industry in submitting logbook data via an E-logbook system. In 2015 the E-logbook coverage rate reached over 80%, and attained 100% in 2016. Therefore, the 2015 and 2016 data were compiled from E-logbooks.

Data preparation and cleaning were performed by adopting the suggestions made by the collaborative work (IOTC, 2015). Each set was allocated to a bigeye region and a yellowfin region (Figure 1). Basically, the region definitions conformed to the 2016 joint work (Hoyle et al, 2016). Except for the conventional region 1 of the region structure used to estimate bigeye CPUE indices, the region was divided into region 1N and region 1S along latitude 0° conforming to the 2015 bigeye assessment model.

Cluster analysis

We adopted the hierarchical clustering method Ward hclust (IOTC, 2015) to identify effort associated with different fishing strategies. The cluster analysis was performed separately for regions for both bigeye and yellowfin. Analyses used species composition to group the data. The data were transformed by centering and scaling, so as to reduce the dominance of species with higher average catches. For this analysis, we aggregated the data by vessel-month to reduce the variability, and therefore reduce misallocation of sets. The assumption is that we believe individual vessels tend to follow a consistent fishing strategy in a month period. More detailed information can be referred to the collaborative work report (IOTC, 2016).

CPUE standardization

CPUE standardization methods adopted the suggestions made from the collaborative work (IOTC, 2016) for Taiwanese fleet to include year-quarter, vessel id, and five by five° latitude and longitude grids as main effects. Cluster is also included as a main effect in the model. Analyses were conducted separately for each region, and for bigeye and yellowfin. CPUE Indices were estimated using two approaches, delta lognormal and lognormal + constant, but the primary approach was the delta lognormal. More detailed information can be obtained from the collaborative work report (IOTC, 2017).

The effects of covariates were examined using the package influ (Bentley *et al.* 2011) to show the influence of each covariate. For the final analyses, data were prepared by selecting operational data by region, for vessels that had fished for 8 quarters in that region. Data in GLM were 'area-weighted', with the weights of the sets adjusted so that the total weight per year-quarter in each 5 degree square would sum to 1. For both species for the GLMs, model fits were examined by plotting the residual densities and using Q-Q plots.

The operational data were standardized using generalized linear models in R. All analyses were performed using R source code freely shared by Simon Hoyle in the collaborative work.

Results and Discussions

The recent status of Taiwanese tuna longline fisheries

Data coverage was 80% in 2015 and 100% in 2016 for this analysis. Figure 2 and Figure 3 showed the Taiwanese tuna longline catch composition, effort, nominal bigeye CPUE, and nominal yellowfin CPUE by 5 degree square in the recently two years. Overall speaking, the performance of Taiwanese tuna longline fisheries in 2015 and 2016 was very similar and showed no significant change than previous years. However, compare to 2015, there were relatively lower yellowfin nominal CPUE in some 5x5 grid and total catch of target species had a higher value over the area of Mozambique Channel in 2016.

Cluster analysis

The aims of the cluster analysis were to identify whether cluster analysis could identify distinct fishing strategies in each region; secondly to use the cluster analysis to identify these fishing strategies in the data for each region, and so to better understand the fishing practices.

In BET region 1N, 1S and 2, we identified 5 clusters as the number with the most support (Figure 4), However, using cluster analysis to identify bigeye and yellowfin targeting is challenging, since targeting is probably less an either/or strategy than a mixture of variables that shift the species composition one way or the other (Table 1).

In BET region 3, we identified 4 clusters as the number with the most support (Figure 5), we found that species composition averaging 80% ‘other’ in one cluster, suggesting that oilfish targeting can represent the majority of the catch, 84% albacore in another cluster, a mix of bigeye, yellowfin, albacore and swordfish in a third cluster, and a mix of albacore, bigeye, shark and southern Bluefin tuna in a fourth cluster were identified at the trip level by hcltrip (Table 1).

In BET region 4, we identified 4 clusters as the number with the most support (Figure 5), we found that species composition averaging 81.6% albacore in one cluster, a mix of 51% albacore and 30% ‘other’ in another cluster, a mix of bigeye, yellowfin, albacore and swordfish in a third cluster, and a mix of 49% albacore, 30% southern Bluefin tuna and 11% bigeye in a fourth cluster, were identified at the trip level by hcltrip (Table 1).

For BET regions, for each cluster in every region, the corresponding fishing strategies were revealed by the various distribution of fishing year, month, number of hooks between floats, location, number of hooks associated with sets in each cluster (Figure 6 ~15).

In YFT region 2, we identified 5 clusters as the number with the most support (Figure 16). Also, except one cluster with 63% albacore, using cluster analysis to identify bigeye and yellowfin targeting is challenging, since targeting is probably less an either/or strategy than a mixture of variables that shift the species composition one way or the other (Table 2).

In YFT region 3, we identified 4 clusters as the number with the most support (Figure 16). We found that species composition averaged 91% ‘other’ in one cluster, suggesting that oilfish targeting can represent the majority of the catch; 76% albacore in another cluster; a mix of bigeye, yellowfin, albacore and swordfish in a third cluster; and a mix of albacore, bigeye, yellowfin in a fourth cluster were identified at the trip level by hcltrip (Table 2).

In YFT region 4, we identified 5 clusters as the number with the most support (Figure 17), we found that species composition averaging 89% albacore in one cluster, 70% albacore in another cluster, a mix of 41% albacore and 44% ‘other’ in third cluster, a mix of bigeye, yellowfin, albacore and swordfish in a fourth cluster, and a mix of 43% albacore, 31% southern Bluefin tuna and 11% bigeye in a fifth cluster, were identified at the trip level by hcltrip (Table 2).

In YFT region 5, we identified 4 clusters as the number with the most support (Figure 17). we found that species composition averaging 68% albacore and 15% bigeye in one cluster, 68% bigeye and 17% yellowfin in another cluster, 42% bigeye and 29% yellowfin in a third cluster, and 56% bigeye and 21% ‘other’ in a fourth cluster were identified at the trip level by hcltrip (Table 2).

For YFT regions, for each cluster in every region, the corresponding fishing strategies were revealed by the various distribution of fishing year, month, number of hooks between floats, location, number of hooks associated with sets in each cluster (Figure 18 ~25).

CPUE indices

Vessel effects for the Taiwanese fleets operating in region 1S and region 4 of BET region (Figure 27 and Figure 30) showed increasing catchability of bigeye tuna, while for other regions, there was little apparent change in catchability through time (Figure 26, 28, 29) Vessel effects for the Taiwanese fleets operating in region 4 of YFT region (Figure 33) showed increasing catchability of yellowfin tuna, while for other regions, there was little apparent change in catchability through time (Figure 31, 32, 34).

For covariate effects, we present an example result for bigeye in region 1N. The coefficients for each vessel (bottom right, Figure 26) show much variation and there are changes in the distribution of records among vessels, resulting in variable changes in annual influence (right panel). The high influence in 1979 arises because there was a greater than usual proportion of effort from vessels with higher coefficients. The spatial distributions of fishing sets (latlong effect) were fairly stable through time with some exceptions. The high influence in around 2012 arises because there was a greater than usual proportion of effort occurred in the Somalia area with the highest coefficients. The coefficients for each cluster (bottom left, Figure 26) show there was one cluster (TW2) with much higher catchability than the other three clusters. There were changes in the distribution of records among clusters, resulting in variable changes in annual influence.

We excluded low-target clusters from the dataset and included the cluster effect in the model.

For bigeye tuna the tropical indices in regions 1N and 1S (blue line, the top two plots in Figure 35) show no strong trend through time. There was a spike in 2012 followed by a moderate decline in the latest 5 years. In the western tropical area (region 2) and temperate area there was also no strong trend through time with relatively lower signal in the last two years. For yellowfin tuna, indices in the western tropical region 2 CPUE (Figure 36) increased from 1979 to 1987 and then declined until 1989, fluctuated during 1990-2006 then declined to 2010, and then increased to a spike in 2012. After that time it remained close to the lowest level observed. The eastern tropical region 5 from 1989 declined steadily to 2006, and declined more dramatically to 2016. It was also close to the lowest level in the time series by 2016.

Yellowfin in western temperate region 3 CPUE declined steadily to 2011, and then remained but with significant variability (Figure 36). Increased showed a followed a similar pattern to the western tropical indices, with a decline until the mid-1970s followed by an increase until the late 1980s, and subsequently a slow decline with significant variability (Figure 36). In eastern temperate region 4 from 1995 CPUE showed a decline pattern with significant variability and reached their lowest observed levels by 2016.

The comparison of the bigeye and yellowfin CPUE indices estimated in this analysis and estimated in the 2015 analysis for regions were shown in Figure 35 and 36. There were three main differences in the process of CPUE standardization between these analyses. First, the data sets of 2002-2004 were excluded in the 2016 analysis regarding the misreporting issue versus those three years data sets were remained in this analysis. Second, all clusters were retained in the 2016 analysis whereas low-target clusters were omitted in this analysis. Third is lognormal constant generalized linear models were adopted in the 2016 analysis versus the delta lognormal models used in this analysis. For both species for the delta lognormal models, model fits were presented by using Q-Q plots (Figure 37 and Figure 38) and plotting the residual densities plots (Figure 39 - 47).

References

Anonymous (1998). Critical review of the data collection and processing system of Chinese Taipei, and revision of statistics for its LL fleet (Taipei, July 1997). SCRS/97/017, ICCAT: 141-204.

Bentley, N., T. H. Kendrick, P. J. Starr and P. A. Breen (2011). "Influence plots and metrics: tools for better understanding fisheries catch-per-unit-effort standardizations." ICES Journal of Marine Science 69(1): 84-88.

Hoyle S. (2014). Spatial considerations in bigeye and yellowfin CPUE from Japanese and Taiwan,China longline fisheries in the Indian Ocean (Hoyle S). Working Party on Tropical Tuna, Indian Ocean Tuna Commission. IOTC–2014–WPTT16–25.

Hoyle, S. D., and H. Okamoto. 2015. Descriptive analyses of the Japanese Indian Ocean longline fishery, focusing on tropical areas. Indian Ocean Tuna Commission Working Party on Tropical Tunas.

Hoyle, S. D., H. Okamoto, Y.-m. Yeh, Z. G. Kim, S. I. Lee, and R. Sharma. 2015b. IOTC–CPUEWS02 2015: Report of the 2nd CPUE Workshop on Longline Fisheries, 30 April – 2 May 2015. Indian Ocean Tuna Commission.

Hoyle, S. D., Y.-M. Yeh, S.-T. Chang, and R.-F. Wu. 2015c. Descriptive analyses of the Taiwanese Indian Ocean longline fishery, focusing on tropical areas. Indian Ocean Tuna Commission Working Party on Tropical Tunas.

Hoyle, S, D., C. Assan, , S.-T. Chang, F. Dan, R. Govinden, D.M. Kim, T. Kitakado, S. I. Lee, J. Lucas, T. Matsumoto, and Y.-M Yeh[1]. Collaborative study of tropical tuna CPUE from multiple Indian Ocean longline fleets in 2017.

IOTC (2015). Report of the 2nd CPUE Workshop on Longline Fisheries. IOTC–2015–CPUEWS02–R[E]

Indian Ocean. Working Party on Tropical Tuna, Indian Ocean Tuna Commission. IOTC–2014–WPTT16–28.

Langley, A., M. Herrera and J. Million (2012). Stock assessment of yellowfin tuna in the Indian Ocean using MULTIFAN-CL. Working Party on Tropical Tuna, Indian Ocean Tuna Commission. IOTC–2012–WPTT14–38 Rev_1.

Langley, A. 2016. Stock assessment of bigeye tuna in the Indian Ocean for 2016-model development and evaluation. IOTC Proceedings, volume IOTC-2016-WPTT18-20, page 98p, Victoria, Seychelles:11-13.

Lee, Y.-C. and H.-C. Liu (1996). The tuna statistics procedures of Taiwan longline and gillnet Fisheries in the Indian Ocean." IPTP Collective Volumes(9): 368-369.

Okamoto H (2014). Provisional analysis on comparison of CPUE trend of bigeye and yellowfin tuna between Japanese and Taiwan-China longline fisheries based on whole and shared strata in the Overseas Fisheries Development Council (2013). Data Collection and Processing System of Statistics for the Taiwanese Deep-Sea Longline Fishery. IOTC Working Party on Tropical Tunas (WPTT) 15. San Sebastian, Spain. IOTC–2013–WPTT15–40 Rev_1.

Simon D. Hoyle, Doo Nam Kim, Sung Il Lee, Takayuki Matsumoto, Kaisuke Satoh, and Yu-Min Yeh. (2016). Collaborative study of tropical tuna CPUE from multiple Indian Ocean longline fleets in 2016. IOTC-2016-WPTT18-XX.

Yeh, Y.-M. (2014). Preliminary analysis of Taiwanese longline fisheries based on operational catch and effort data for bigeye and yellowfin tuna in the Indian Ocean. Working Party on Tropical Tuna, Indian Ocean Tuna Commission. IOTC–2014–WPTT16–42.

[1] Nanhua University, invited Taiwanese expert.

R Core Team. 2016. R: A Language and Environment for Statistical Computing. R Foundation for Statistical Computing, Vienna, Austria.

Table 1. For Taiwanese effort in the BET region 1N, 1S, 2, 3, and 4, average percentage of each species per set, by cluster, as estimated by cluster analysis.

Region	Cluster	Albacore	Bigeye tuna	Yellowfin tuna	Other tuna	Swordfish	Strip marlin	Blue marlin	Black marline	Other billfish	Skipjack	Shark	Other fishes	Southern Bluefin tuna
1N	1	1.6%	43.5%	19.9%	0.1%	11.1%	4.1%	6.3%	0.4%	2.5%	0.3%	4.6%	4.6%	0.8%
	2	0.2%	61.3%	20.5%	0.0%	8.4%	1.6%	2.6%	0.2%	0.4%	0.1%	1.3%	3.3%	0.0%
	3	0.3%	39.8%	13.3%	0.0%	37.7%	1.6%	2.5%	0.2%	0.3%	0.0%	1.1%	3.4%	0.0%
	4	0.1%	28.1%	51.2%	0.0%	7.4%	1.4%	2.8%	0.1%	0.6%	0.0%	2.9%	5.4%	0.0%
	5	0.3%	39.2%	14.7%	0.0%	12.5%	1.4%	3.9%	0.1%	0.2%	0.0%	3.0%	24.8%	0.0%
1S	1	75.2%	6.3%	13.9%	0.0%	1.3%	0.4%	0.6%	0.1%	0.1%	0.1%	0.9%	1.0%	0.1%
	2	5.9%	37.0%	19.2%	0.0%	6.5%	1.0%	3.3%	0.2%	0.5%	0.0%	10.5%	15.8%	0.0%
	3	1.6%	42.5%	23.8%	0.2%	12.9%	2.9%	4.2%	0.6%	1.4%	0.5%	2.9%	5.4%	1.1%
	4	1.3%	61.8%	20.0%	0.0%	5.5%	0.9%	1.8%	0.1%	0.5%	0.0%	2.1%	5.9%	0.0%
	5	1.2%	29.3%	54.6%	0.0%	5.8%	0.8%	1.9%	0.1%	0.5%	0.0%	1.6%	4.0%	0.0%
2	1	2.0%	72.1%	13.8%	0.0%	4.2%	2.0%	2.0%	0.4%	0.3%	0.0%	1.3%	1.9%	0.0%
	2	0.5%	44.9%	33.4%	0.0%	3.7%	8.4%	3.8%	1.2%	0.4%	0.1%	2.4%	1.1%	0.0%
	3	66.5%	15.2%	11.9%	0.0%	2.0%	1.0%	0.9%	0.2%	0.1%	0.2%	0.7%	1.4%	0.0%
	4	1.8%	50.5%	16.1%	0.2%	11.9%	2.3%	4.4%	1.0%	1.6%	0.4%	5.0%	4.1%	0.7%
	5	2.3%	54.4%	8.0%	0.0%	4.8%	0.6%	2.0%	0.2%	0.4%	0.0%	6.1%	21.2%	0.0%
3	1	83.5%	5.2%	4.5%	0.0%	1.4%	0.2%	0.3%	0.0%	0.1%	0.1%	0.7%	3.0%	0.8%
	2	19.2%	31.5%	16.6%	0.2%	20.5%	1.3%	0.8%	0.2%	0.4%	0.1%	3.2%	5.5%	0.5%
	3	30.0%	18.3%	6.1%	1.1%	4.9%	0.9%	0.7%	0.5%	3.6%	3.0%	10.4%	9.3%	11.2%
	4	8.6%	3.9%	1.8%	0.0%	3.3%	0.0%	0.1%	0.0%	0.0%	0.0%	2.1%	79.9%	0.2%
4	1	81.6%	8.1%	2.7%	0.1%	1.3%	0.5%	0.2%	0.1%	0.1%	0.1%	0.6%	2.7%	1.8%
	2	29.1%	29.7%	14.7%	1.5%	9.7%	1.3%	0.8%	0.2%	0.7%	1.0%	2.3%	6.2%	2.8%
	3	49.1%	11.2%	2.3%	0.0%	2.0%	0.2%	0.3%	0.0%	0.0%	0.1%	0.6%	4.5%	29.7%

	4	51.1%	5.0%	0.9%	0.0%	1.3%	0.0%	0.0%	0.0%	0.1%	0.0%	2.0%	30.4%	9.1%

Table 2. For Taiwanese effort in the YFT region 2, 3, 4, and 5, average percentage of each species per set, by cluster, as estimated by cluster analysis.

Region	Cluster	Albacore	Bigeye tuna	Yellowfin tuna	Other tuna	Swordfish	Strip marlin	Blue marlin	Black marline	Other billfish	Skipjack	Shark	Other fishes	Southern Bluefin tuna
2	1	63.1%	13.9%	13.4%	0.0%	2.5%	0.8%	1.4%	0.3%	0.2%	0.1%	1.7%	2.6%	0.1%
	2	0.6%	40.9%	22.1%	0.2%	14.6%	4.3%	5.7%	0.5%	1.6%	0.5%	3.2%	4.9%	1.0%
	3	0.5%	39.4%	43.2%	0.0%	6.7%	1.0%	2.3%	0.1%	0.5%	0.0%	1.9%	4.4%	0.0%
	4	1.2%	62.6%	16.9%	0.0%	8.4%	1.2%	2.3%	0.1%	0.6%	0.0%	1.7%	4.9%	0.0%
	5	1.0%	36.8%	16.0%	0.0%	8.4%	1.1%	4.0%	0.2%	0.5%	0.0%	11.2%	20.8%	0.0%
3	1	75.9%	7.7%	8.1%	0.0%	2.3%	0.3%	0.4%	0.1%	0.2%	0.0%	1.1%	3.8%	0.2%
	2	10.2%	44.2%	18.9%	0.1%	4.6%	1.2%	1.5%	0.2%	1.1%	0.4%	6.9%	9.5%	1.2%
	3	16.5%	24.7%	12.4%	0.0%	38.9%	0.8%	0.6%	0.1%	0.0%	0.1%	2.1%	3.6%	0.2%
	4	4.3%	1.4%	0.8%	0.0%	1.0%	0.0%	0.0%	0.0%	0.0%	0.0%	1.4%	90.8%	0.2%
4	1	89.0%	6.0%	2.2%	0.1%	0.9%	0.2%	0.1%	0.0%	0.1%	0.0%	0.4%	0.9%	0.3%
	2	69.9%	8.1%	4.1%	0.0%	1.8%	0.6%	0.2%	0.1%	0.2%	0.2%	1.3%	8.5%	5.0%
	3	24.4%	33.6%	16.2%	1.3%	11.0%	1.3%	1.2%	0.3%	0.8%	1.0%	2.3%	4.0%	2.6%
	4	42.7%	10.5%	2.1%	0.0%	2.0%	0.2%	0.3%	0.0%	0.1%	0.1%	1.4%	10.0%	30.7%
	5	40.5%	5.0%	2.0%	0.0%	1.6%	0.1%	0.1%	0.0%	0.1%	0.0%	2.4%	44.2%	4.0%
5	1	1.7%	67.8%	16.8%	0.0%	4.5%	2.6%	2.4%	0.5%	0.3%	0.1%	1.5%	1.8%	0.0%
	2	1.1%	42.4%	28.6%	0.1%	7.1%	5.7%	3.5%	1.0%	1.2%	0.3%	4.7%	3.9%	0.4%
	3	67.8%	15.1%	9.8%	0.0%	2.2%	1.1%	1.0%	0.2%	0.1%	0.1%	0.9%	1.6%	0.0%
	4	1.8%	56.2%	7.5%	0.0%	4.9%	0.7%	2.3%	0.2%	0.3%	0.0%	5.3%	20.7%	0.0%

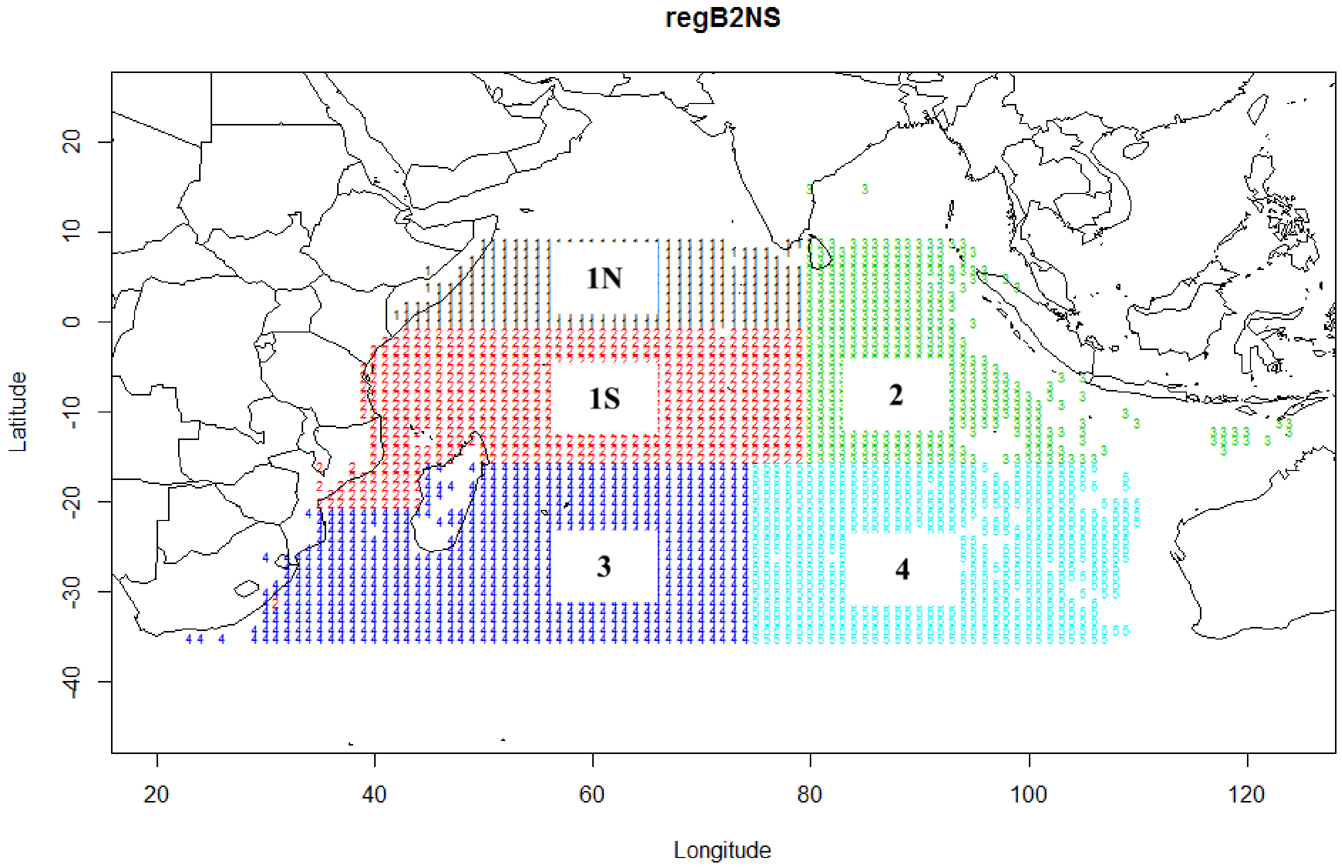

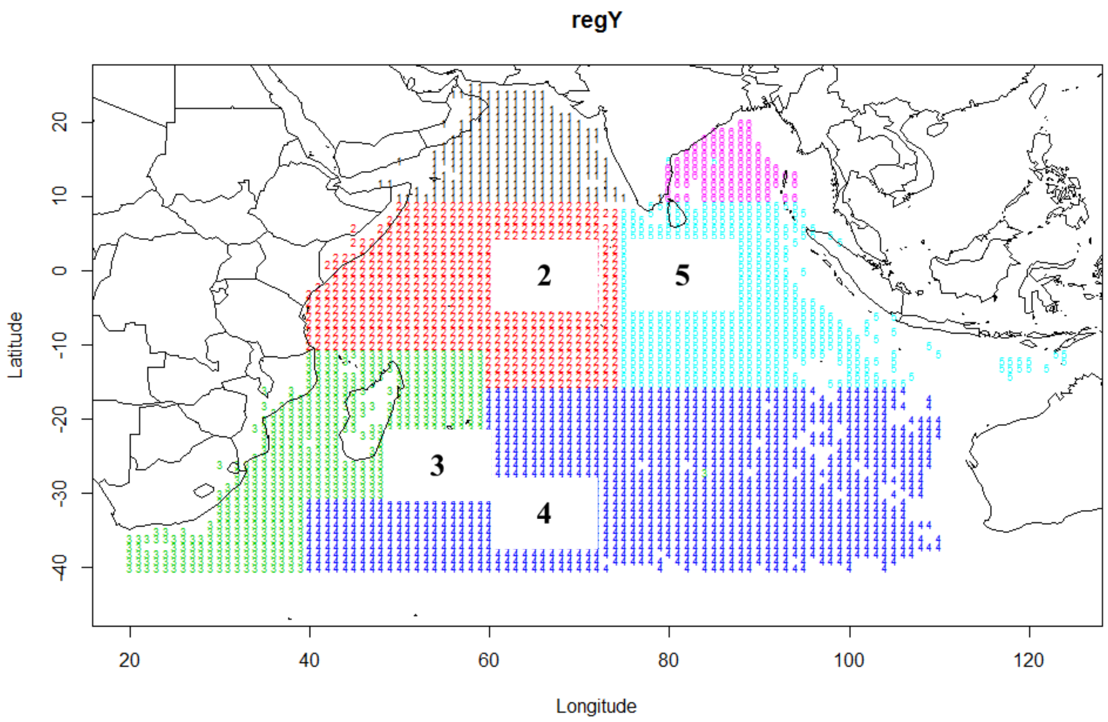

Figure 1. Spatial stratification of the Indian Ocean for this analysis.

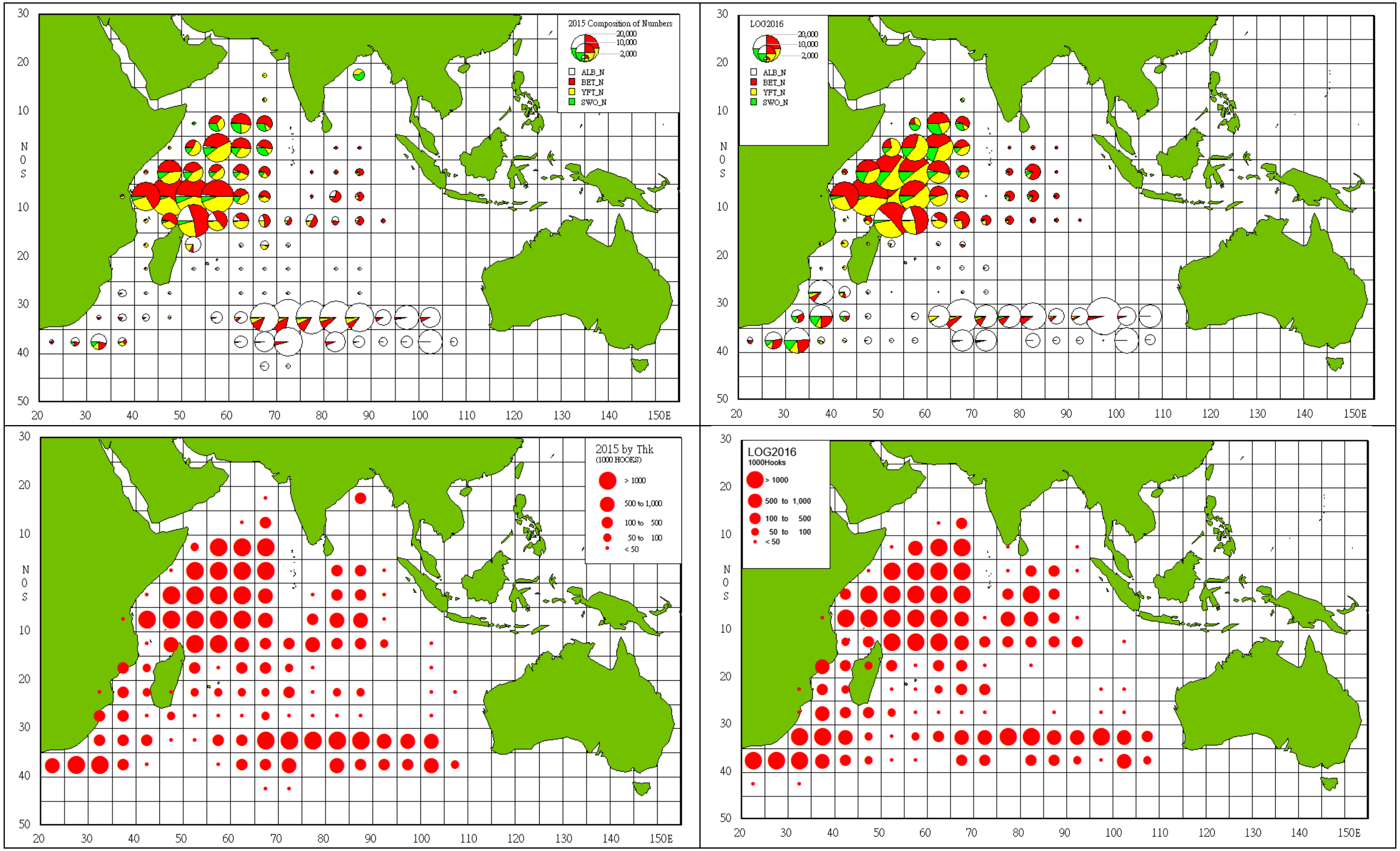
2015 Composition of Numbers
20,000
10,000
2,000
ALB_N
BET_N
YFT_N
SWO_N
LOG2016
20,000
10,000
2,000
ALB_N
BET_N
YFT_N
SWO_N
2015 by Thk
(1000 HOOKS)
> 1000
500 to 1,000
100 to 500
50 to 100
< 50
LOG2016
1000Hooks
> 1000
500 to 1,000
100 to 500
50 to 100
< 50
30
20
10
N
0
S
10
20
30
40
50
20
30
40
50
60
70
80
90
100
110
120
130
140
150E

Figure 2. Comparison of 2015 and 2016 data used in this analysis. Map of catch composition for 2015 (top_left), for 2016 (top_right), fishing effort by for 2015 (bottom_left), and for 2016 (bottom_right), by 5 degree square.

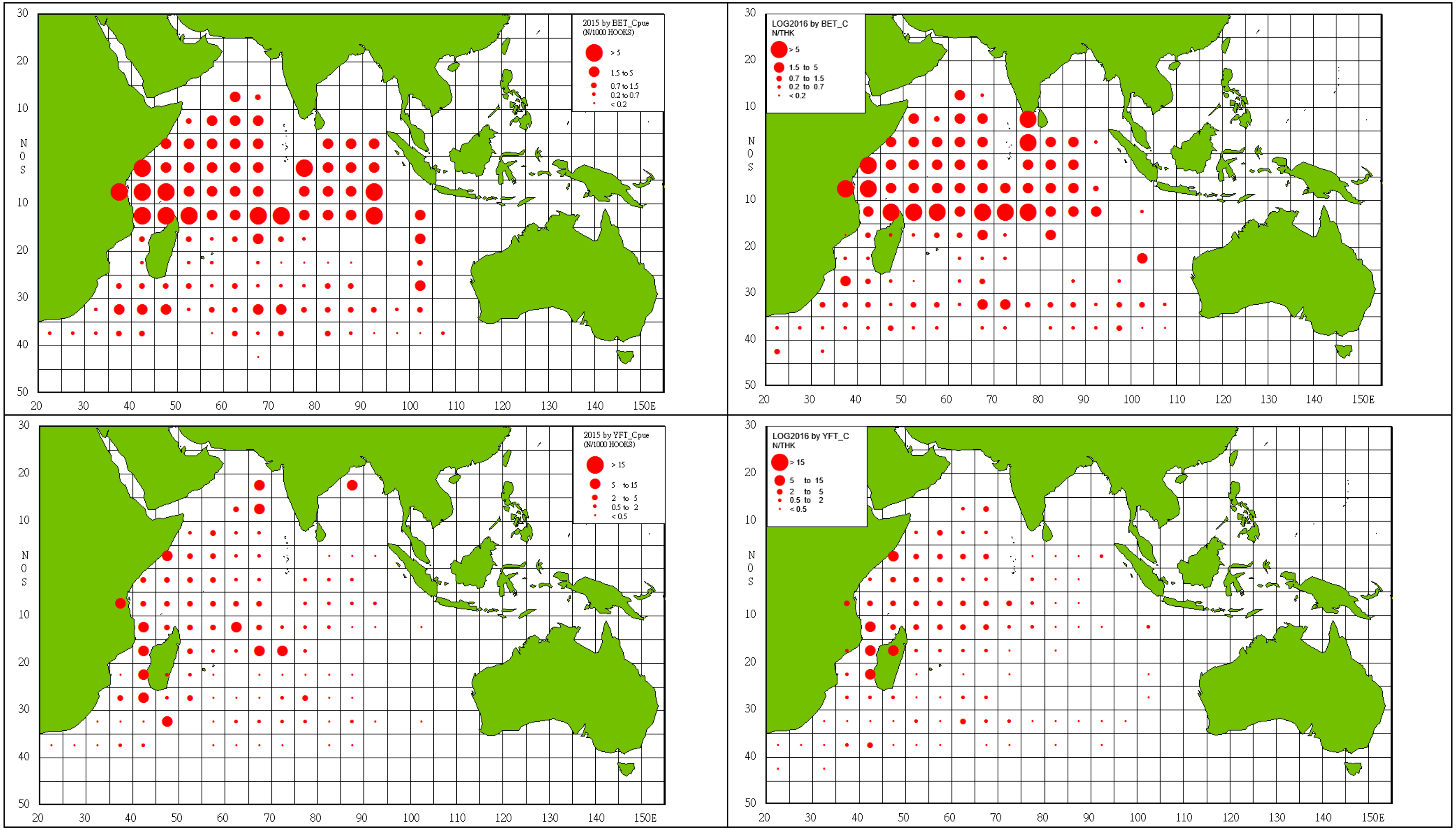

Figure 3. Comparison of 2015 and 2016 data used in this analysis. Map of nominal bigeye CPUE for 2015 (top_left), for 2016(top_right), nominal yellowfin CPUE for

2015 (bottom_left), for 2016(bottom_right), by 5 degree square.

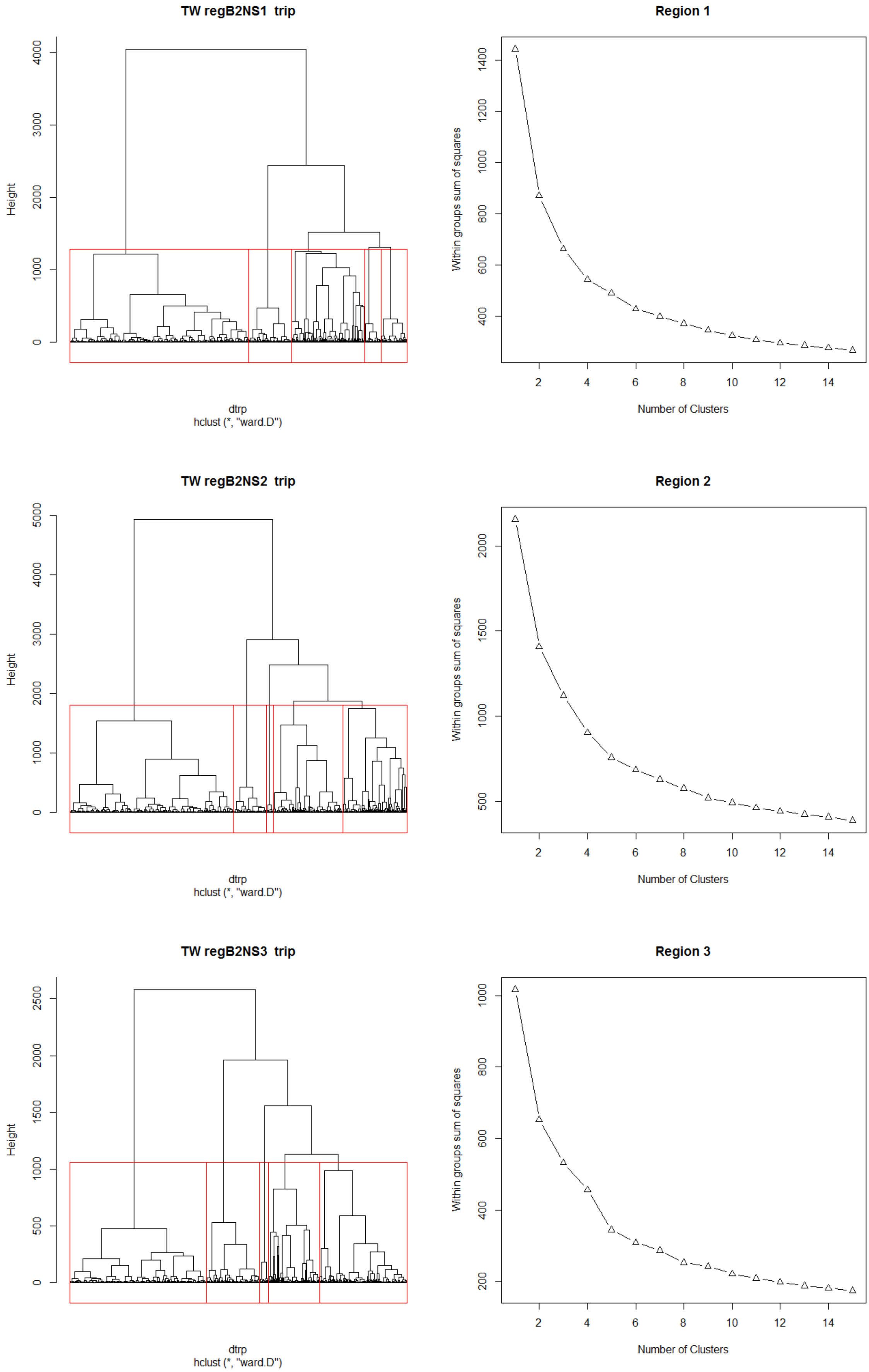

Figure 4. Plots showing analyses to estimate the number of distinct classes of species composition in Taiwanese region 1N, 1S, 2 of B2NS. These are based on a hierarchical Ward clustering analysis of trip-level data (top left);

within-group sums of squares from kmeans analyses with a range of numbers of clusters (top right); and analyses of the numbers of components to retain from a principal component analysis of trip-level (bottom left) data.

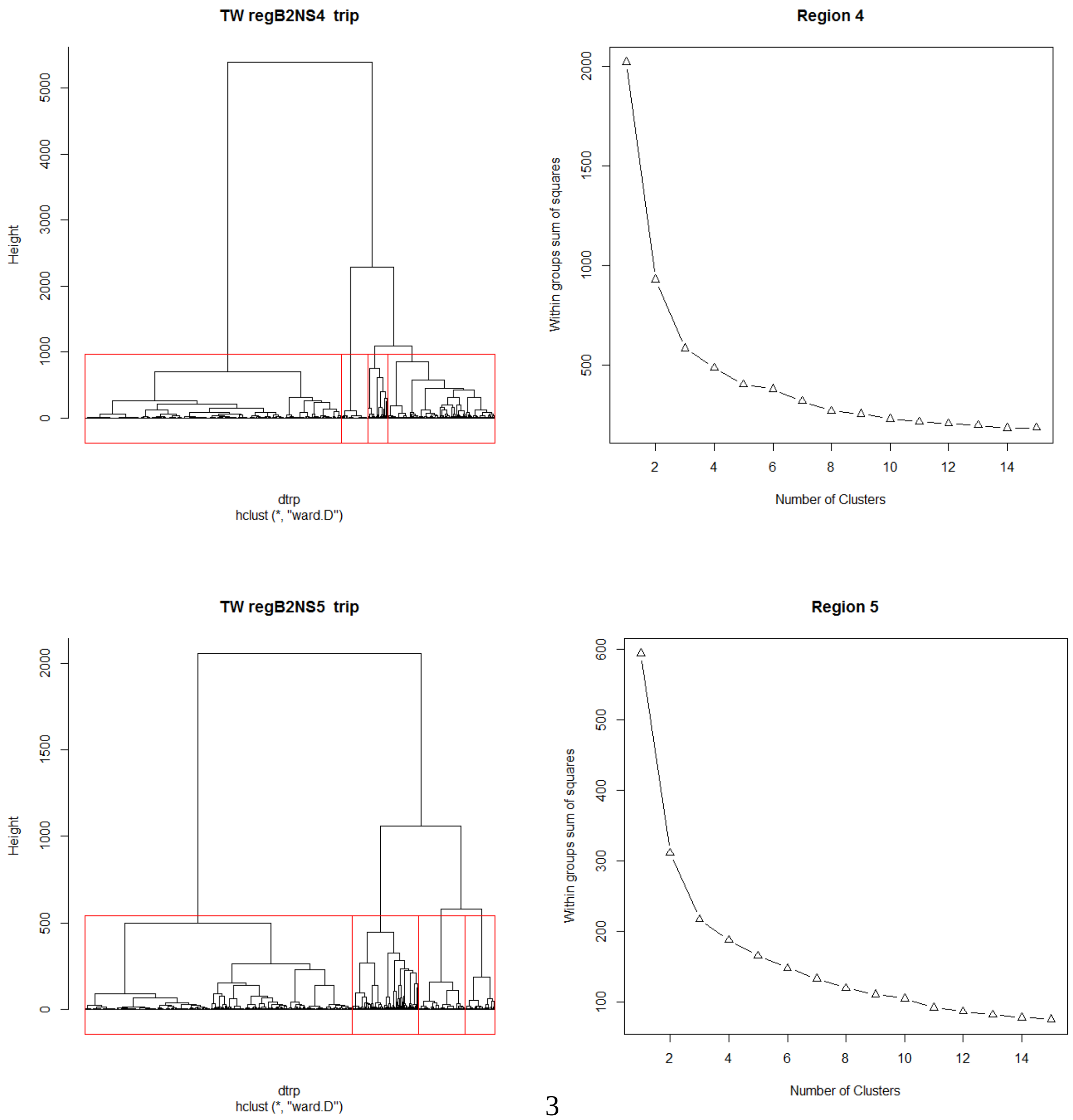

Figure 5. Plots showing analyses to estimate the number of distinct classes of species composition in Taiwanese region 3 and 4 of B2NS. These are based on a hierarchical Ward clustering analysis of trip-level data (top left); within-group sums of squares from kmeans analyses with a range of numbers of clusters (top right); and analyses of the numbers of components to retain from a principal component analysis of trip-level (bottom left) data.

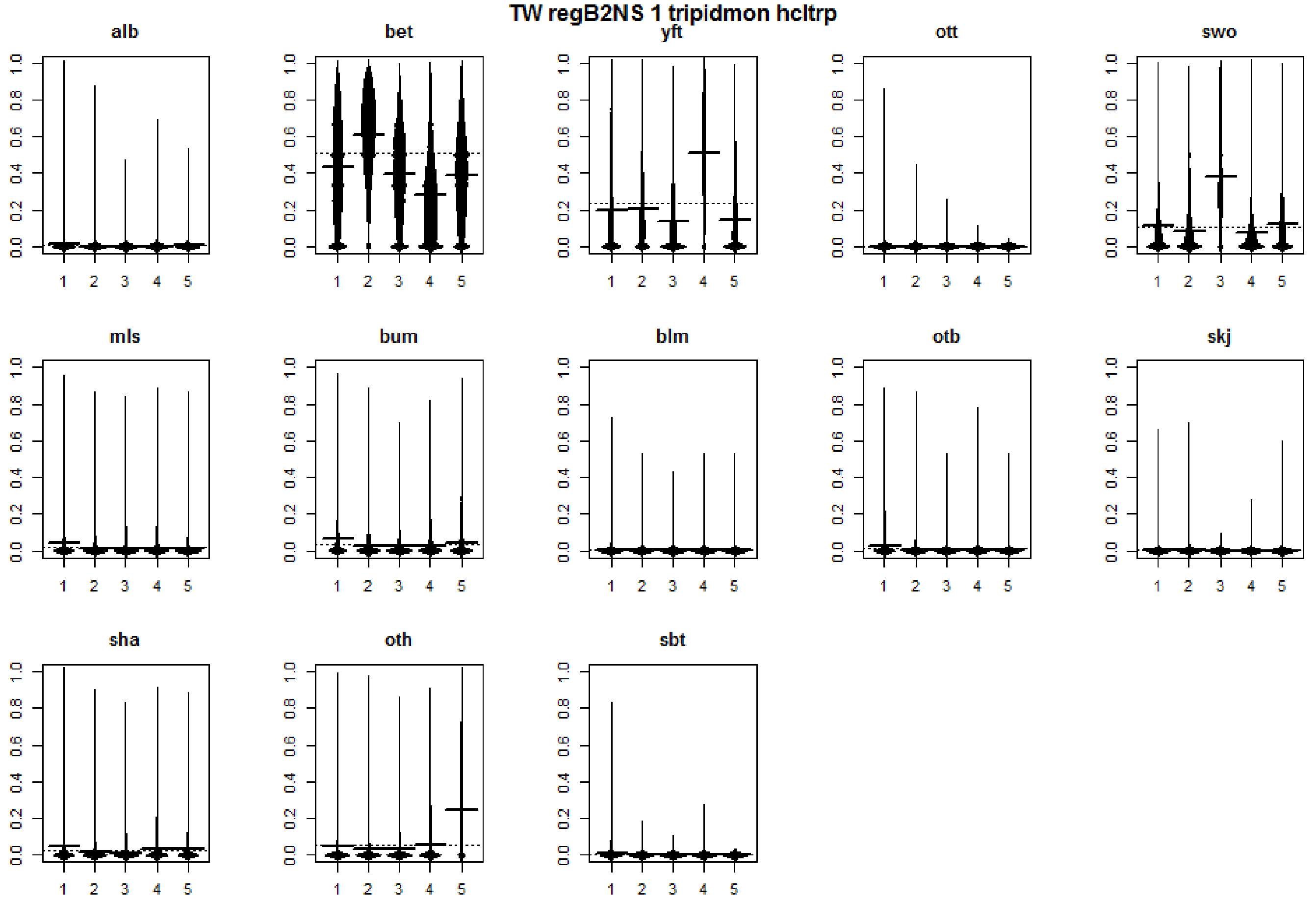

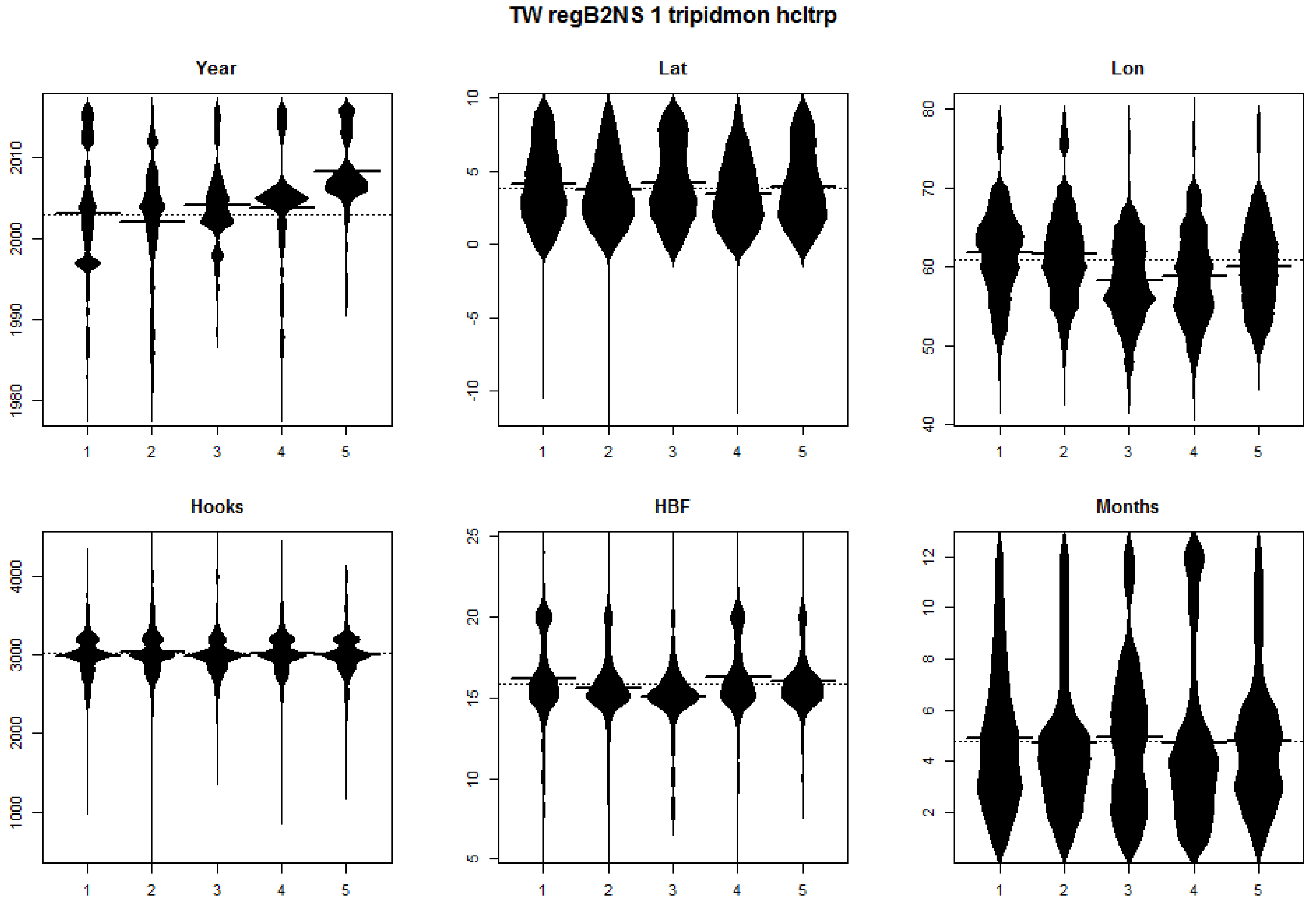

Figure 6. For Taiwanese effort in region 1N of B2NS for the period 1979-2016, for each species, boxplot of the

proportion of the species in the trip versus the cluster. The widths of the boxes are proportional to the numbers of trips in each cluster (above). Boxplot showing the distributions of variables associated with sets in each hcltrp cluster (below). Clustering was performed using a hierarchical Ward clustering analysis of trip-level data.

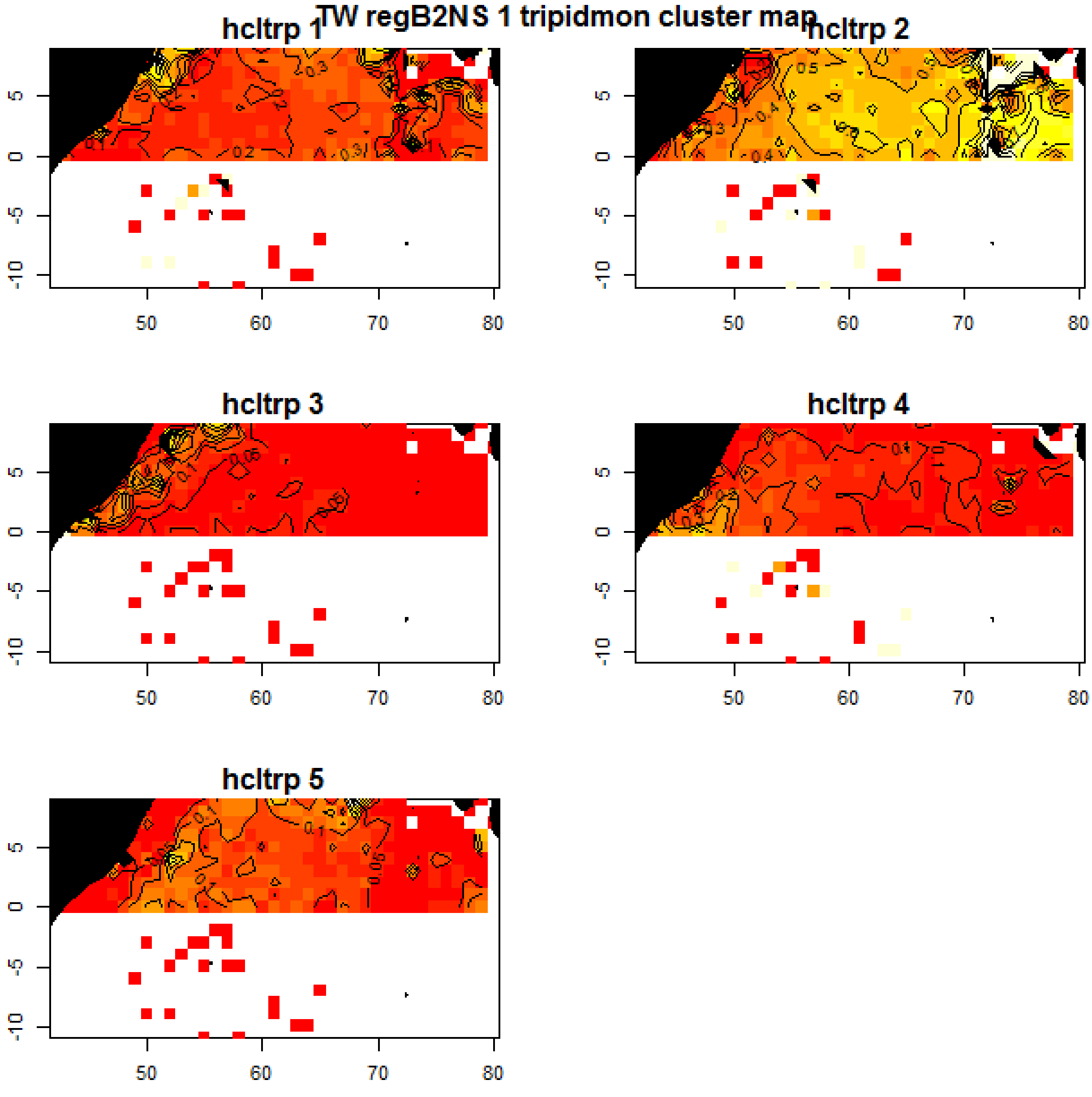

Figure 7. Maps of the spatial distributions of clusters in region 1N of B2NS for Taiwanese effort.

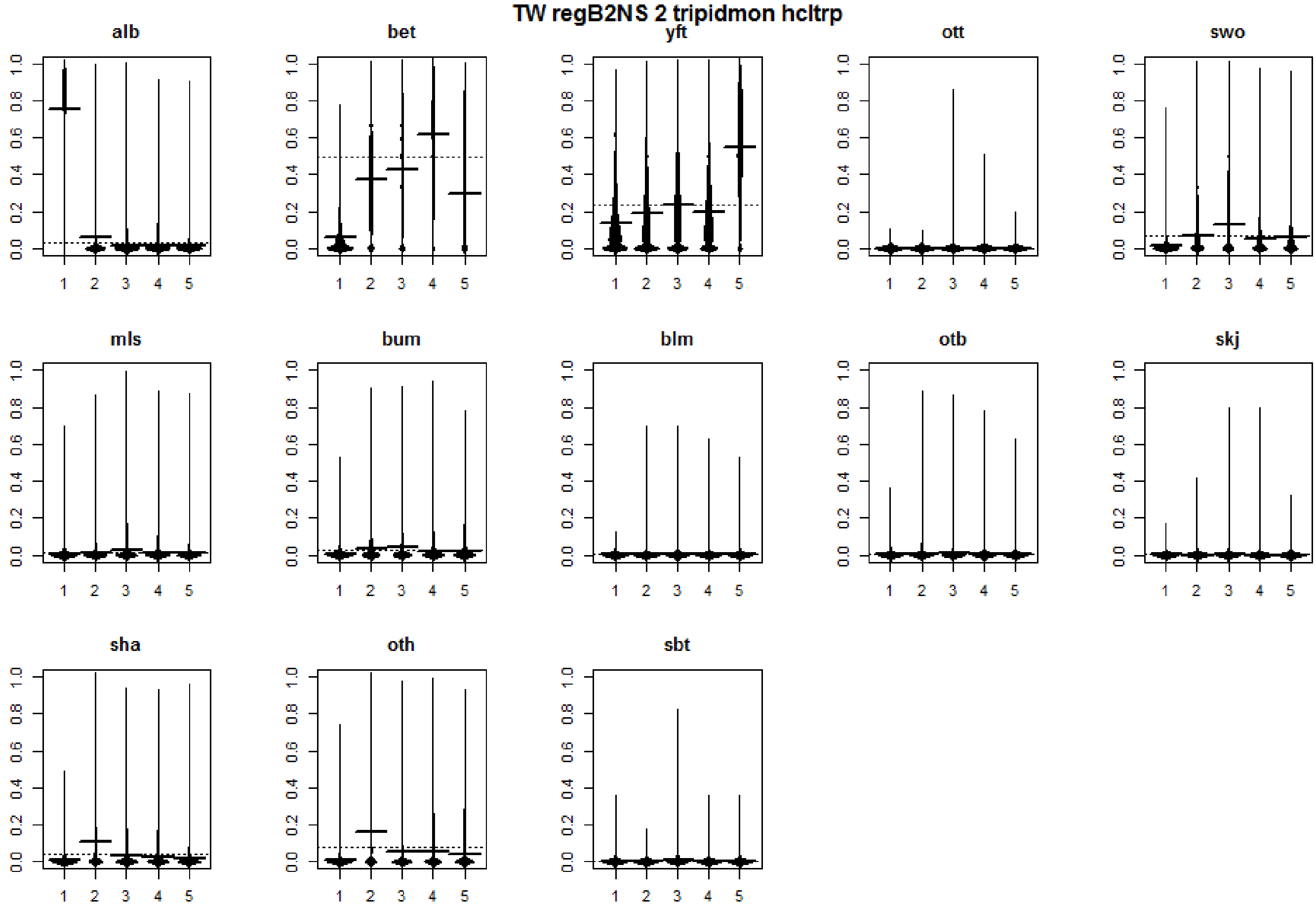

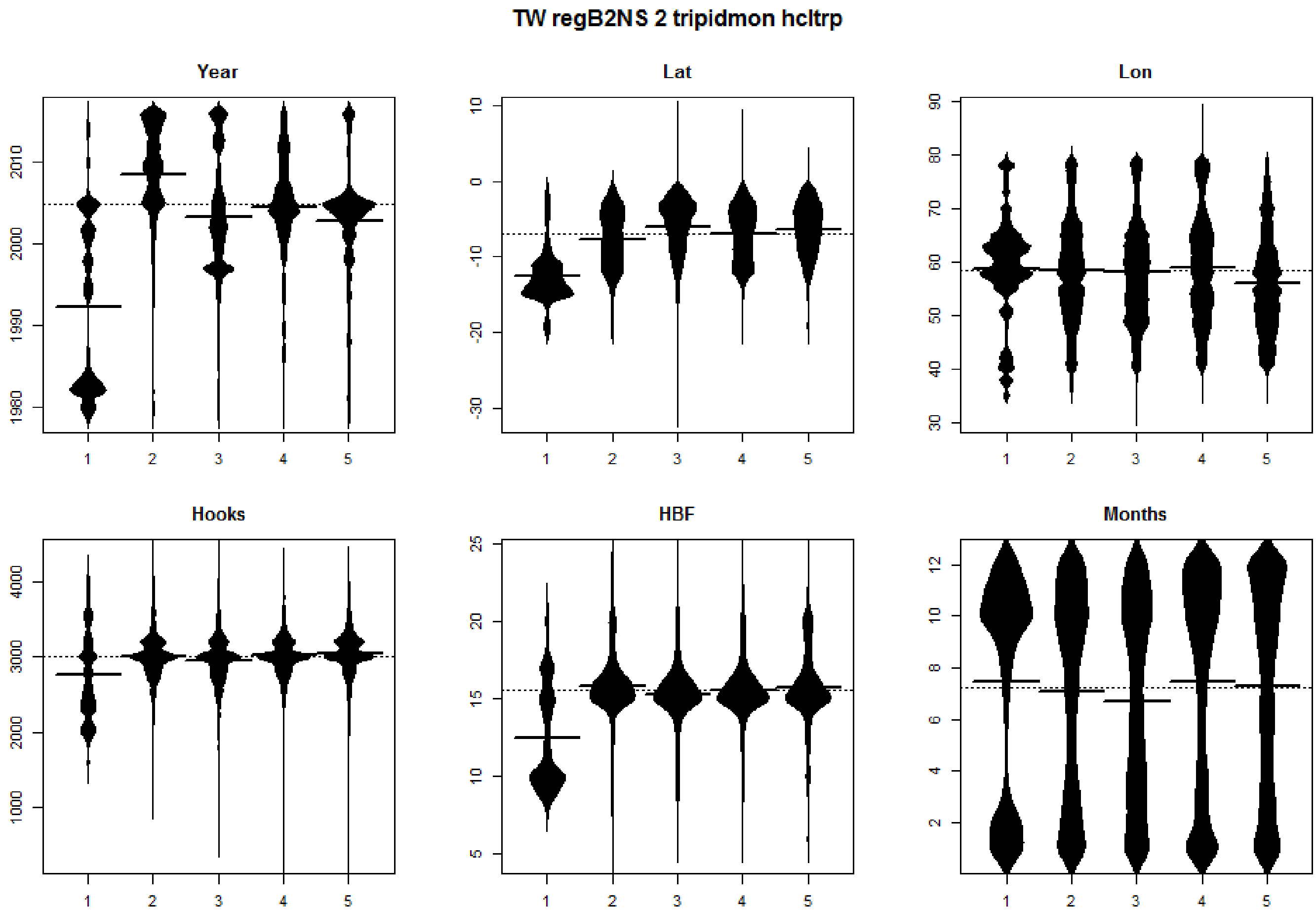

Figure 8. For Taiwanese effort in region 1S of B2NS for the period 1979-2016, for each species, boxplot of the

proportion of the species in the trip versus the cluster. The widths of the boxes are proportional to the numbers of trips in each cluster (above). Boxplot showing the distributions of variables associated with sets in each hcltrp cluster (below). Clustering was performed using a hierarchical Ward clustering analysis of trip-level data.

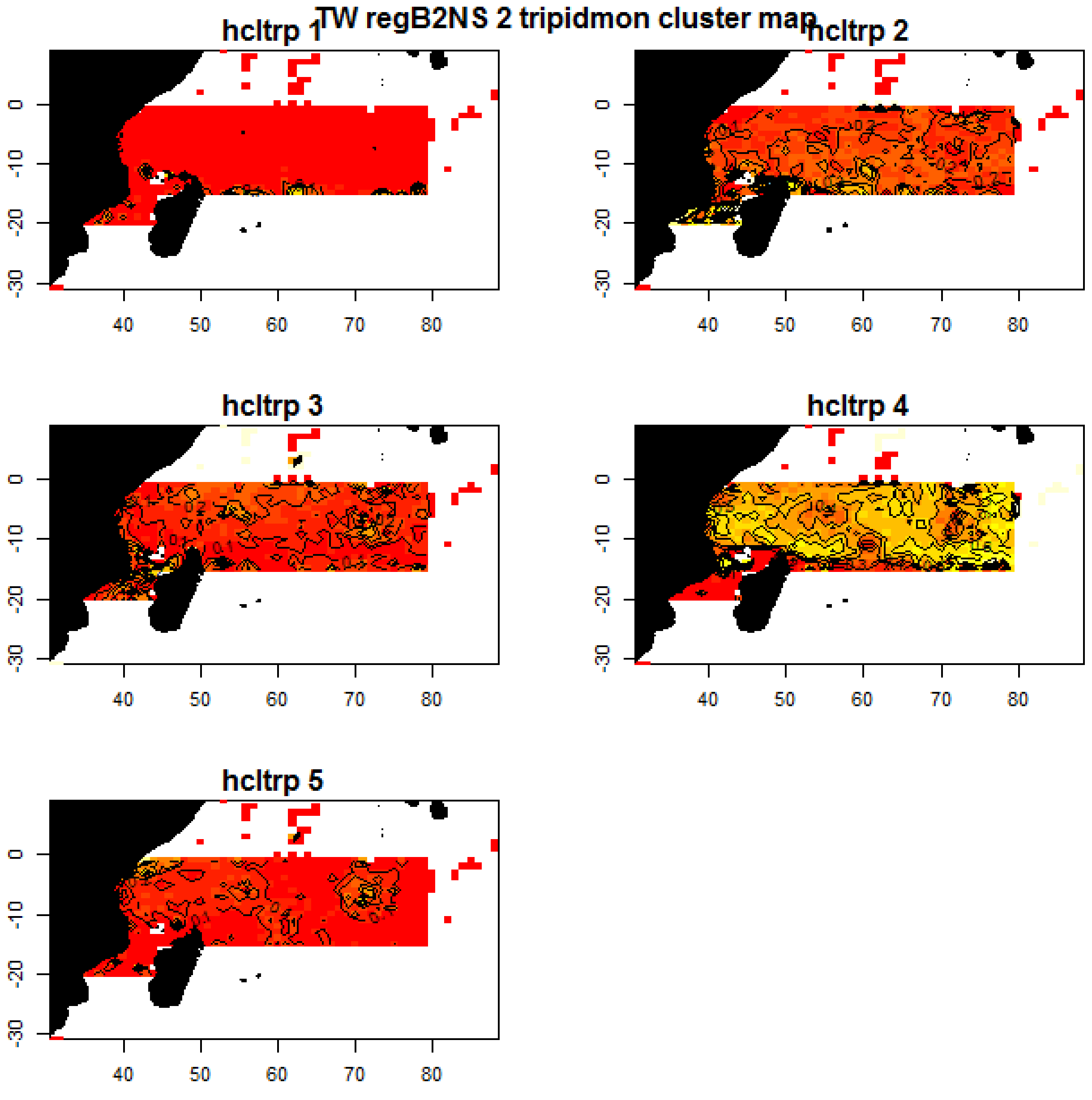

Figure 9. Maps of the spatial distributions of clusters in region 1S of B2NS for Taiwanese effort.

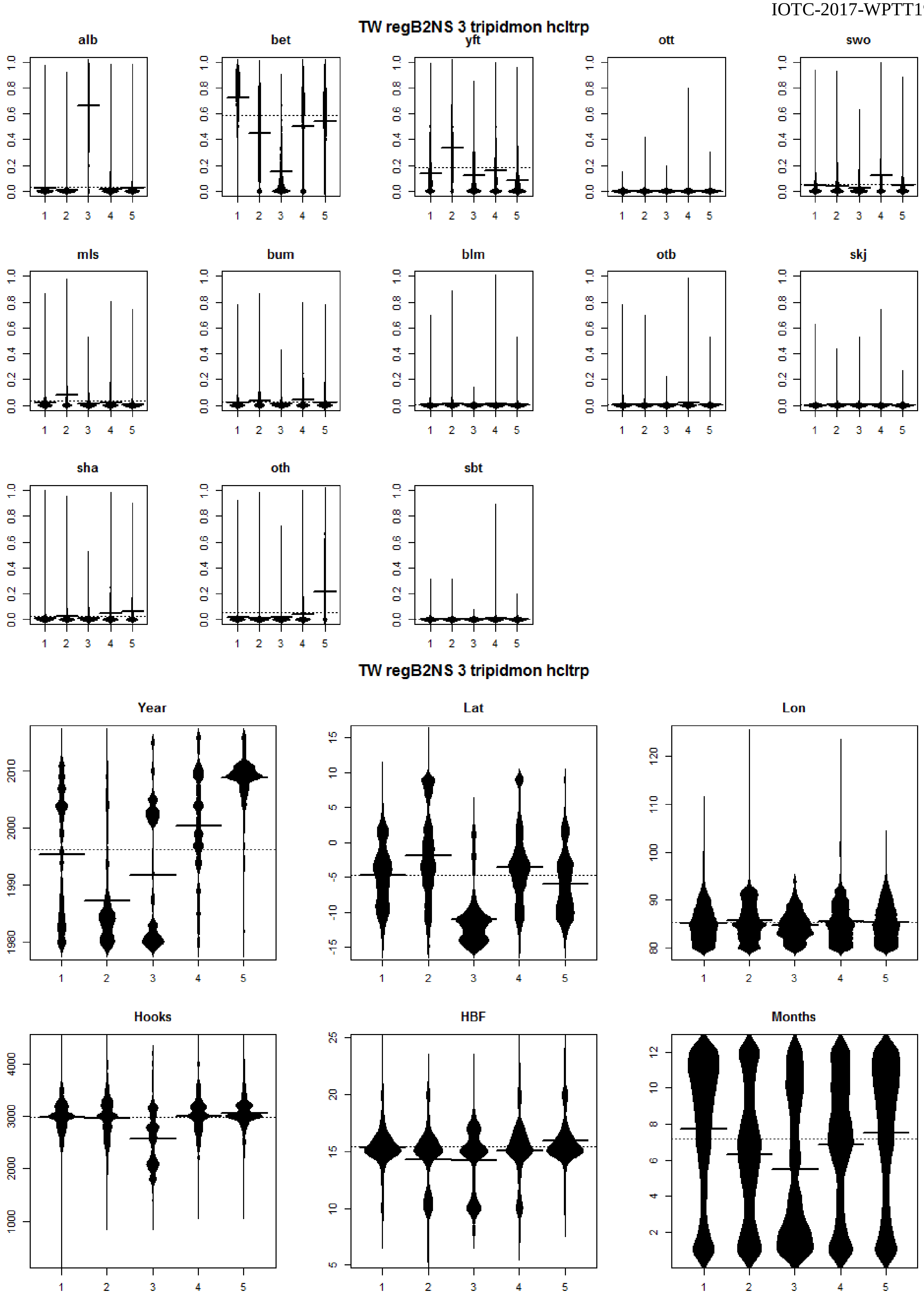

Figure 10. For Taiwanese effort in region 2 of B2NS for the period 1979-2016, for each species, boxplot of the proportion of the species in the trip versus the cluster. The widths of the boxes are proportional to the numbers of

trips in each cluster (above). Boxplot showing the distributions of variables associated with sets in each hcltrp cluster (below). Clustering was performed using a hierarchical Ward clustering analysis of trip-level data.

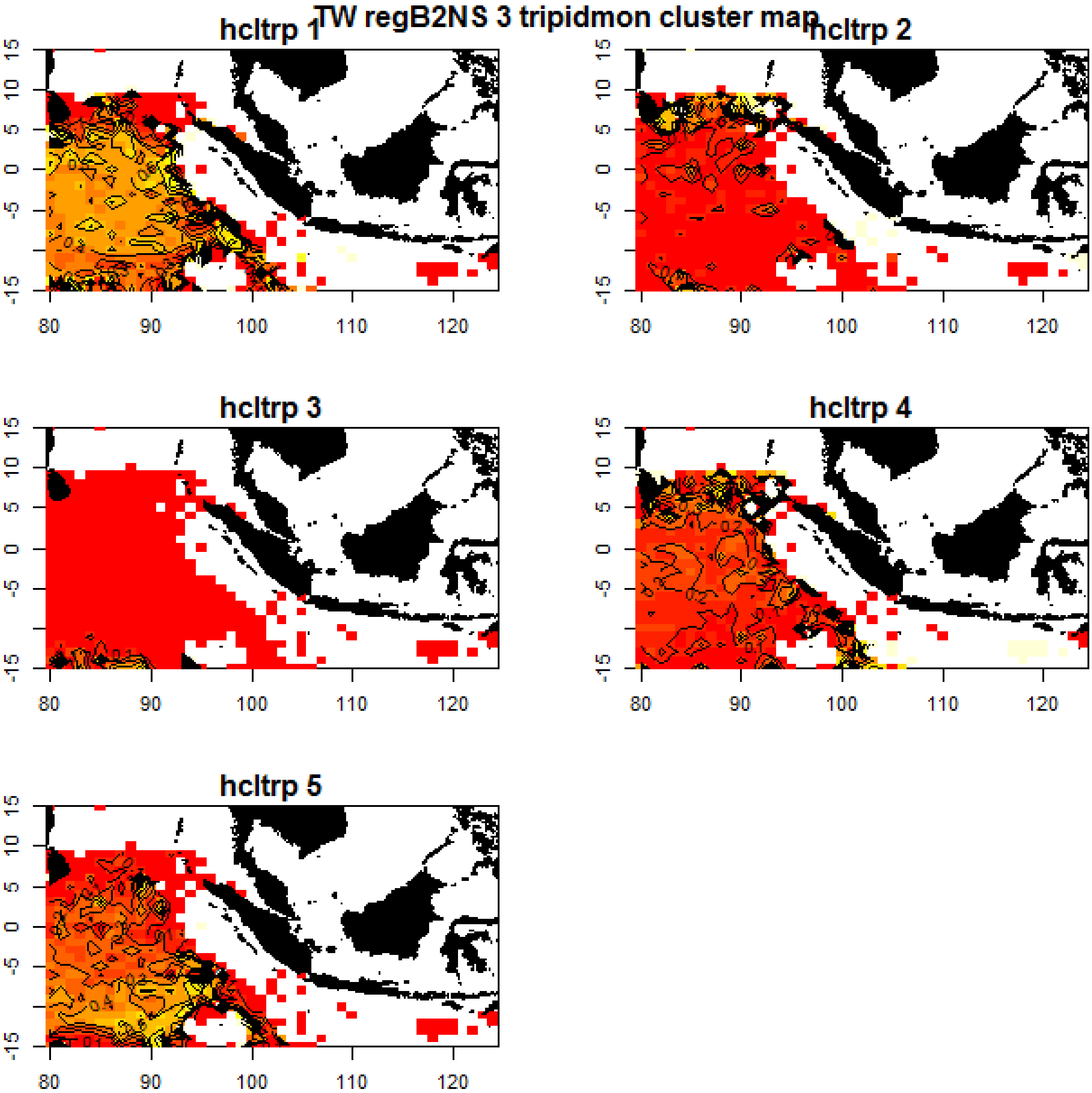

Figure 11. Maps of the spatial distributions of clusters in region 2 of B2NS for Taiwanese effort.

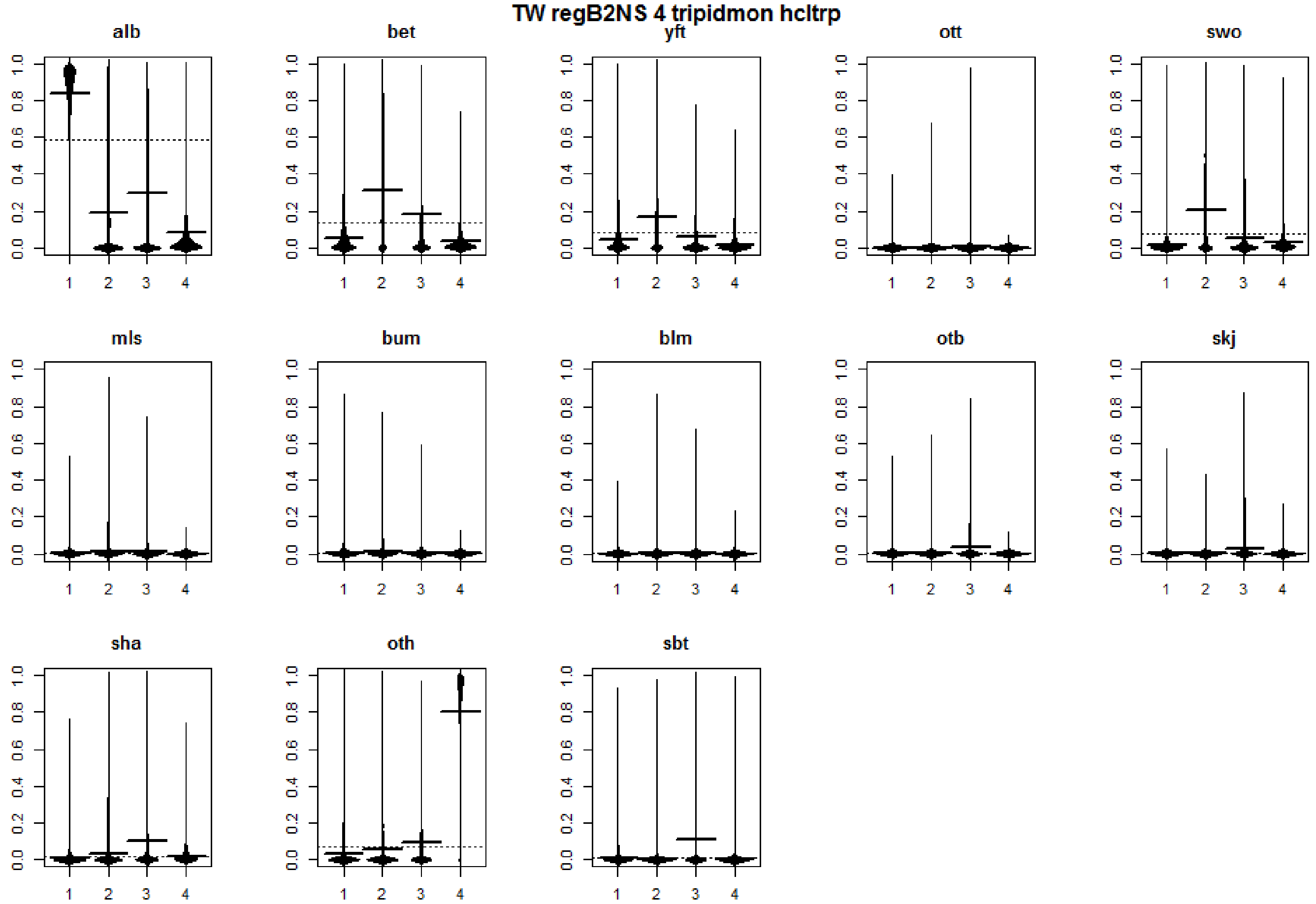

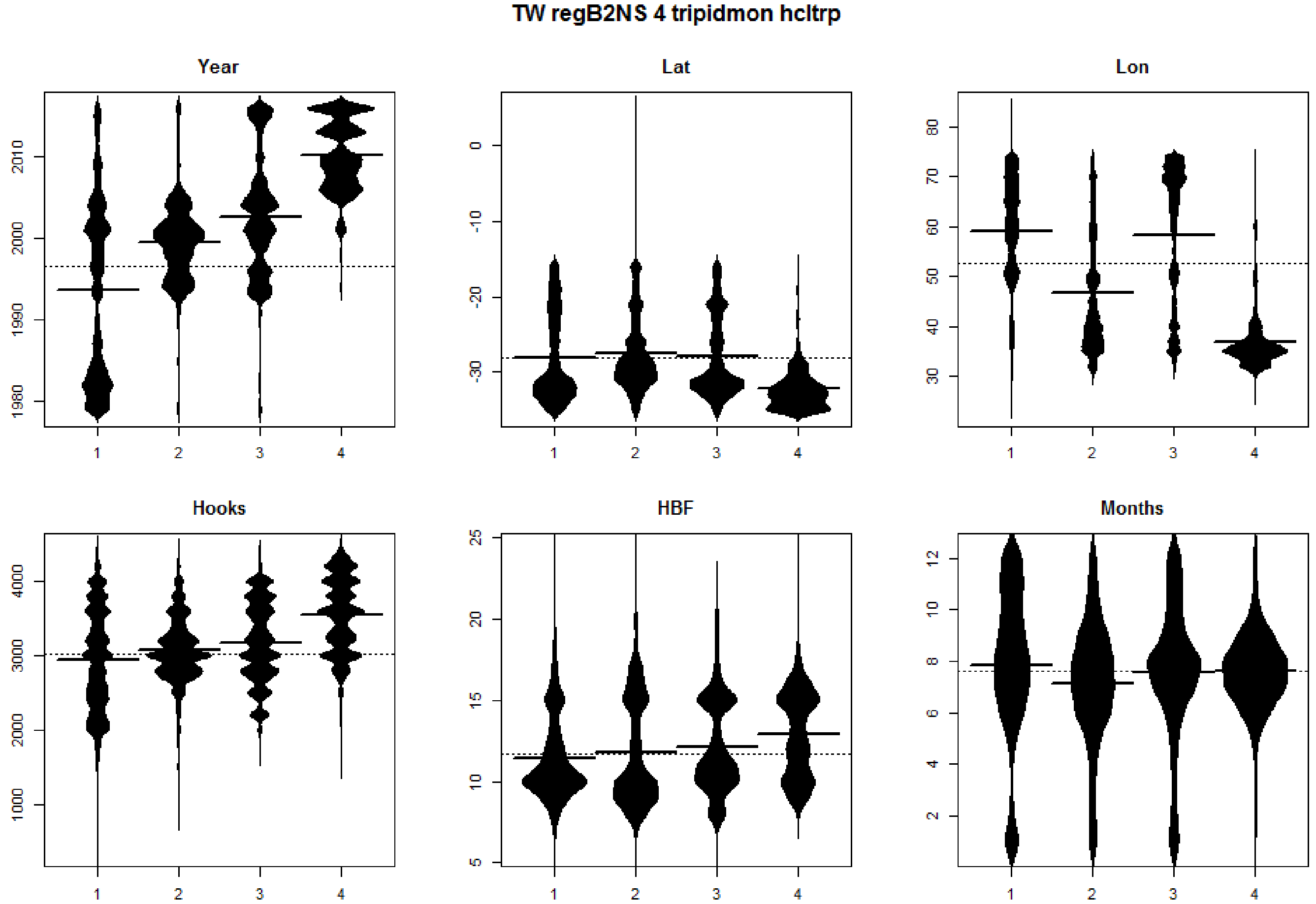

Figure 12. For Taiwanese effort in region 3 of B2NS for the period 1979-2016, for each species, boxplot of the

proportion of the species in the trip versus the cluster. The widths of the boxes are proportional to the numbers of trips in each cluster (above). Boxplot showing the distributions of variables associated with sets in each hcltrp cluster (below). Clustering was performed using a hierarchical Ward clustering analysis of trip-level data.

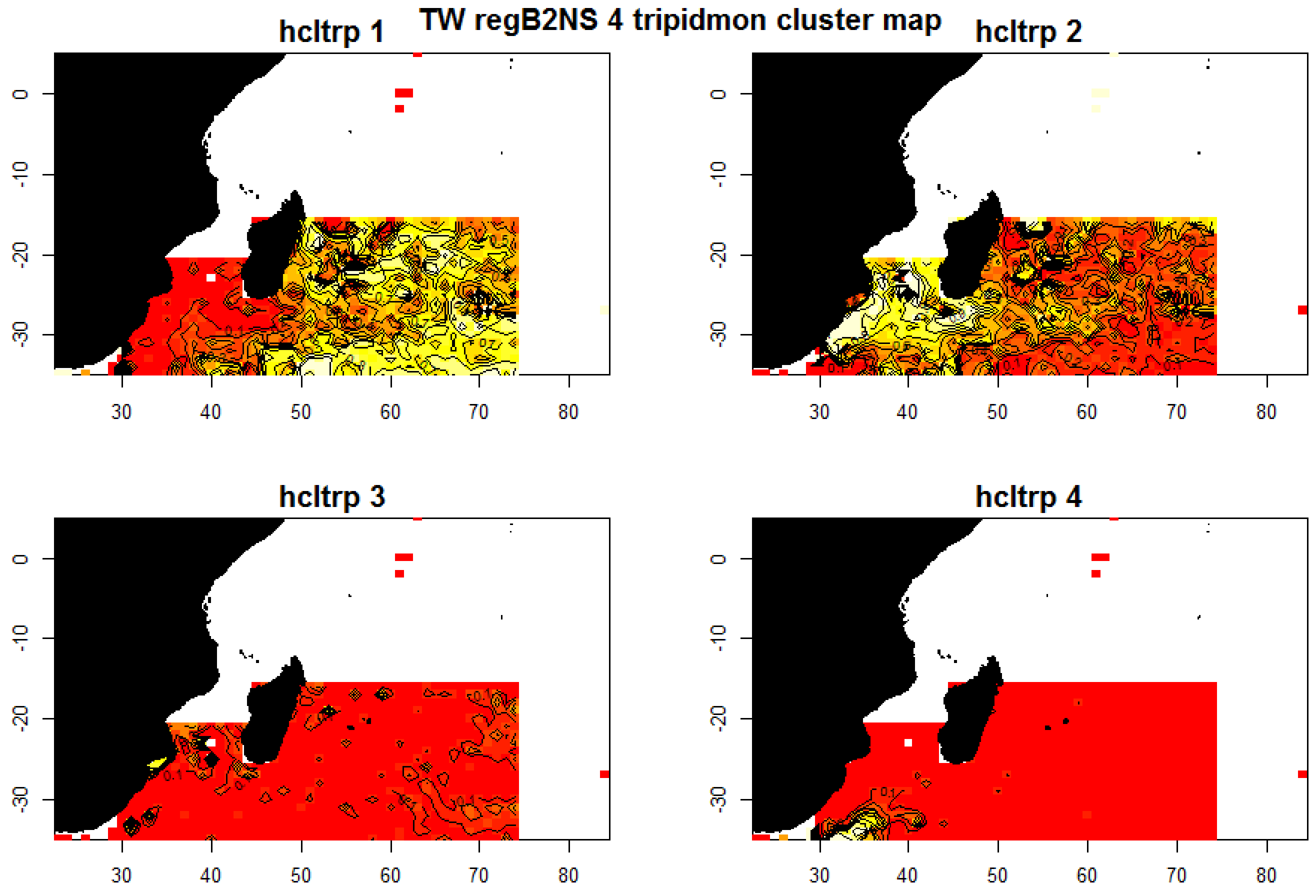

Figure 13. Maps of the spatial distributions of clusters in region 3 of B2NS for Taiwanese effort.

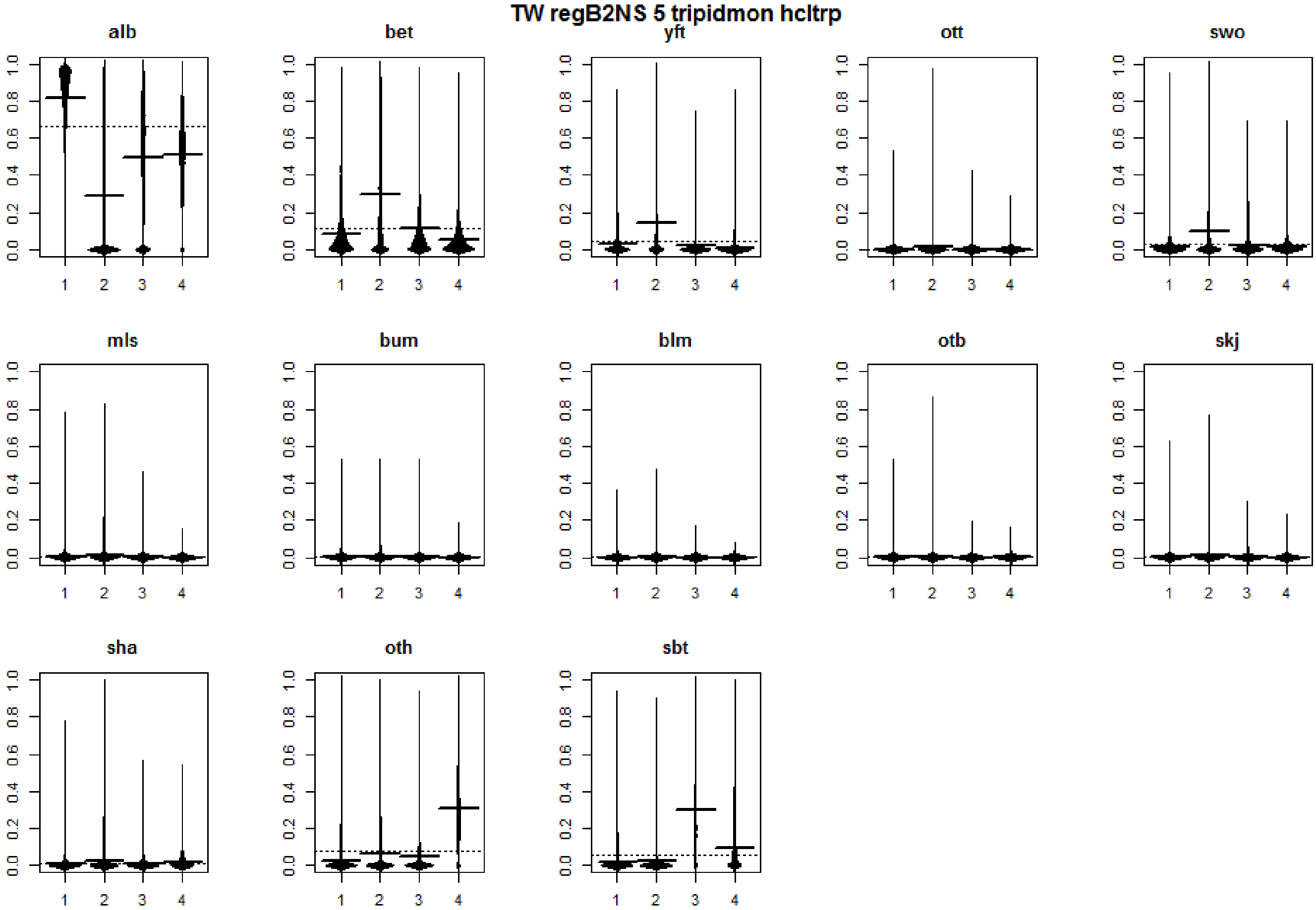

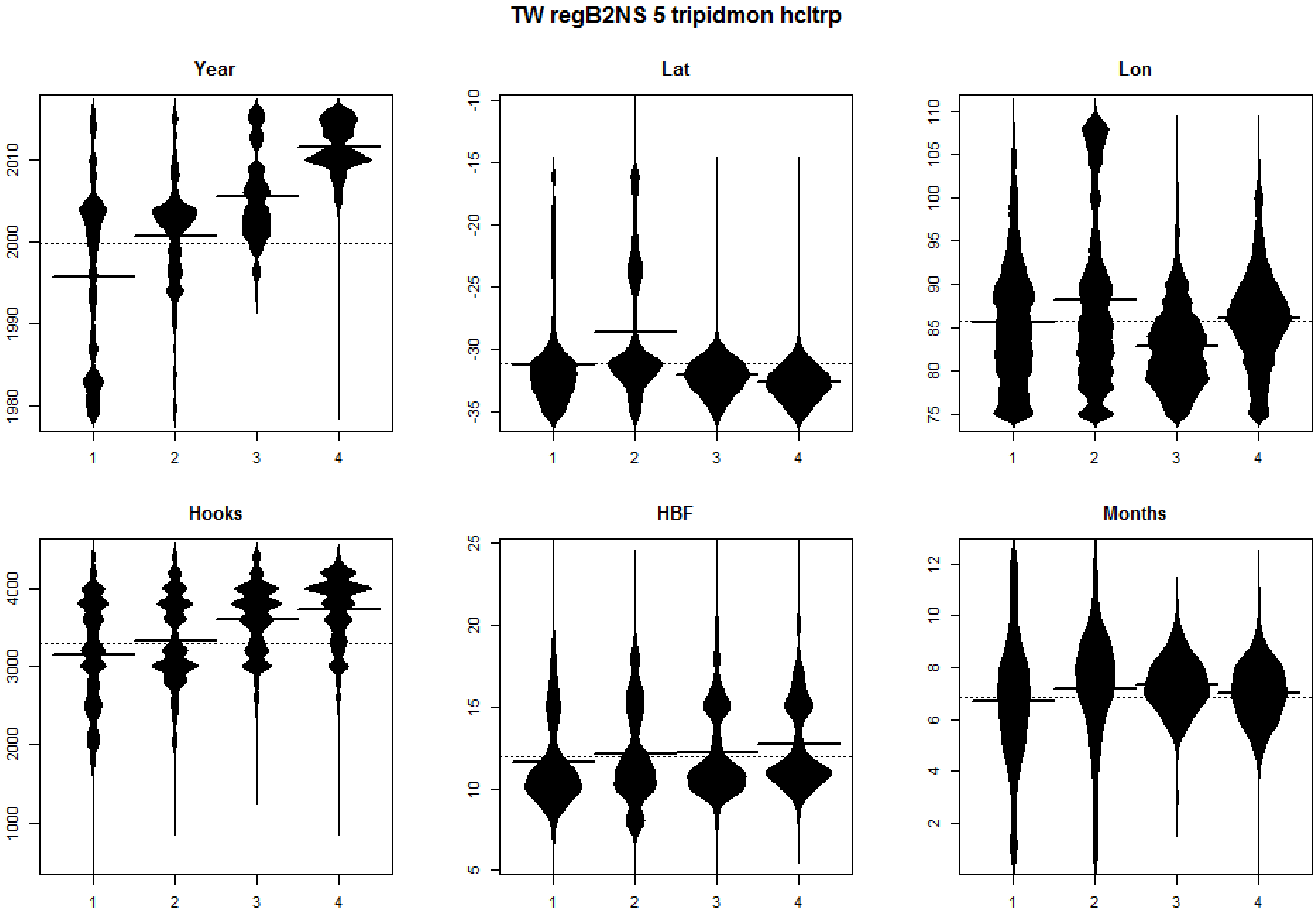

Figure 14. For Taiwanese effort in region 4 of B2NS for the period 1979-2016, for each species, boxplot of the

proportion of the species in the trip versus the cluster. The widths of the boxes are proportional to the numbers of trips in each cluster (above). Boxplot showing the distributions of variables associated with sets in each hcltrp cluster (below). Clustering was performed using a hierarchical Ward clustering analysis of trip-level data.

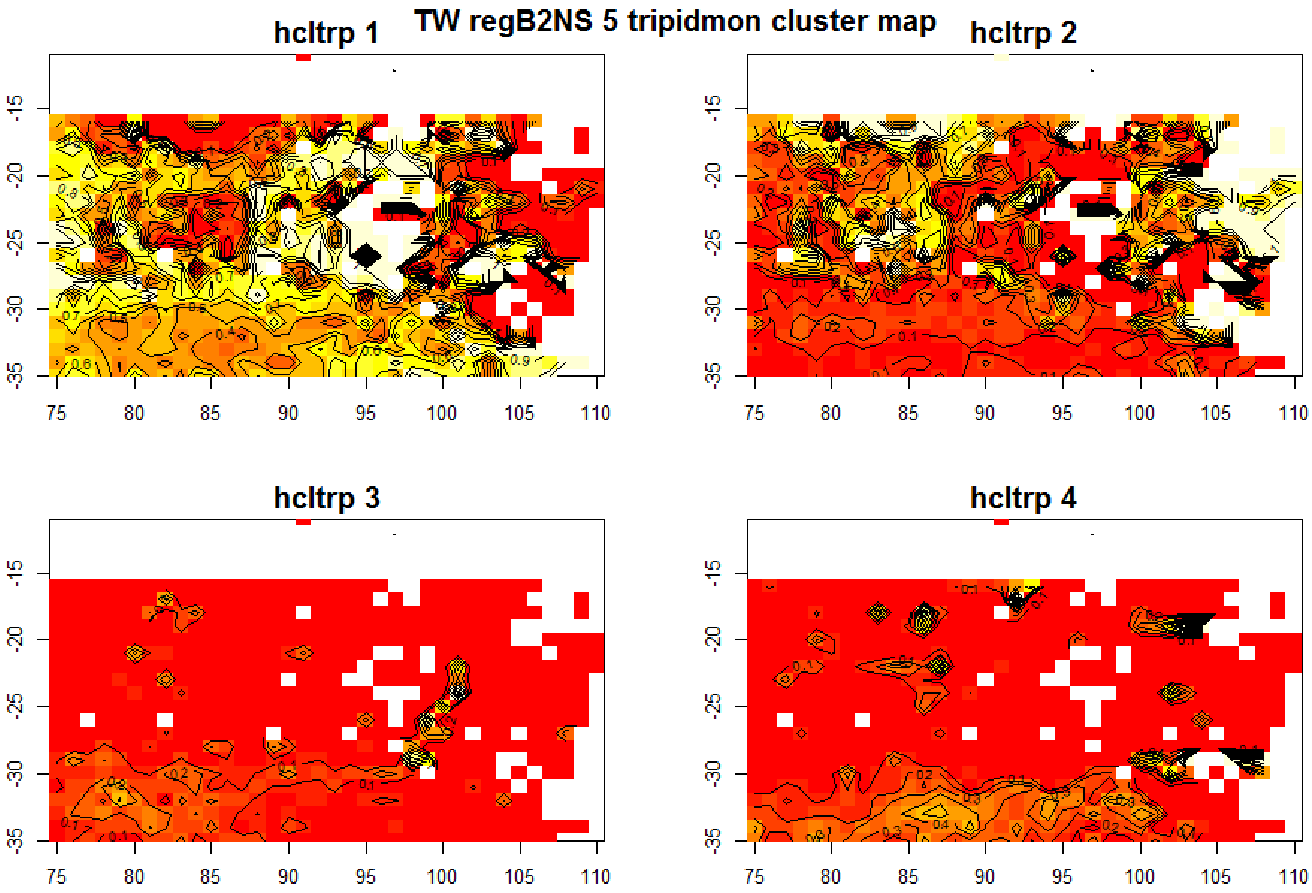

Figure 15. Maps of the spatial distributions of clusters in region 4 of B2NS for Taiwanese effort.

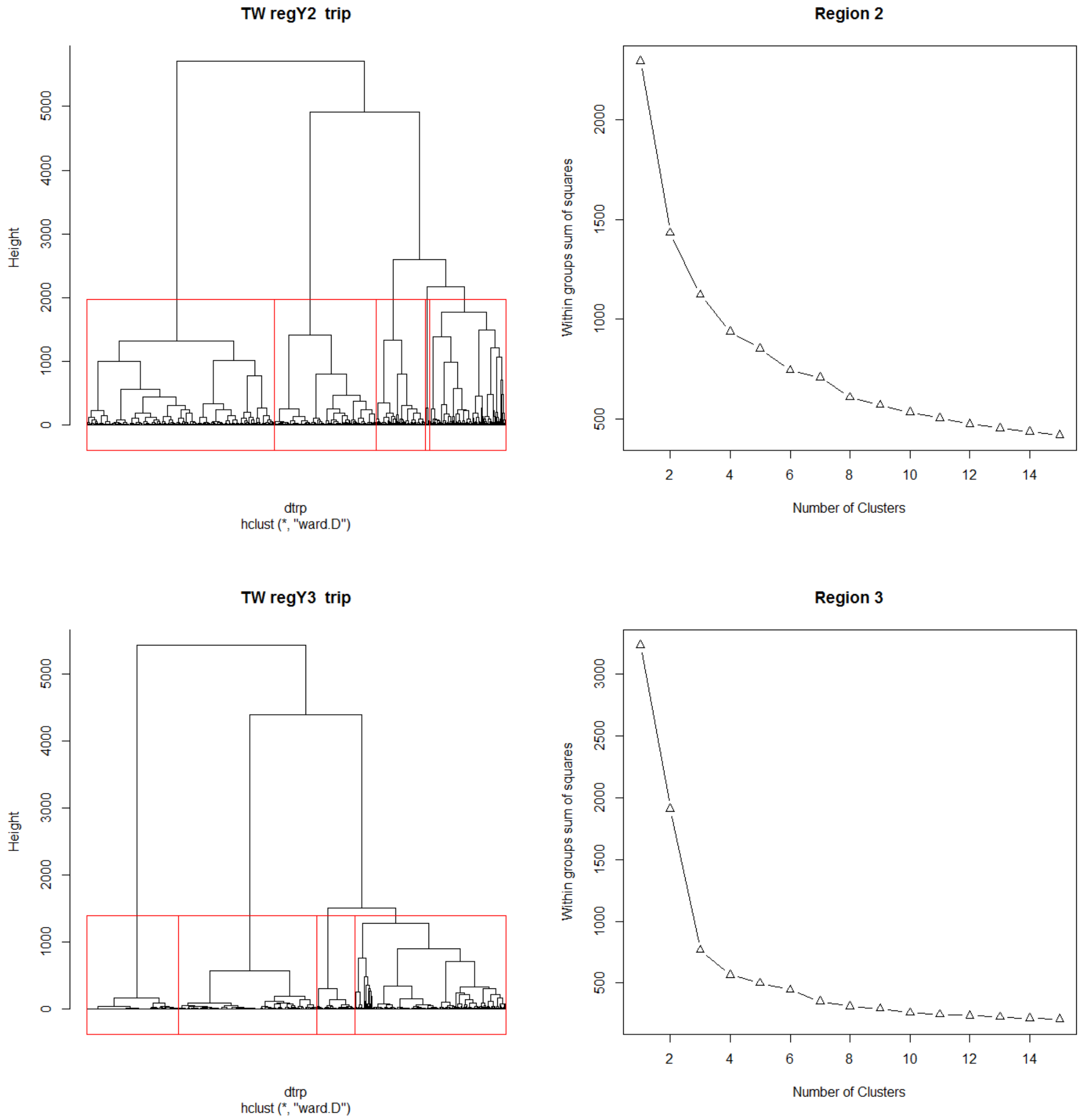

Figure 16. Plots showing analyses to estimate the number of distinct classes of species composition in Taiwanese region 2 & 3 of Y. These are based on a hierarchical Ward clustering analysis of trip-level data (top left); within-group sums of squares from kmeans analyses with a range of numbers of clusters (top right); and analyses of the numbers of components to retain from a principal component analysis of trip-level (bottom left) data.

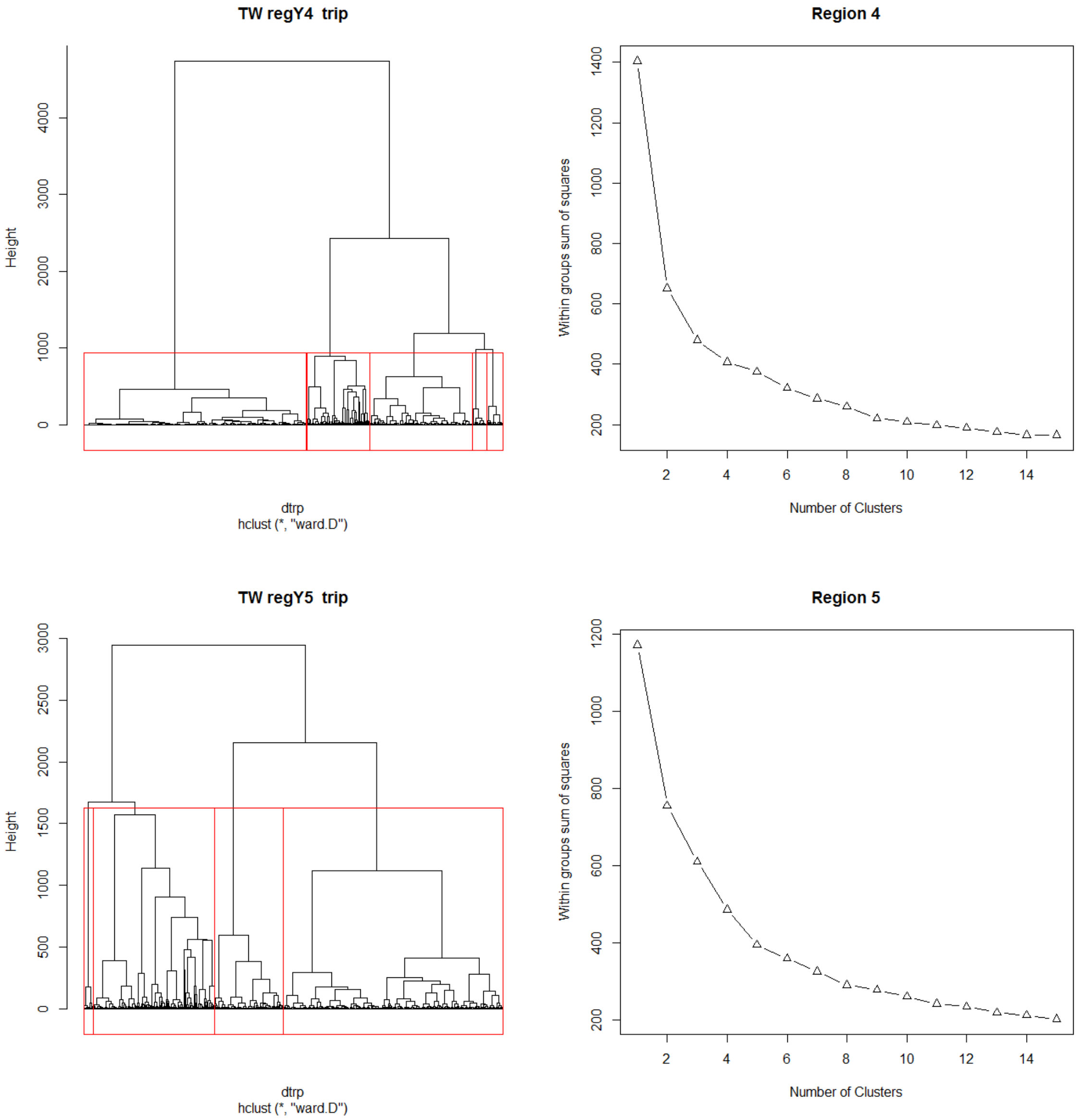

Figure 17. Plots showing analyses to estimate the number of distinct classes of species composition in Taiwanese region 4 & 5 of Y. These are based on a hierarchical Ward clustering analysis of trip-level data (top left); within-group sums of squares from kmeans analyses with a range of numbers of clusters (top right); and analyses of the numbers of components to retain from a principal component analysis of trip-level (bottom left) data.

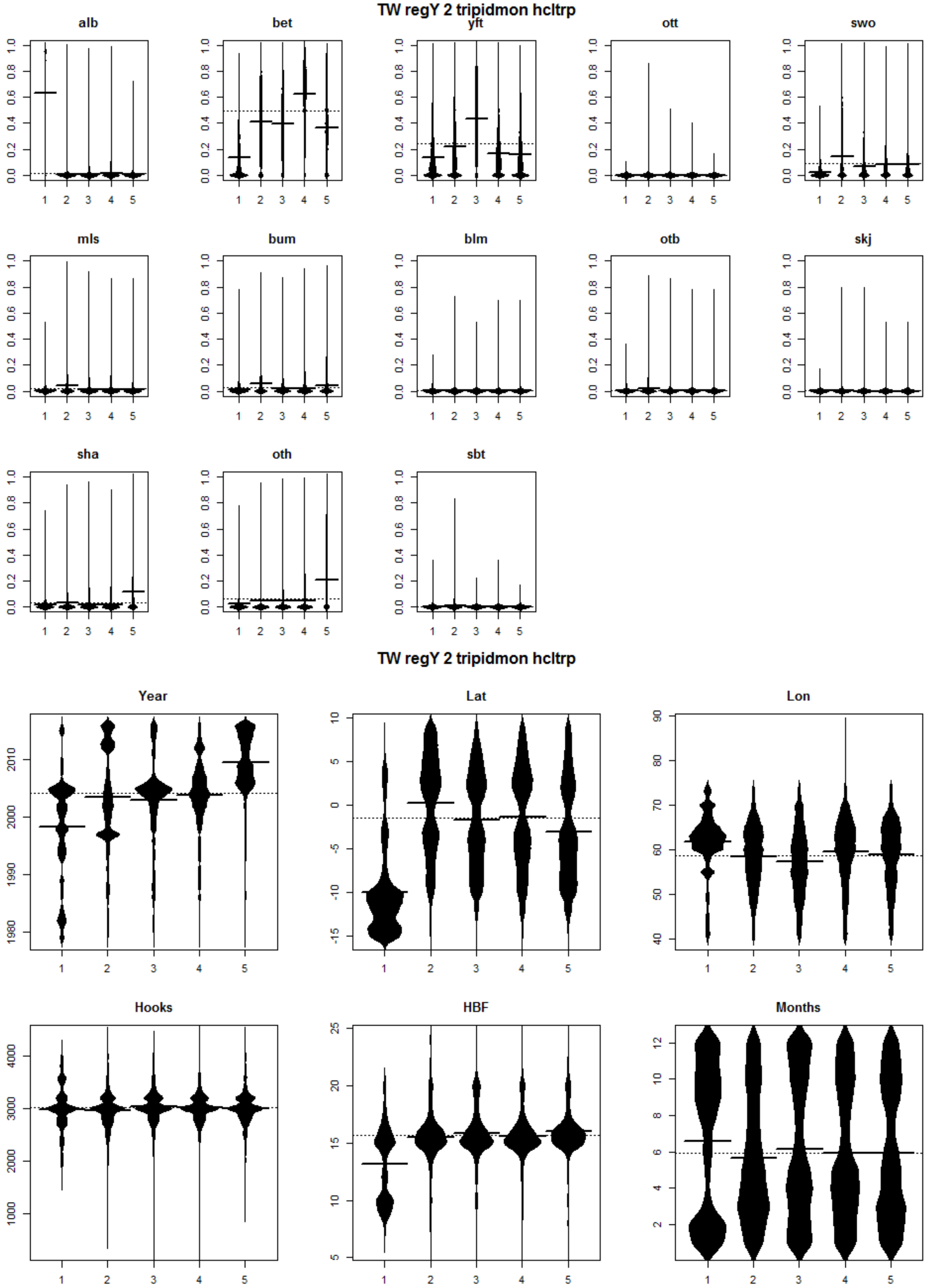

Figure 18. Plots showing analyses to estimate the number of distinct classes of species composition in Taiwanese region 4 & 5 of Y. These are based on a hierarchical Ward clustering analysis of trip-level data (top left); within-

group sums of squares from kmeans analyses with a range of numbers of clusters (top right); and analyses of the numbers of components to retain from a principal component analysis of trip-level (bottom left) data.

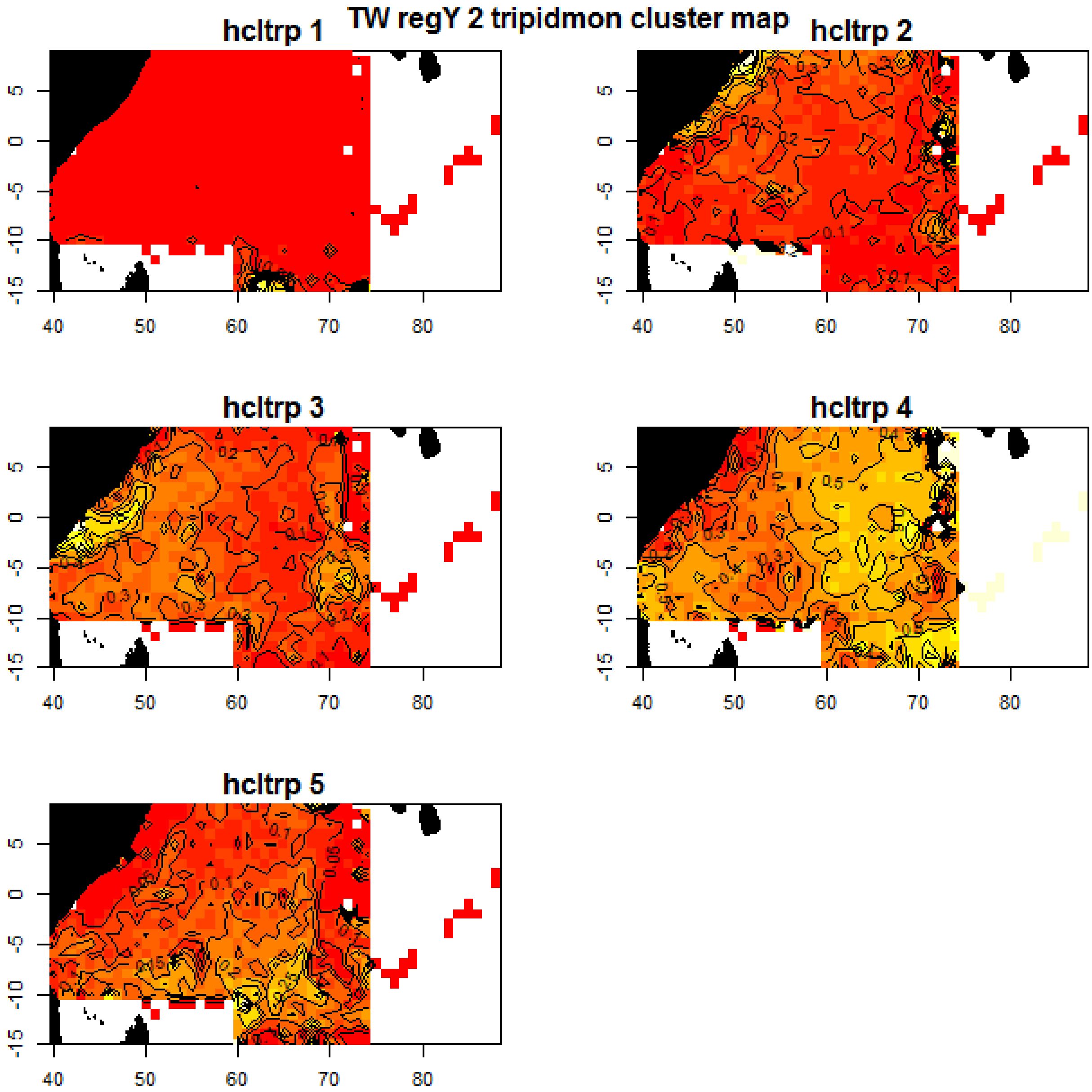

Figure 19. Maps of the spatial distributions of clusters in region 2 of Y for Taiwanese effort.

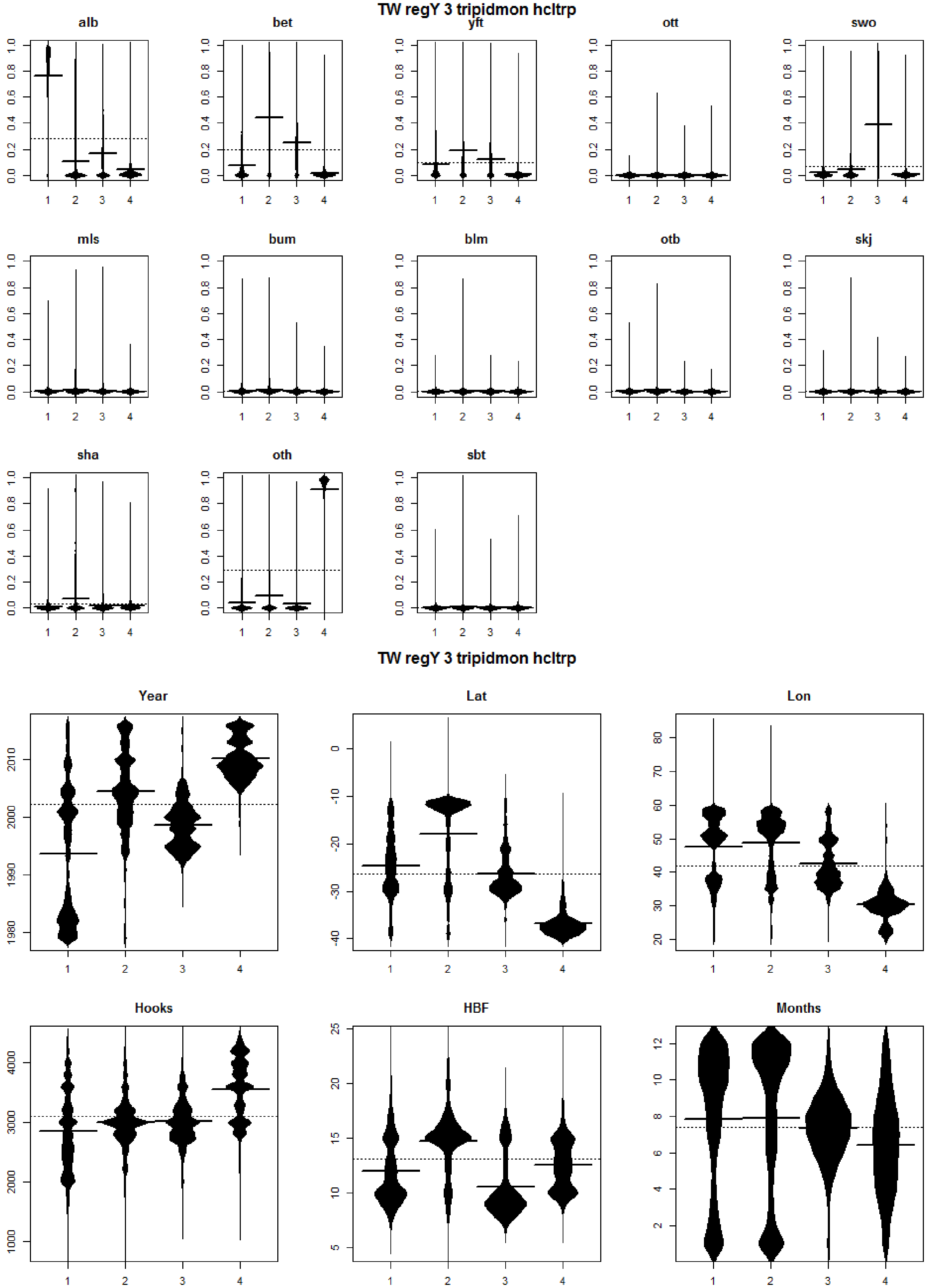

Figure 20. For Taiwanese effort in region 3 of Y for the period 1979-2016, for each species, boxplot of the

proportion of the species in the trip versus the cluster. The widths of the boxes are proportional to the numbers of trips in each cluster (above). Boxplot showing the distributions of variables associated with sets in each hcltrp cluster (below). Clustering was performed using a hierarchical Ward clustering analysis of trip-level data.

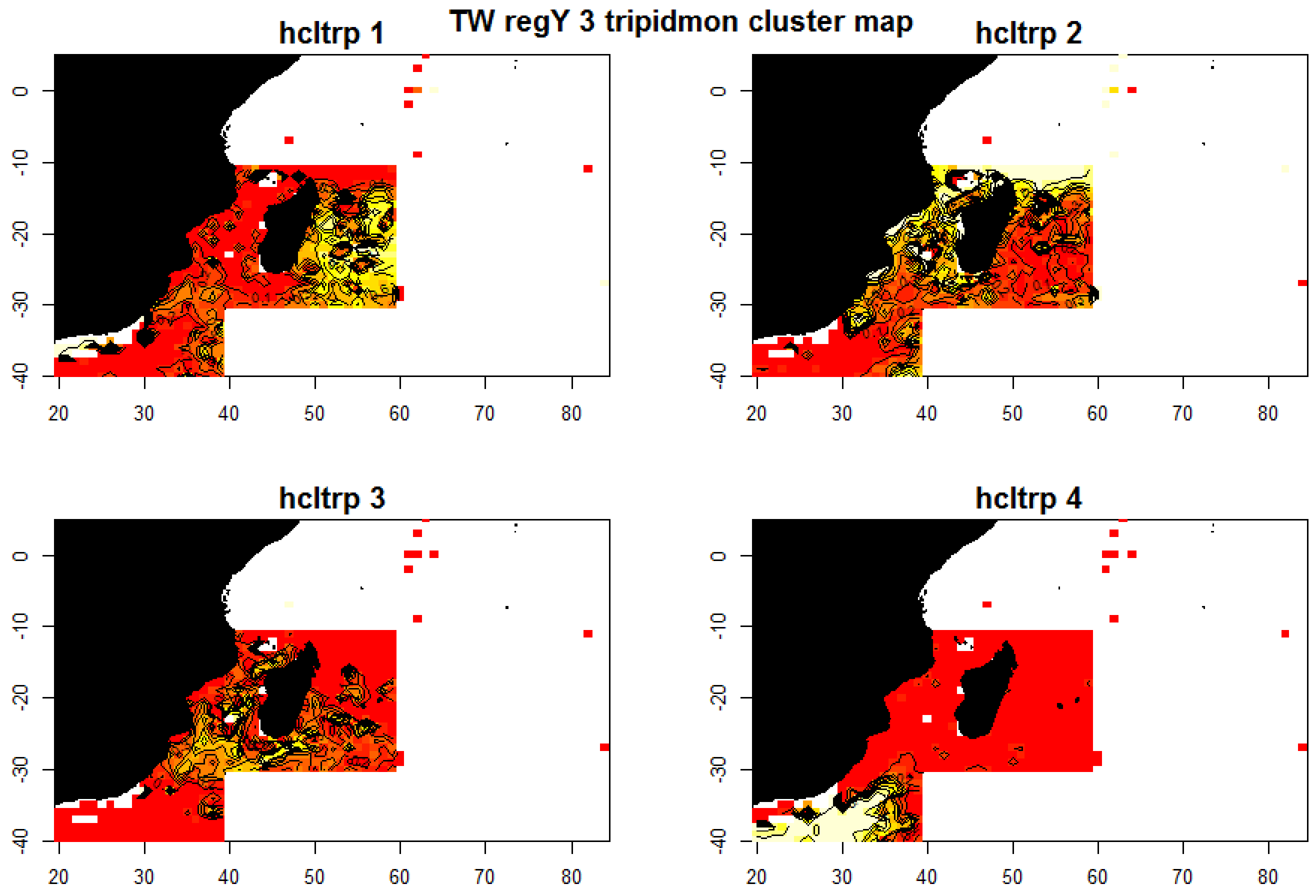

Figure 21. Maps of the spatial distributions of clusters in region 3 of Y for Taiwanese effort.

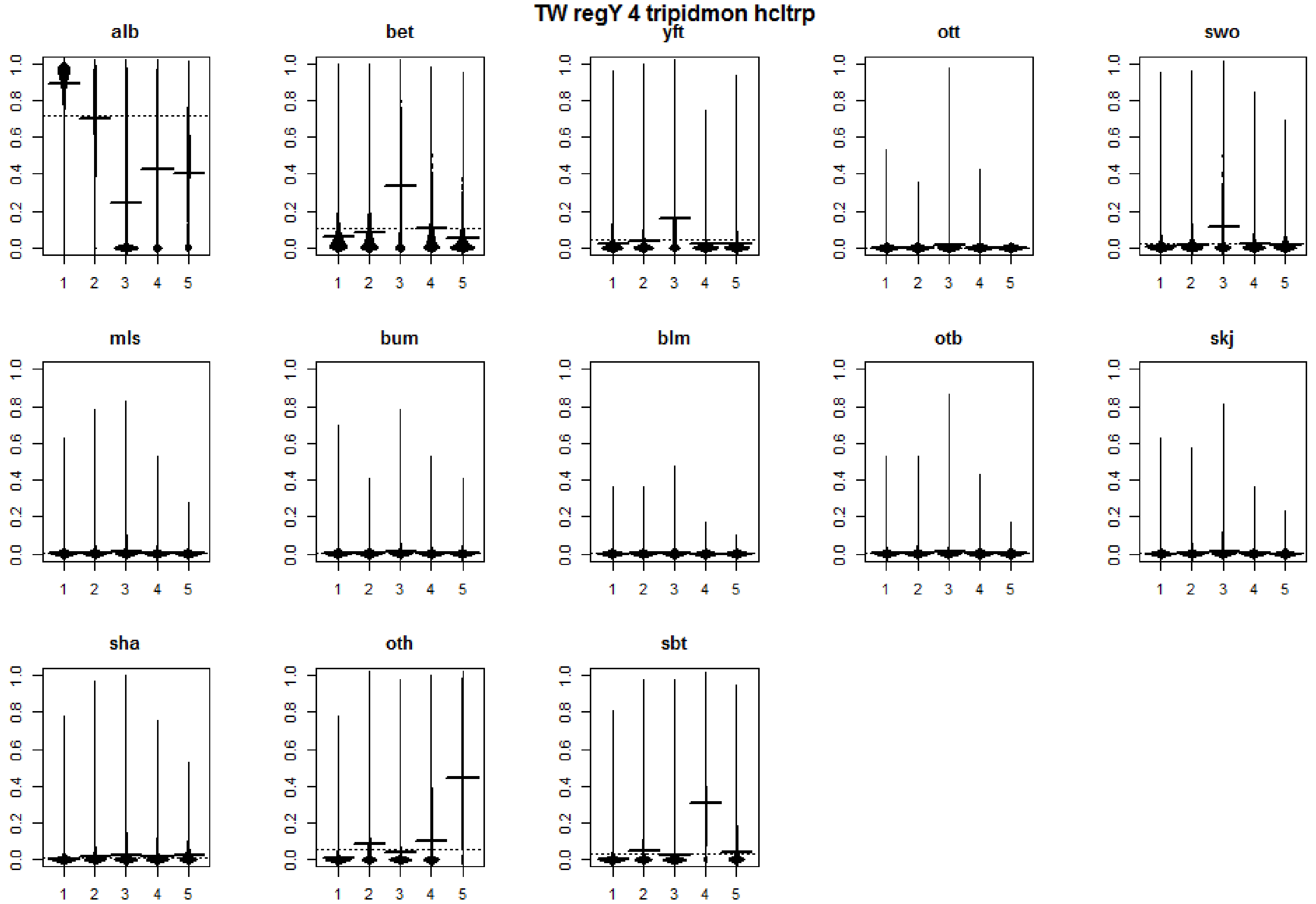

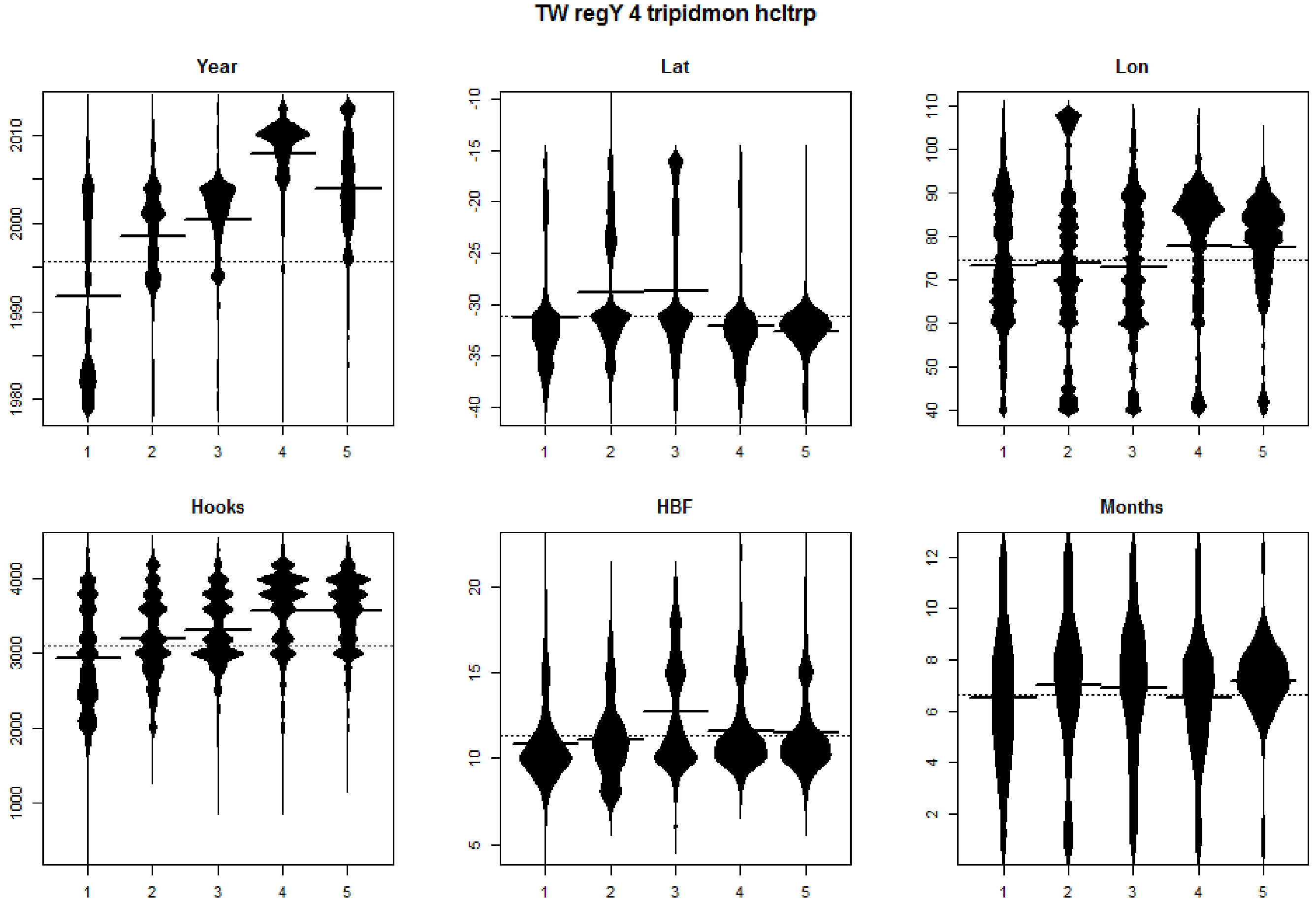

Figure 22. For Taiwanese effort in region 4 of Y for the period 1979-2016, for each species, boxplot of the

proportion of the species in the trip versus the cluster. The widths of the boxes are proportional to the numbers of trips in each cluster (above). Boxplot showing the distributions of variables associated with sets in each hcltrp cluster (below). Clustering was performed using a hierarchical Ward clustering analysis of trip-level data.

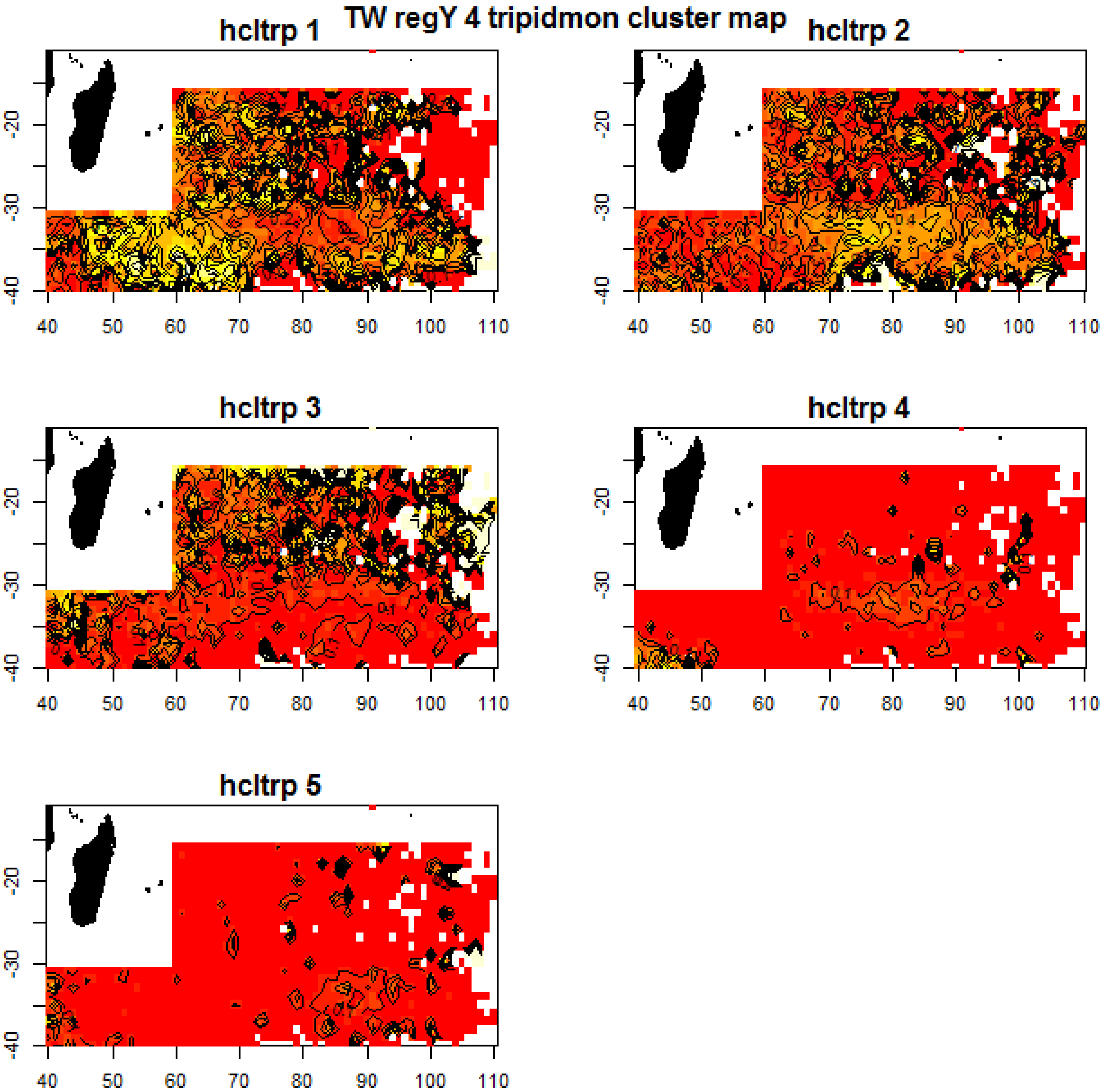

Figure 23. Maps of the spatial distributions of clusters in region 4 of Y for Taiwanese effort.

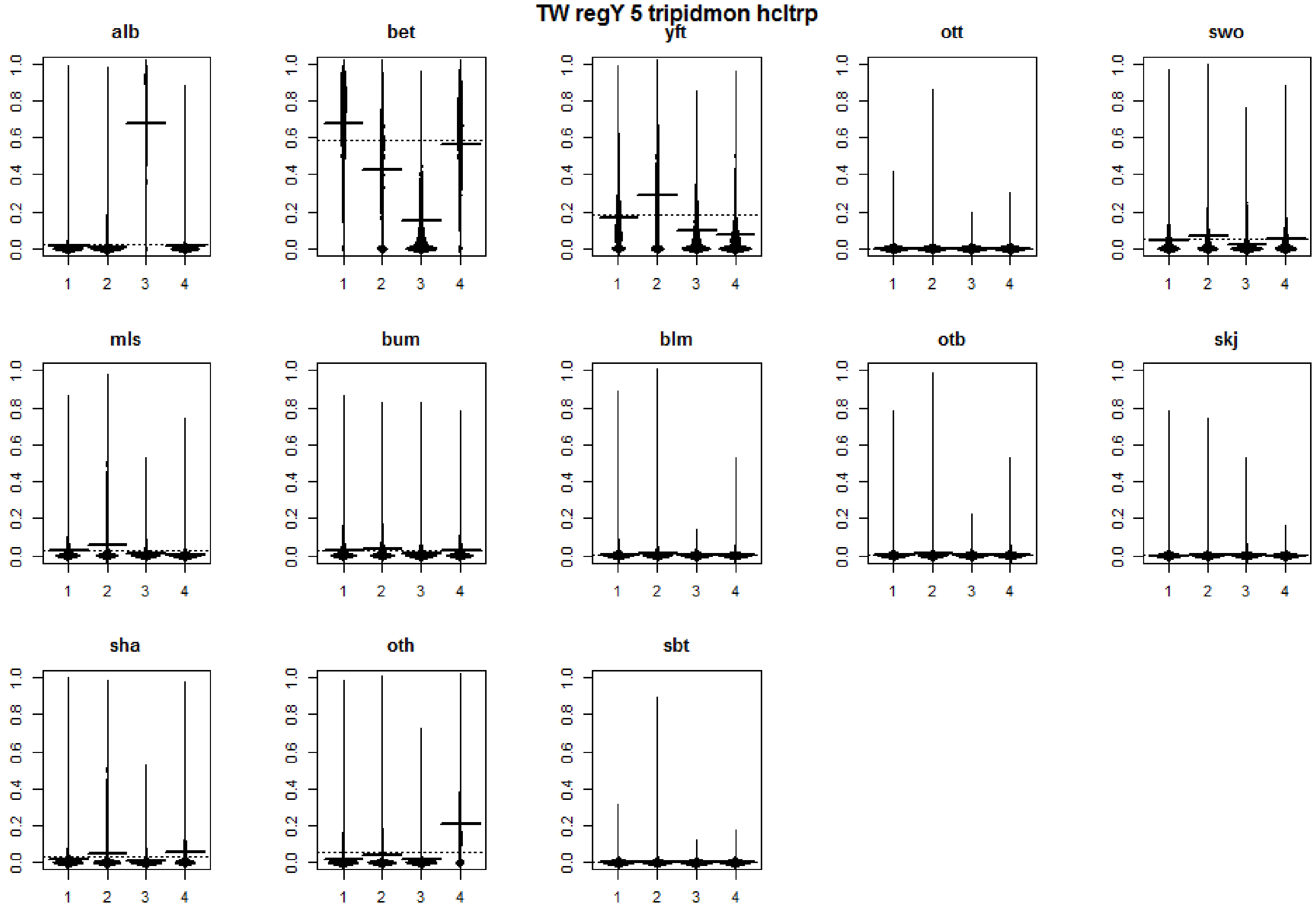

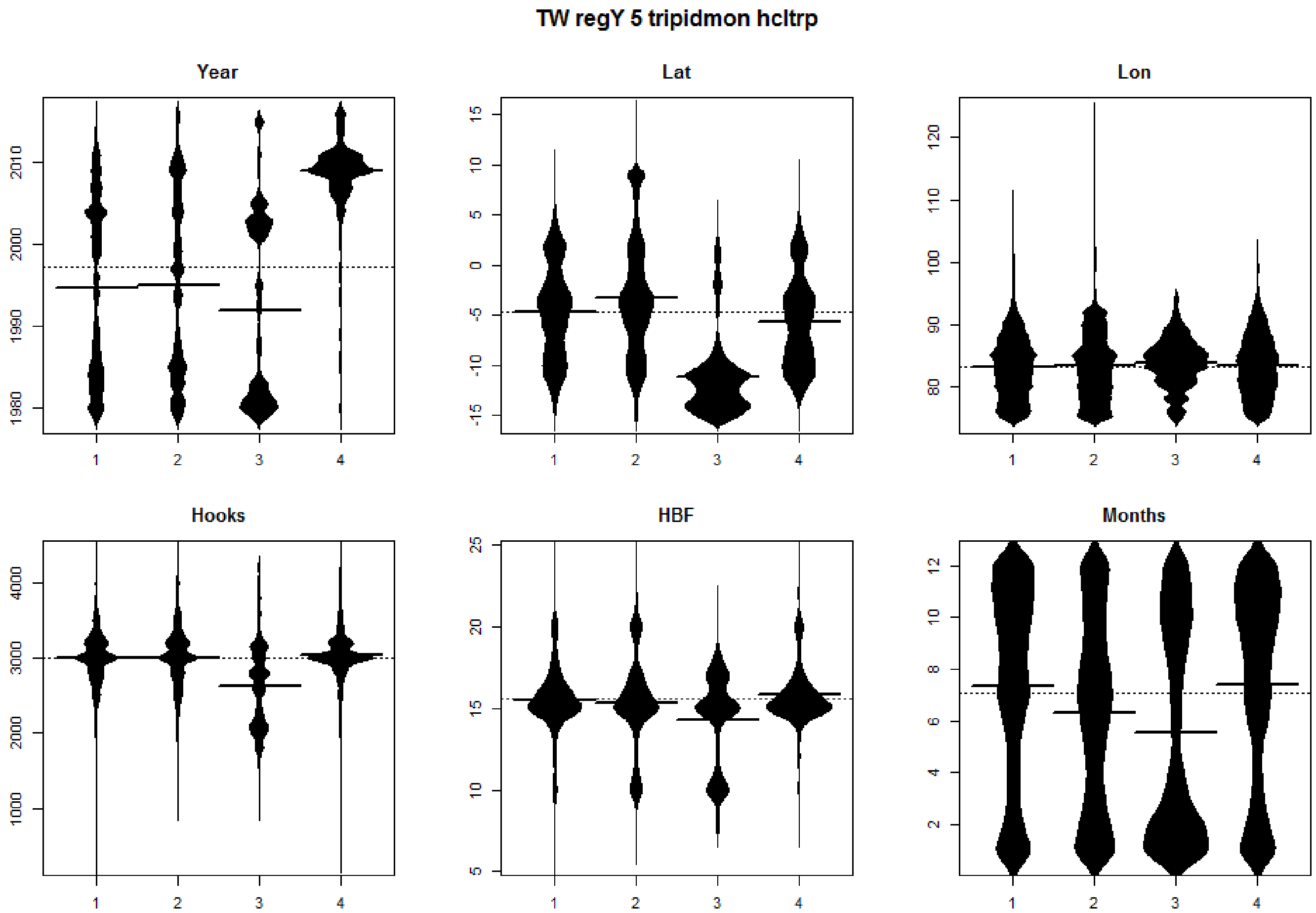

Figure 24. For Taiwanese effort in region 5 of Y for the period 1979-2016, for each species, boxplot of the

proportion of the species in the trip versus the cluster. The widths of the boxes are proportional to the numbers of trips in each cluster (above). Boxplot showing the distributions of variables associated with sets in each hcltrp cluster (below). Clustering was performed using a hierarchical Ward clustering analysis of trip-level data.

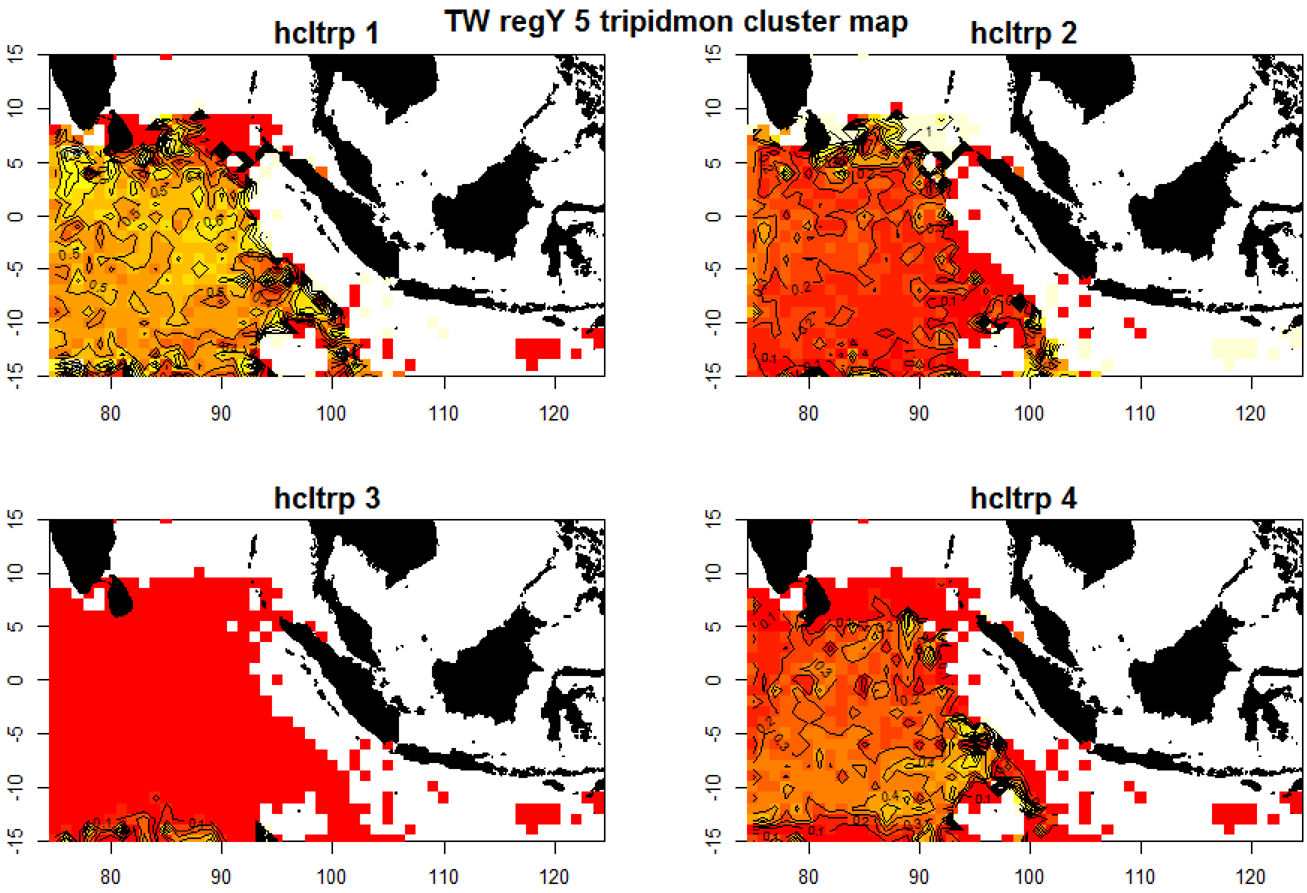

Figure 25. Maps of the spatial distributions of clusters in region 5 of Y for Taiwanese effort.

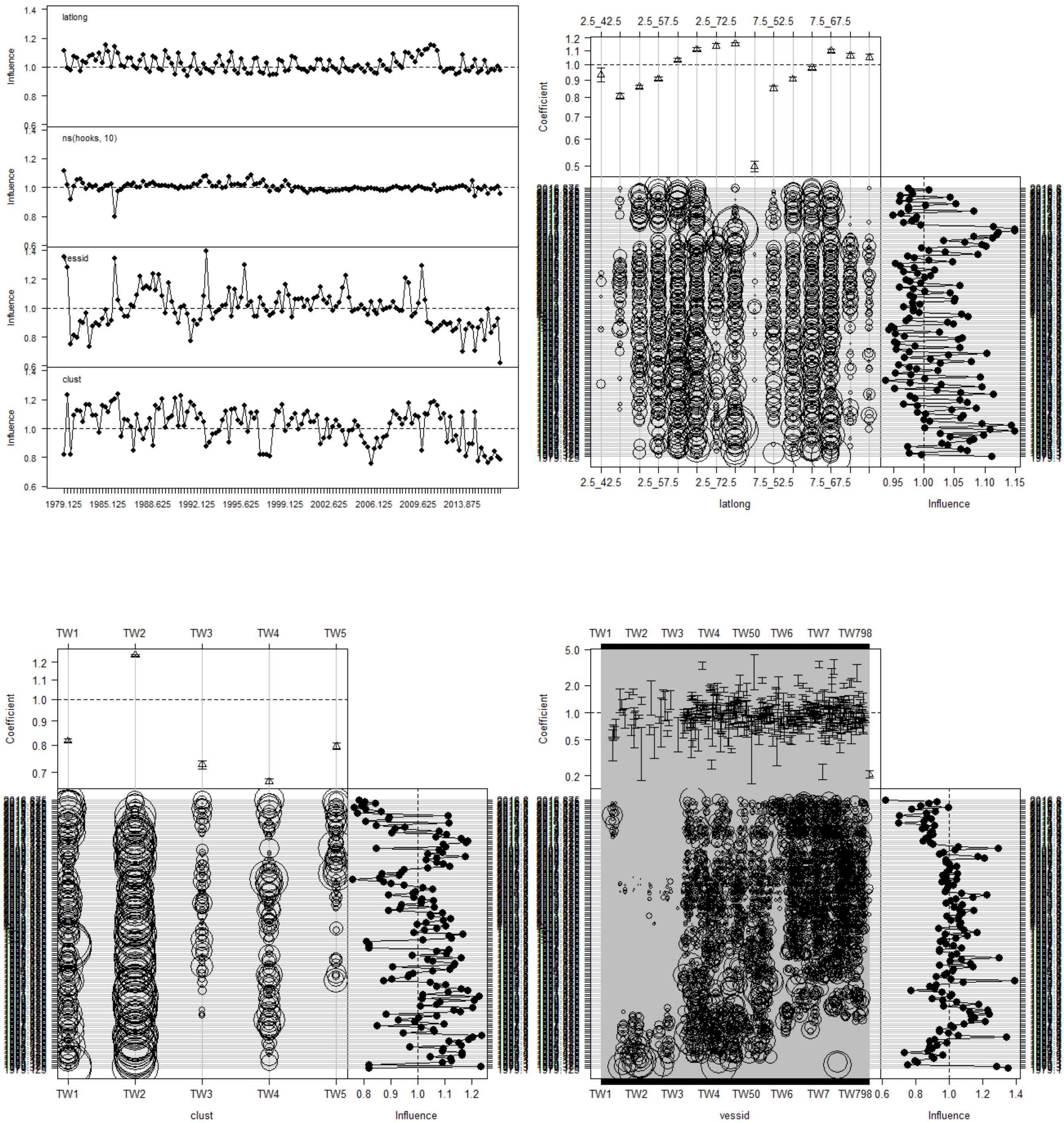

Figure 26. Influence plots for bigeye tuna CPUE in region 1N by the Taiwanese fleet. The top left plots shows the change in the CPUE time series caused by each covariate. The top right plot shows the influence of the latlong effect. The bottom left plot shows the influence of the cluster effect, and the bottom right plot shows the influence of the vessid effect.

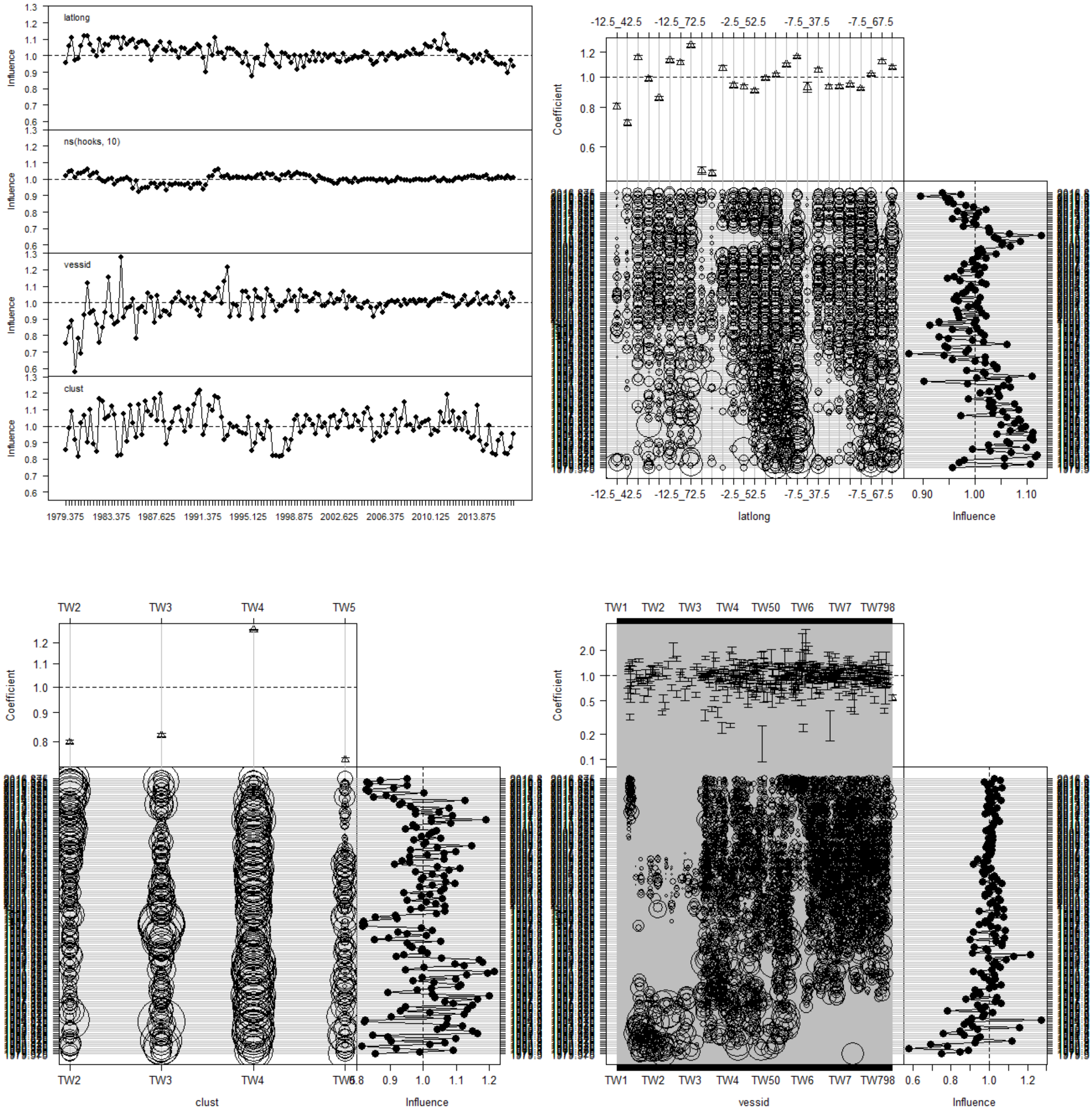

Figure 27 Influence plots for bigeye tuna CPUE in region 1S by the Taiwanese fleet. The top left plots shows the change in the CPUE time series caused by each covariate. The top right plot shows the influence of the latlong effect. The bottom left plot shows the influence of the cluster effect, and the bottom right plot shows the influence of the vessid effect.

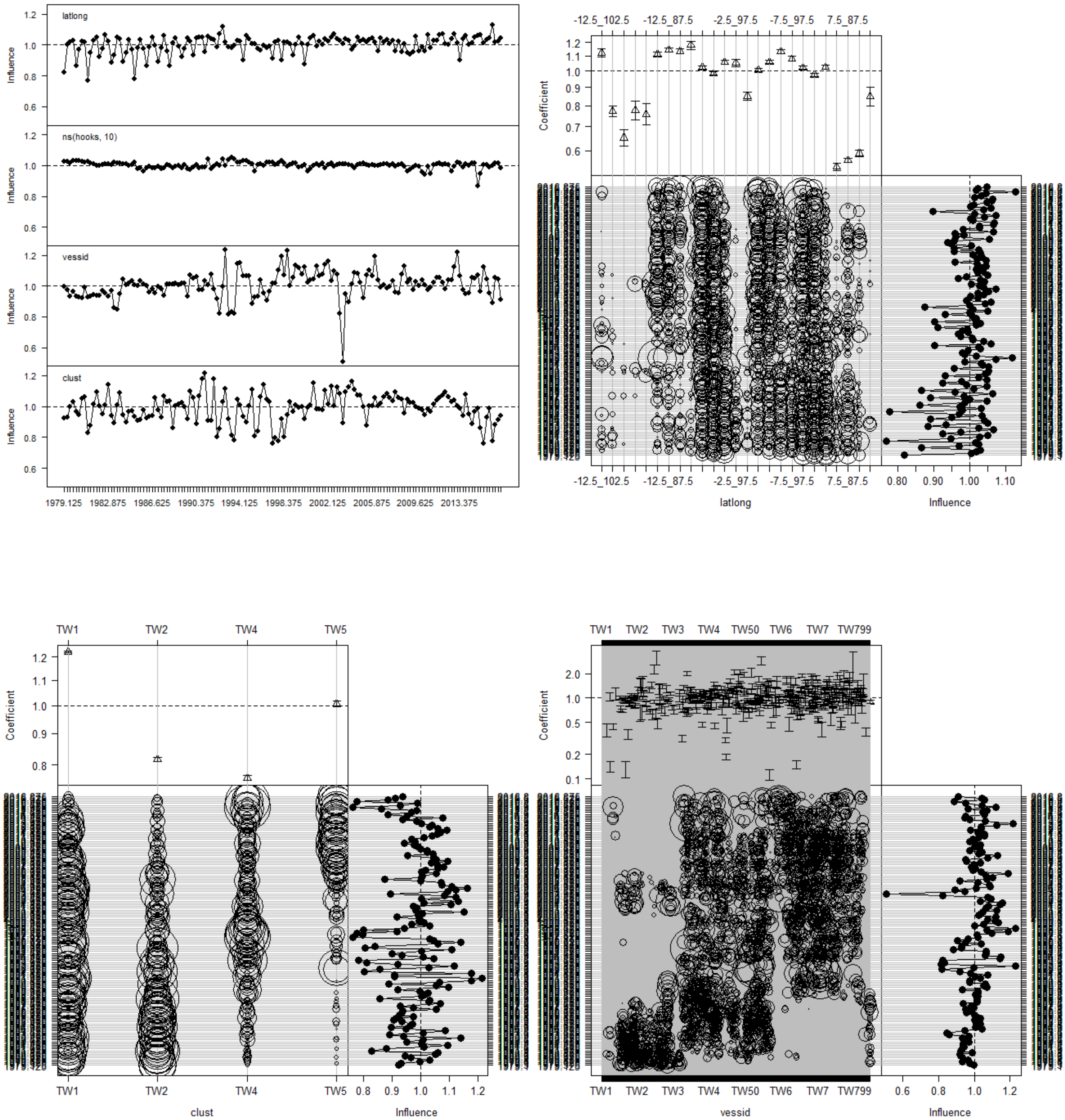

Figure 28 Influence plots for bigeye tuna CPUE in region 2 by the Taiwanese fleet. The top left plots shows the change in the CPUE time series caused by each covariate. The top right plot shows the influence of the latlong effect. The bottom left plot shows the influence of the cluster effect, and the bottom right plot shows the influence of the vessid effect.

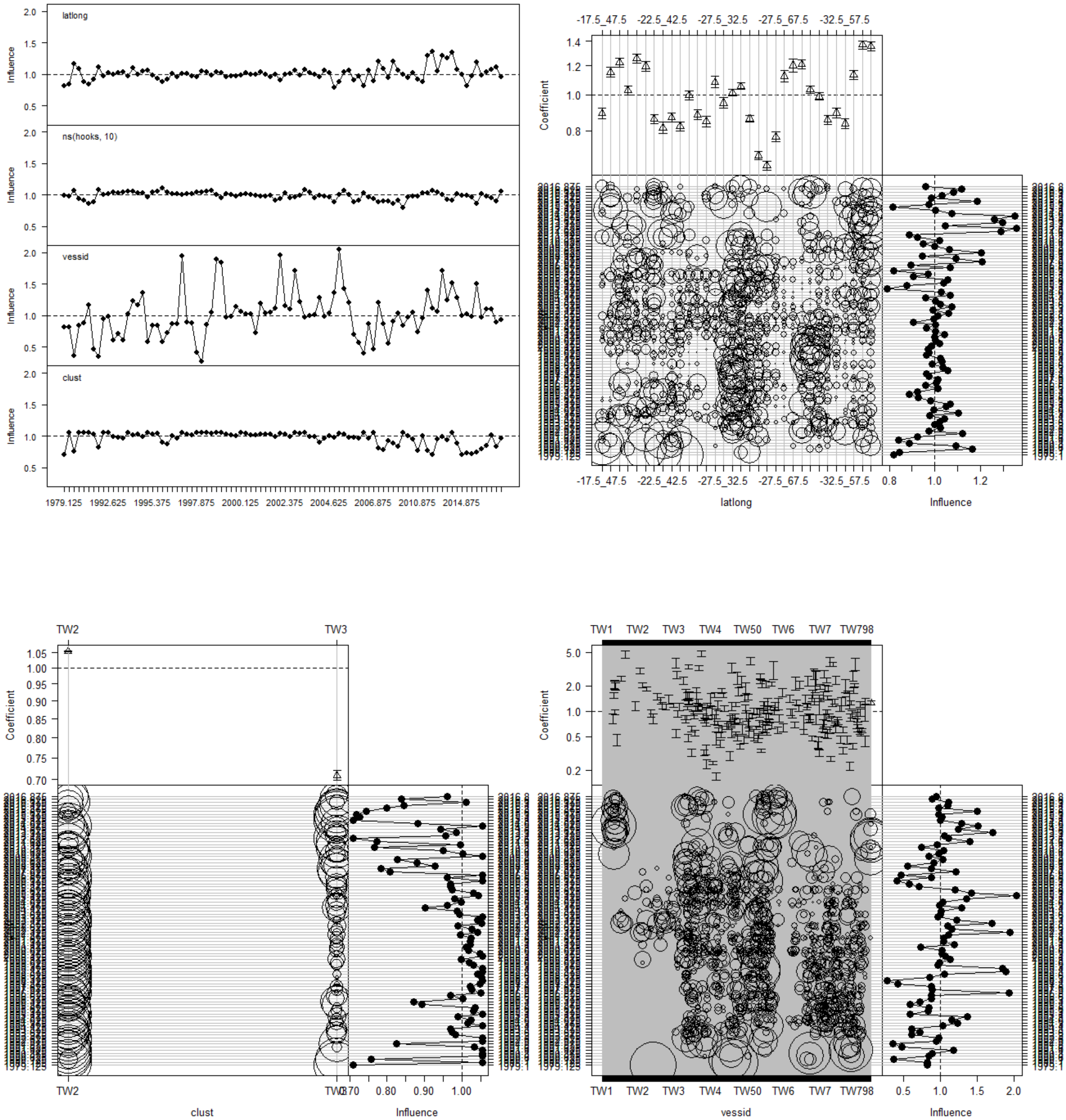

Figure 29 Influence plots for bigeye tuna CPUE in region 3 by the Taiwanese fleet. The top left plots shows the change in the CPUE time series caused by each covariate. The top right plot shows the influence of the latlong effect. The bottom left plot shows the influence of the cluster effect, and the bottom right plot shows the influence of the vessid effect.

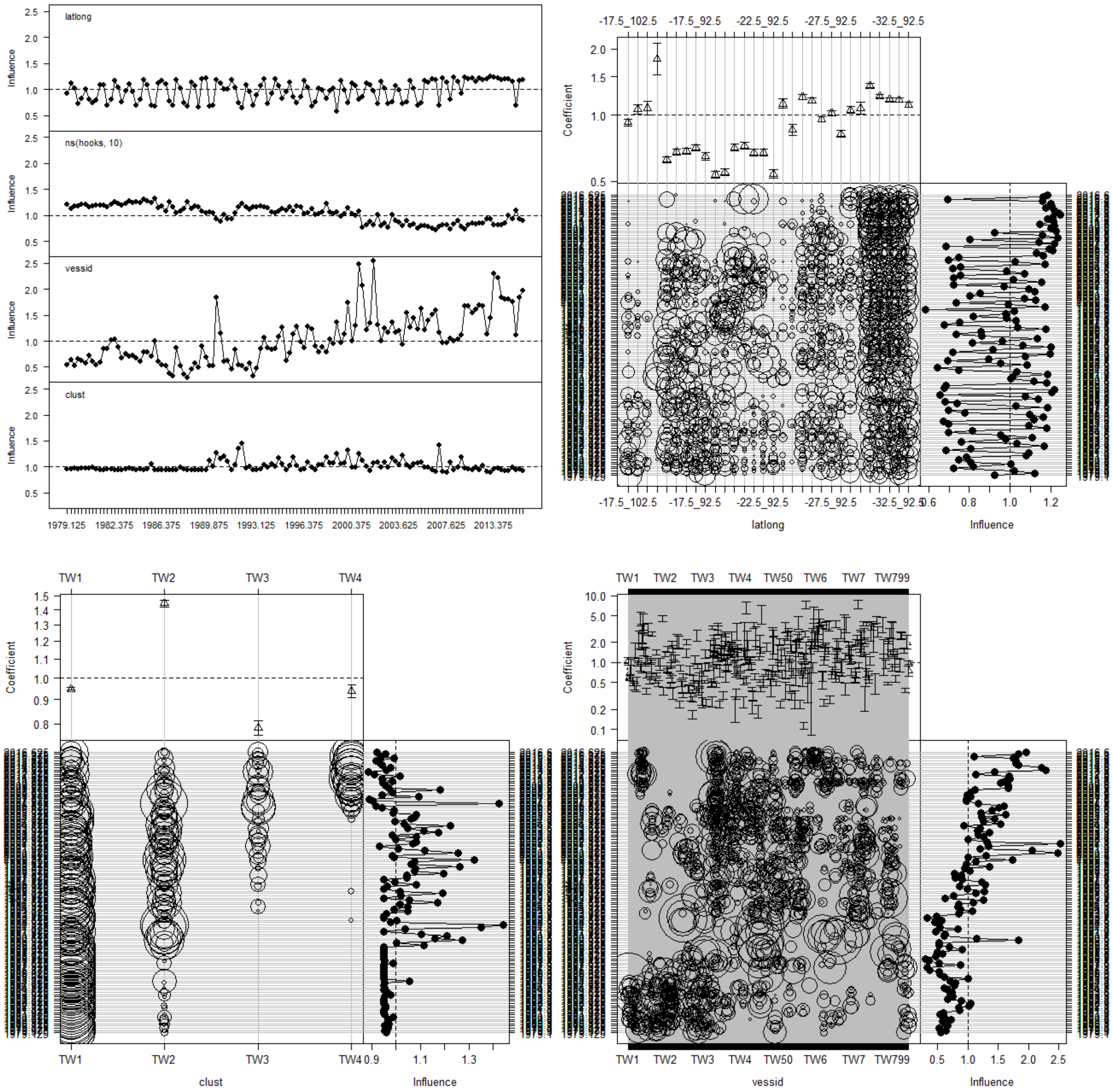

Figure 30 Influence plots for bigeye tuna CPUE in region 4 by the Taiwanese fleet. The top left plots shows the change in the CPUE time series caused by each covariate. The top right plot shows the influence of the latlong effect. The bottom left plot shows the influence of the cluster effect, and the bottom right plot shows the influence of the vessid effect.

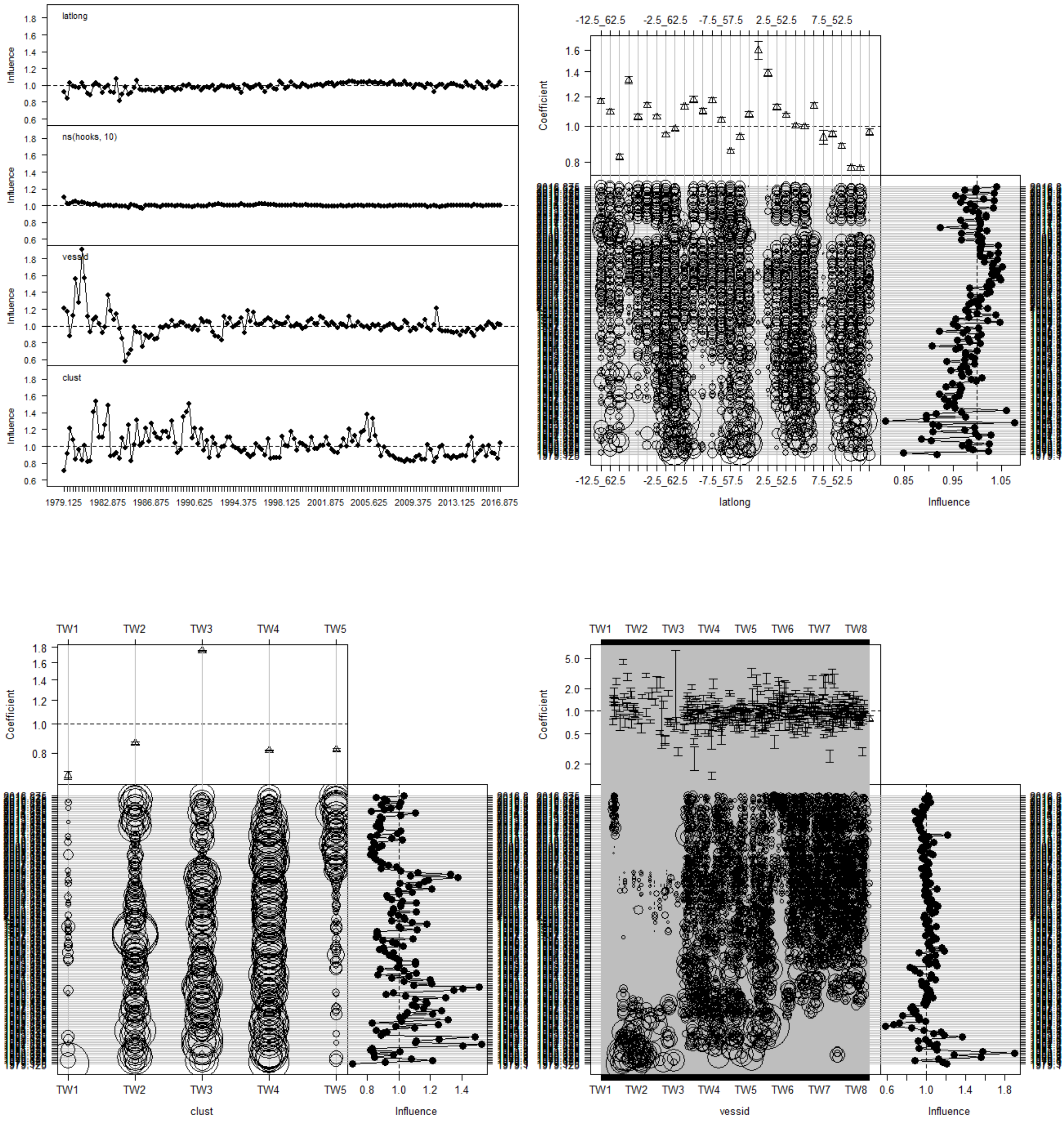

Figure 31 Influence plots for yellowfin tuna CPUE in region 2 by the Taiwanese fleet. The top left plots shows the change in the CPUE time series caused by each covariate. The top right plot shows the influence of the latlong effect. The bottom left plot shows the influence of the cluster effect, and the bottom right plot shows the influence of the vessid effect.

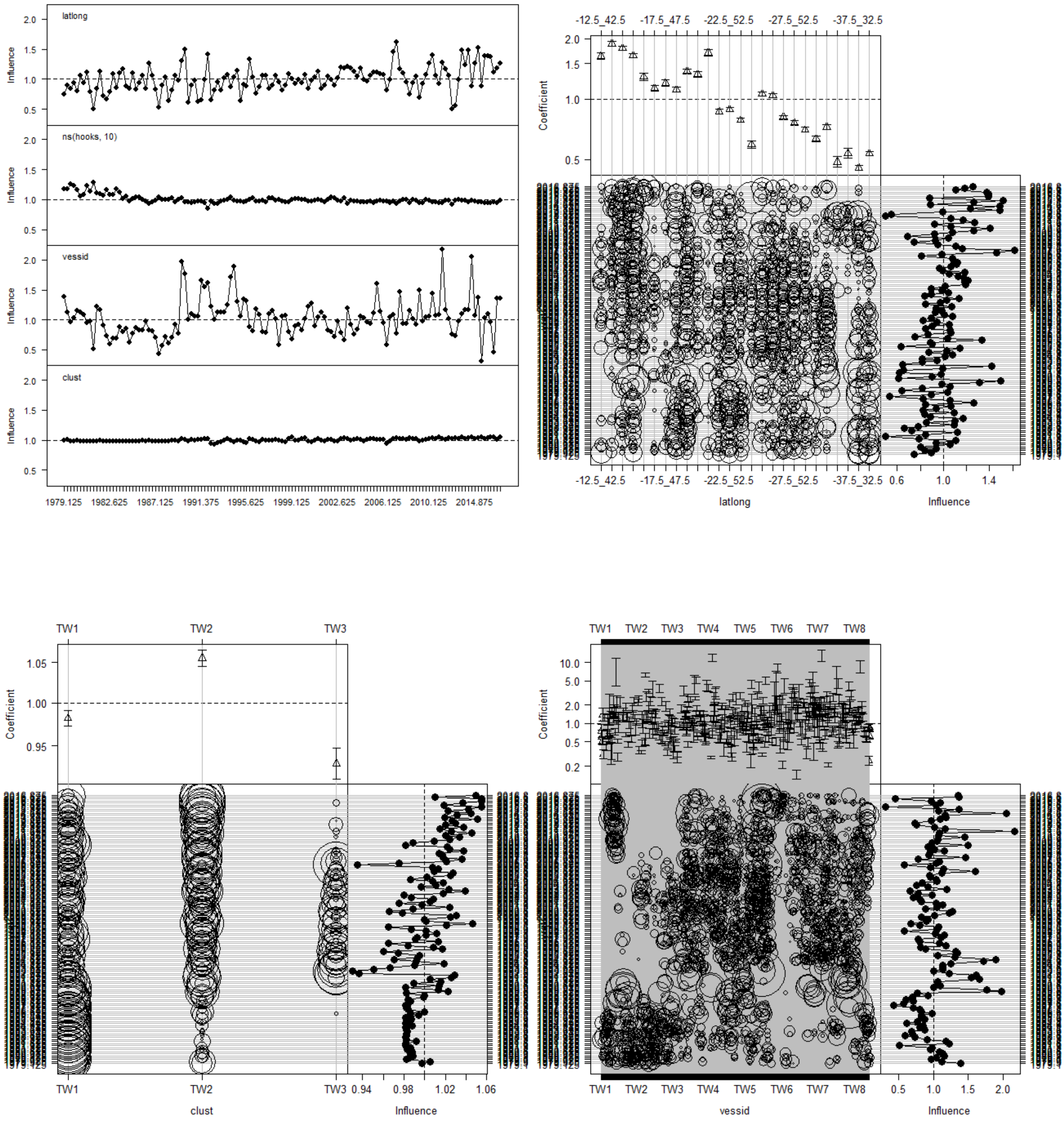

Figure 32 Influence plots for yellowfin tuna CPUE in region 3 by the Taiwanese fleet. The top left plots shows the change in the CPUE time series caused by each covariate. The top right plot shows the influence of the latlong effect. The bottom left plot shows the influence of the cluster effect, and the bottom right plot shows the influence of the vessid effect.

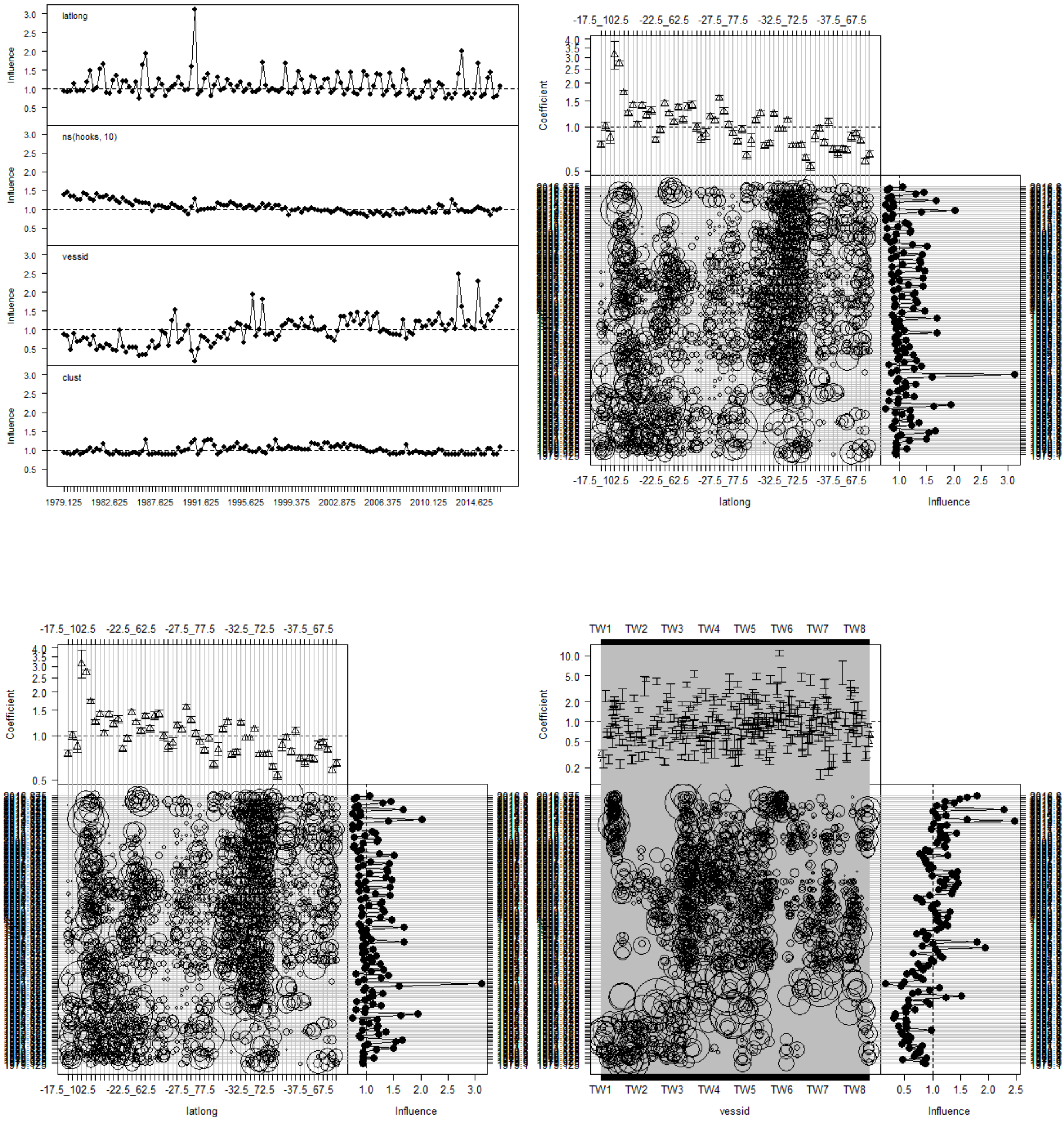

Figure 33 Influence plots for yellowfin tuna CPUE in region 4 by the Taiwanese fleet. The top left plots shows the change in the CPUE time series caused by each covariate. The top right plot shows the influence of the latlong effect. The bottom left plot shows the influence of the cluster effect, and the bottom right plot shows the influence of the vessid effect.

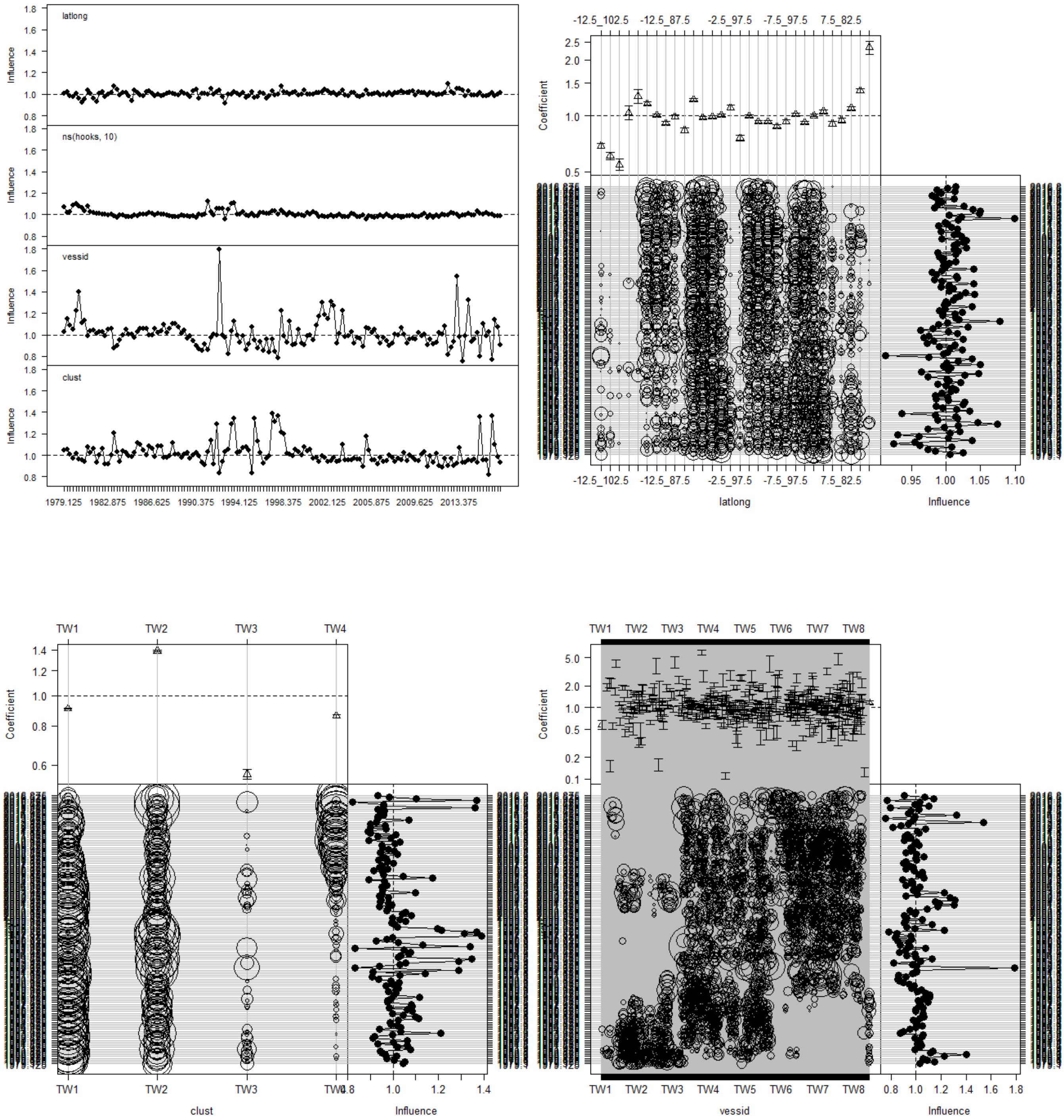

Figure 34 Influence plots for yellowfin tuna CPUE in region 5 by the Taiwanese fleet. The top left plots shows the change in the CPUE time series caused by each covariate. The top right plot shows the influence of the latlong effect. The bottom left plot shows the influence of the cluster effect, and the bottom right plot shows the influence of the vessid effect.

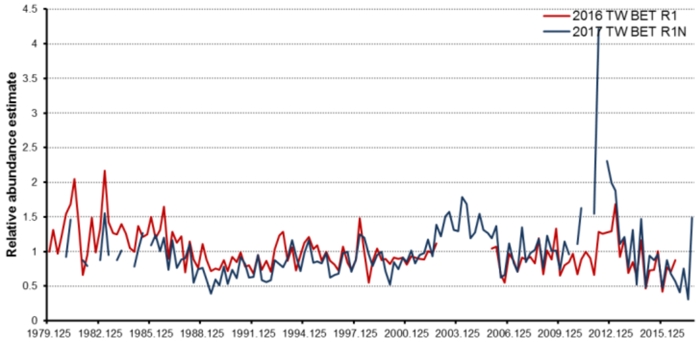
2016 TW BET R1
2017 TW BET R1N
Relative abundance estimate
0
0.5
1
1.5
2
2.5
3
3.5
4
4.5
1979.125
1982.125
1985.125
1988.125
1991.125
1994.125
1997.125
2000.125
2003.125
2006.125
2009.125
2012.125
2015.125

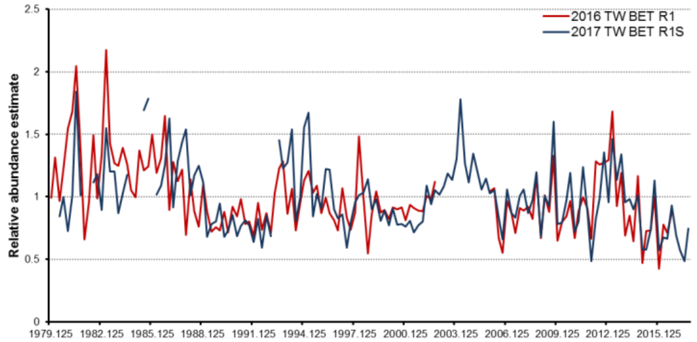
2016 TW BET R1
2017 TW BET R1S
Relative abundance estimate
0
0.5
1
1.5
2
2.5
1979.125
1982.125
1985.125
1988.125
1991.125
1994.125
1997.125
2000.125
2003.125
2006.125
2009.125
2012.125
2015.125

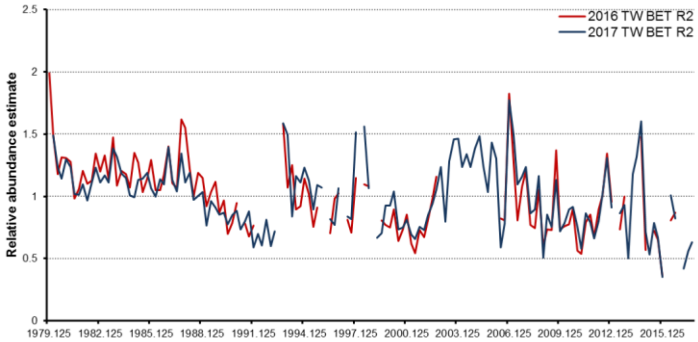
2016 TW BET R2
2017 TW BET R2
Relative abundance estimate
0
0.5
1
1.5
2
2.5
1979.125
1982.125
1985.125
1988.125
1991.125
1994.125
1997.125
2000.125
2003.125
2006.125
2009.125
2012.125
2015.125

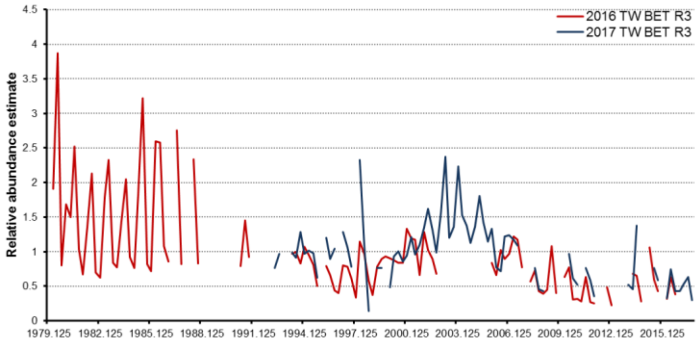
2016 TW BET R3
2017 TW BET R3
Relative abundance estimate
0
0.5
1
1.5
2
2.5
3
3.5
4
4.5
1979.125
1982.125
1985.125
1988.125
1991.125
1994.125
1997.125
2000.125
2003.125
2006.125
2009.125
2012.125
2015.125

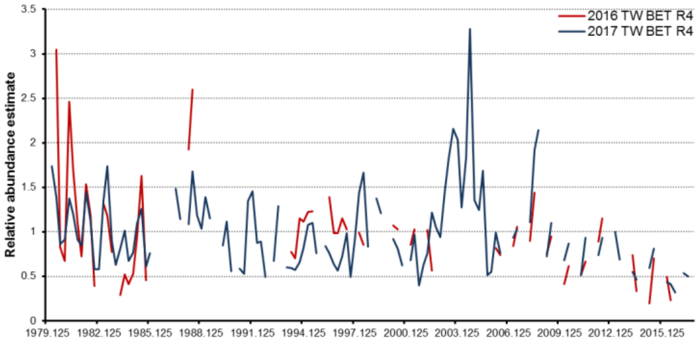

Figure 35. Comparisons of bigeye CPUE time series estimated in this analysis (red) and estimated in 2016 (blue) by regions.

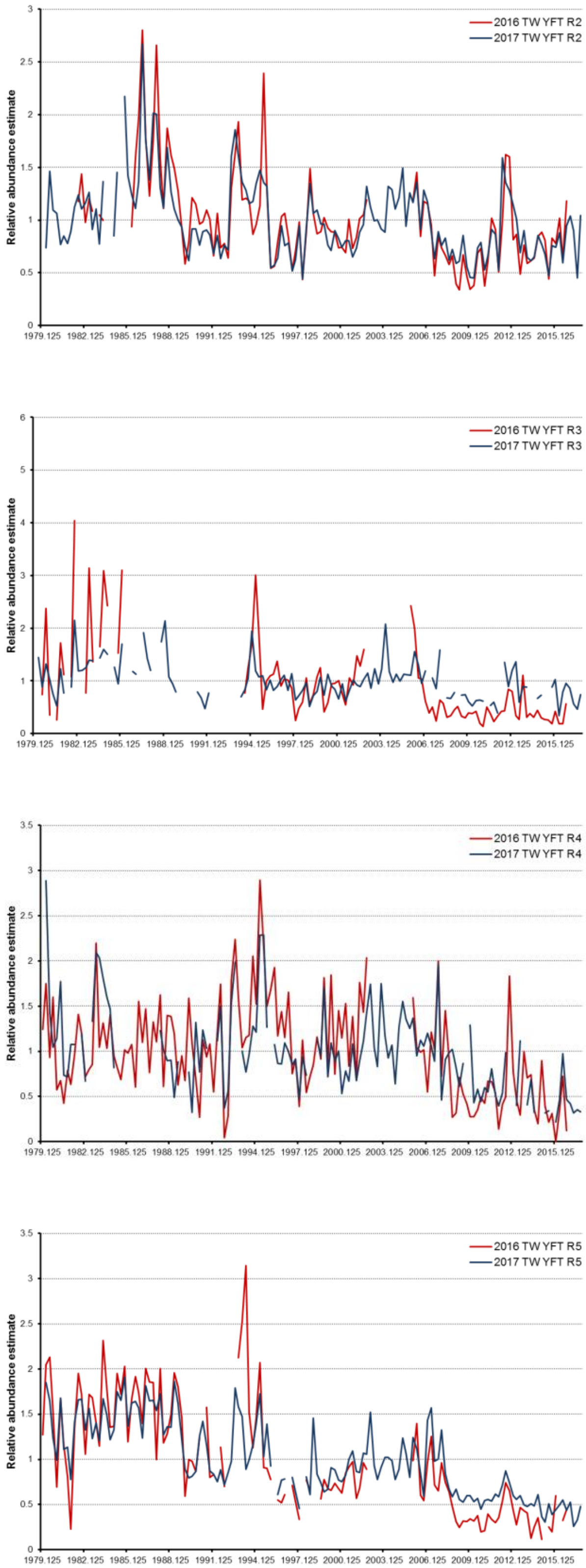

Figure 36. Comparisons of yellowfin CPUE time series estimated in this analysis (red) and estimated in 2016 (blue) by regions.

Region 1N

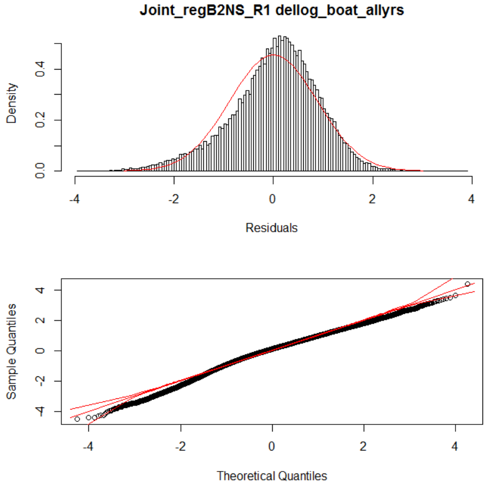

Region 1S

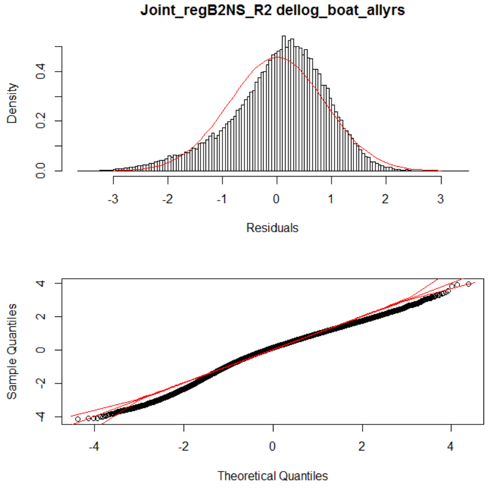

Region 2

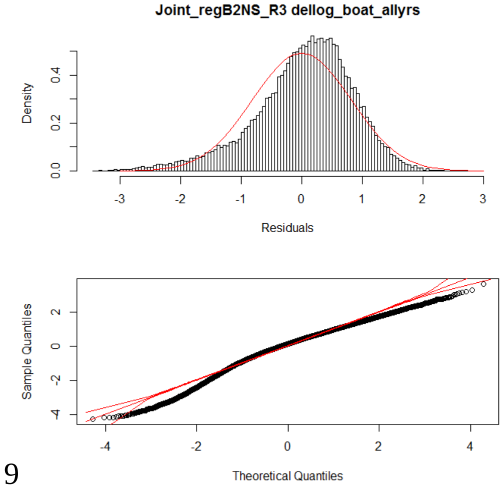

Region 3

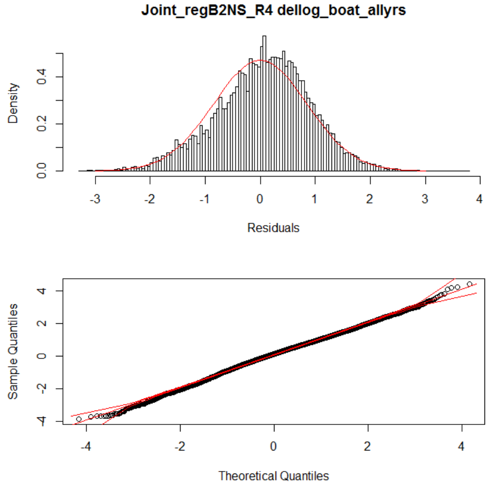

Region 4

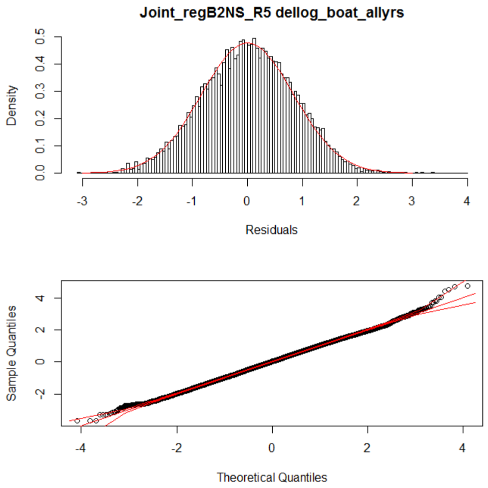

Figure 37. Residual diagnostics (as histogram and QQ plot) on bigeye tuna CPUE indices by regions.

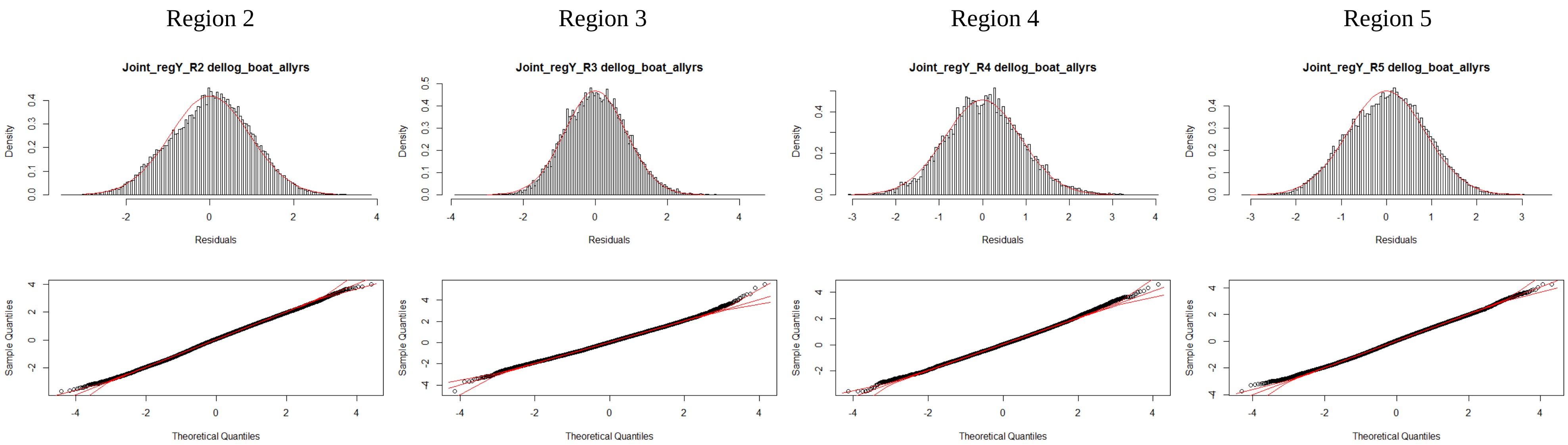

Figure 38. Residual diagnostics (as histogram and QQ plot) on yellowfin tuna CPUE indices by regions.

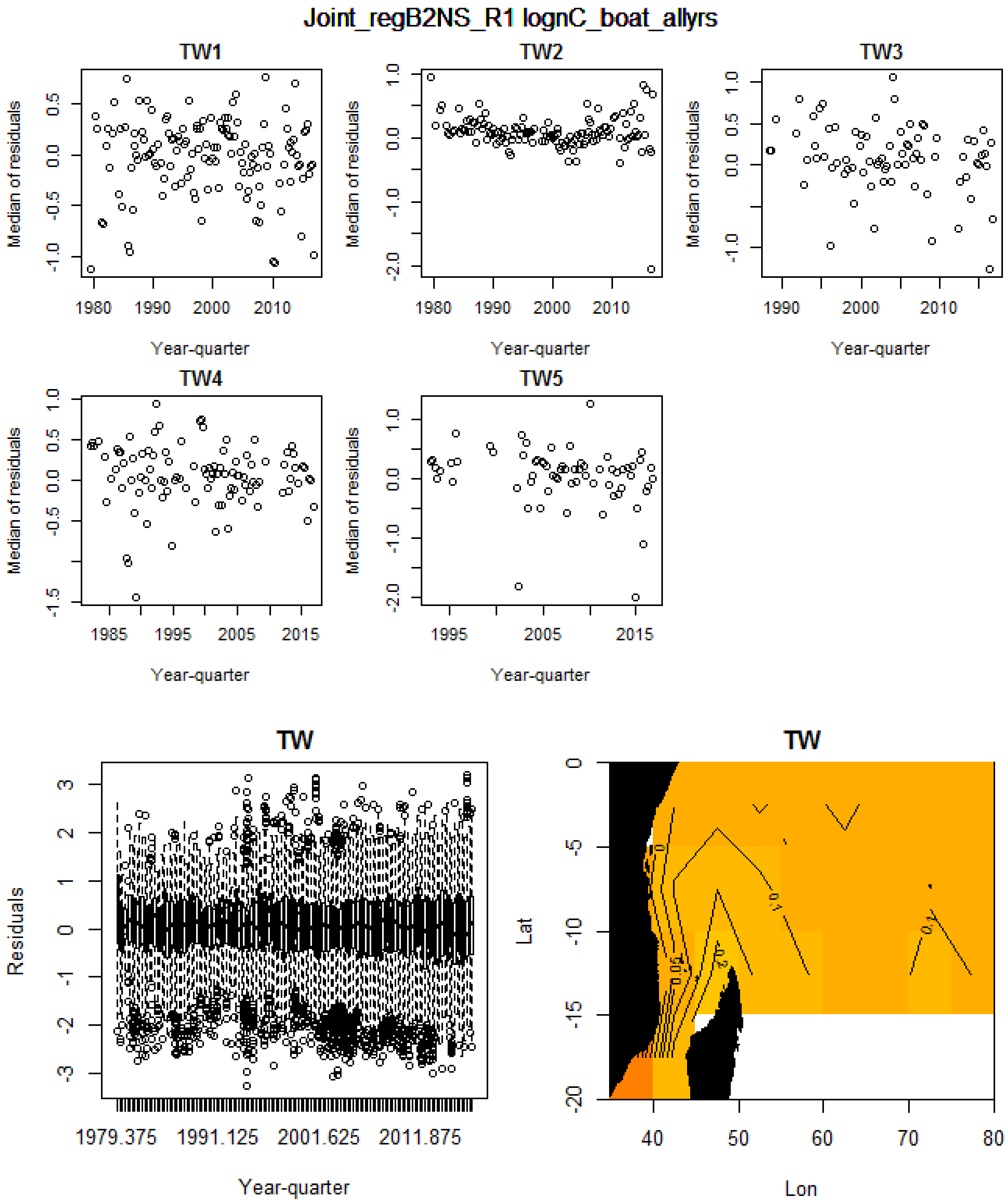

Figure 39. (Top) Median residuals from the lognormal constant model per year-quarter (x-axis), by cluster (subplots), for bigeye tuan in region 1N. (Bottom) Bigeye tuna residuals for regions 1N, median residuals are mapped by 5 cell (left) and plotted by year-quarter (right).

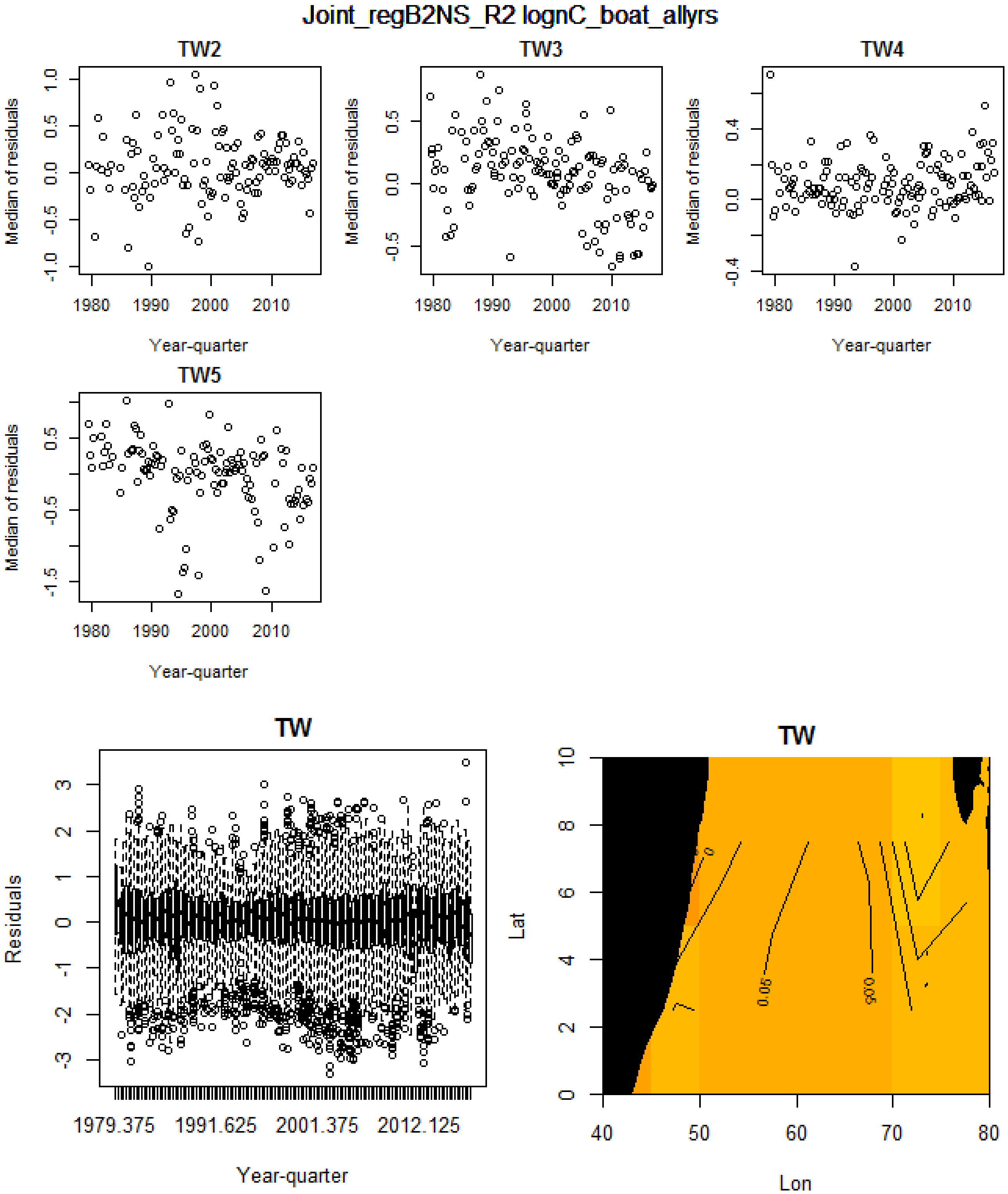

Figure 40. (Top) Median residuals from the lognormal constant model per year-quarter (x-axis), by cluster (subplots), for bigeye tuan in region 1S. (Bottom) Bigeye tuna residuals for regions 1S, median residuals are mapped by 5 cell (left) and plotted by year-quarter (right).

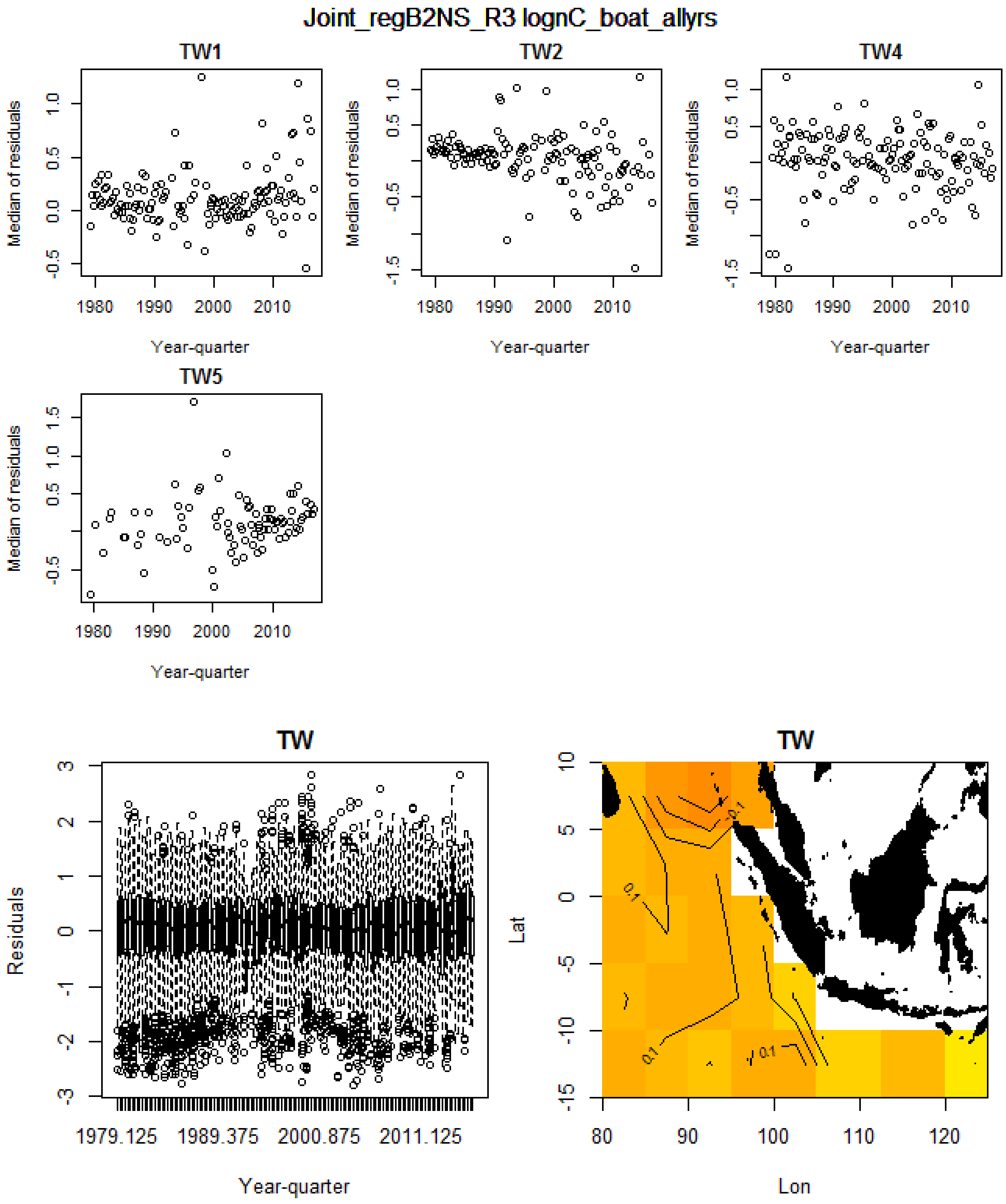

Figure 41. : (Top) Median residuals from the lognormal constant model per year-quarter (x-axis), by cluster (subplots), for bigeye tuan in region 2. (Bottom) Bigeye tuna residuals for regions 2, median residuals are mapped by 5 cell (left) and plotted by year-quarter (right).

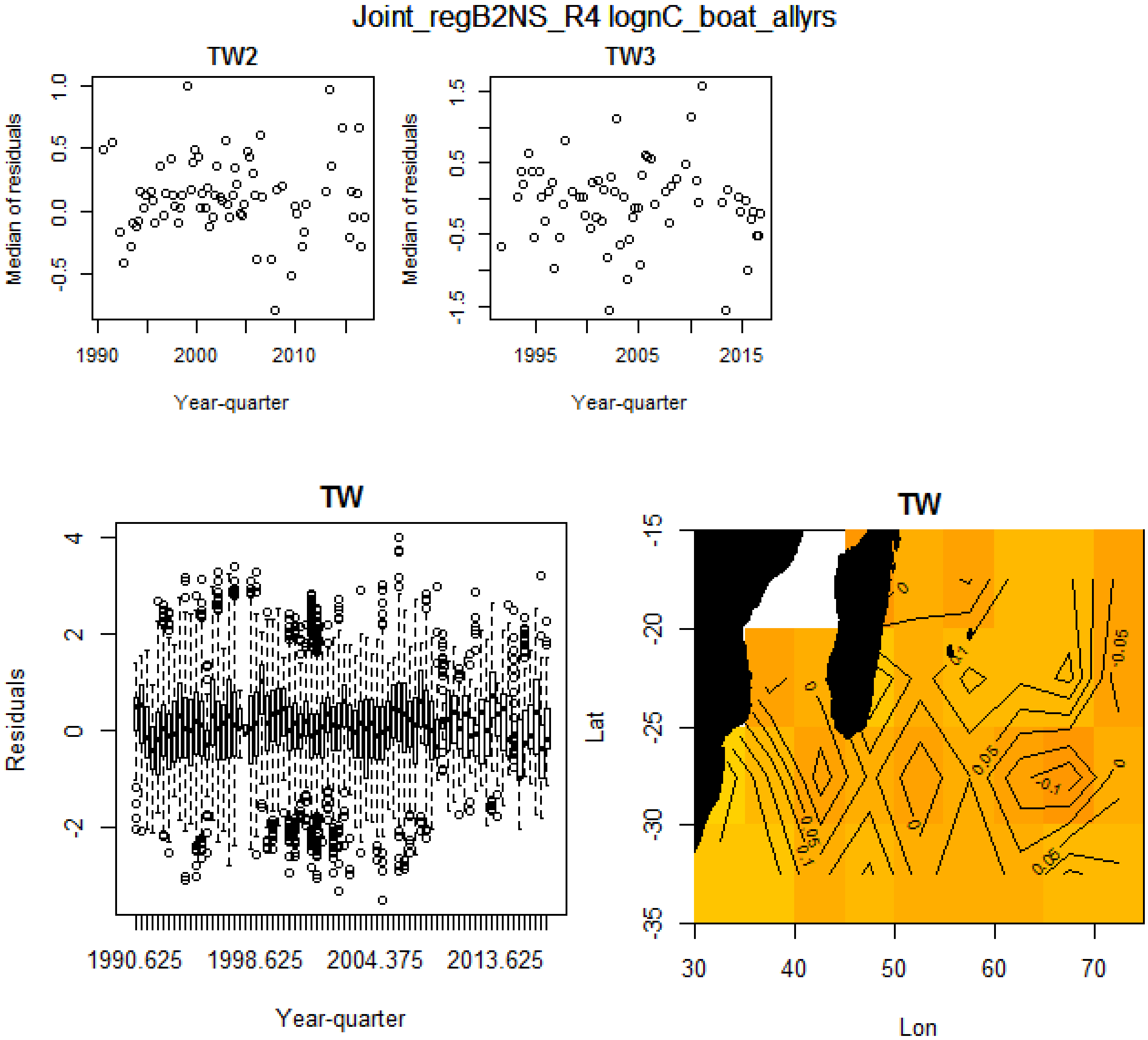

Figure 42. (Top) Median residuals from the lognormal constant model per year-quarter (x-axis), by cluster (subplots), for bigeye tuan in region 3. (Bottom) Bigeye tuna residuals for regions 3, median residuals are mapped by 5 cell (left) and plotted by year-quarter (right).

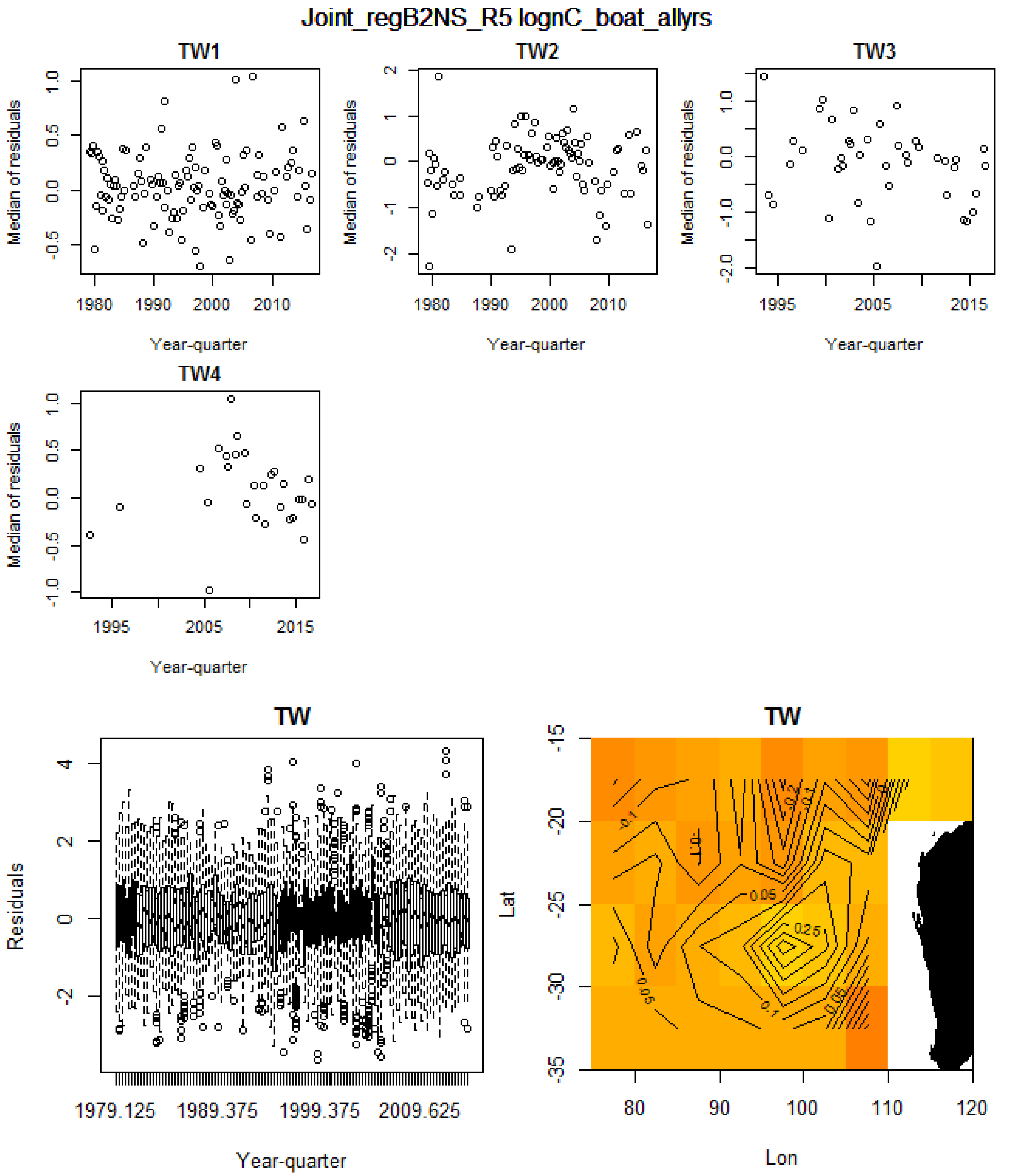

Figure 43. (Top) Median residuals from the lognormal constant model per year-quarter (x-axis), by cluster (subplots), for bigeye tuan in region 4. (Bottom) Bigeye tuna residuals for regions 4, median residuals are mapped by 5 cell (left) and plotted by year-quarter (right).

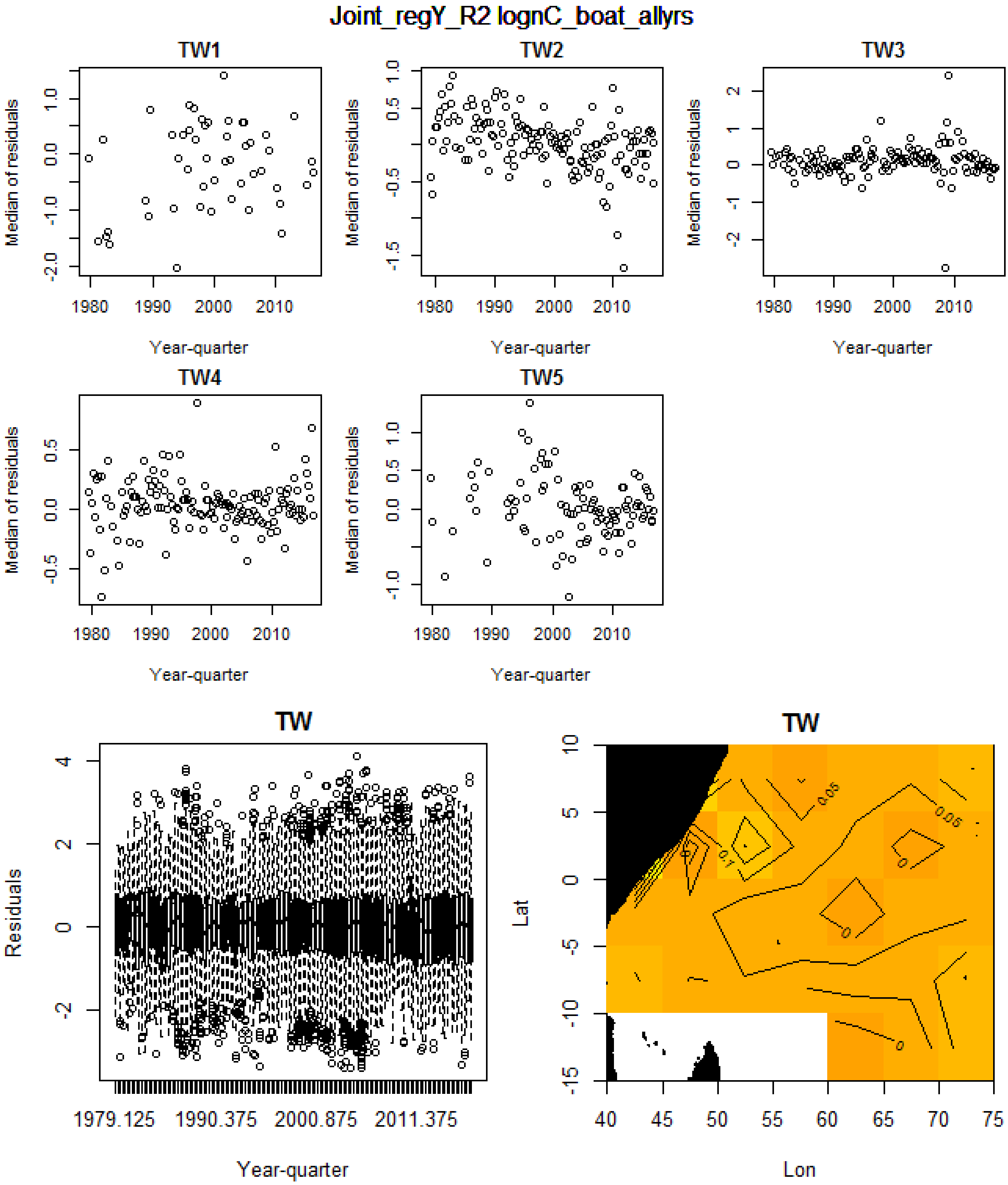

Figure 44. (Top) Median residuals from the lognormal constant model per year-quarter (x-axis), by cluster (subplots), for yellowfin in region 2. (Bottom) Bigeye tuna residuals for regions 2, median residuals are mapped by 5 cell (left) and plotted by year-quarter (right).

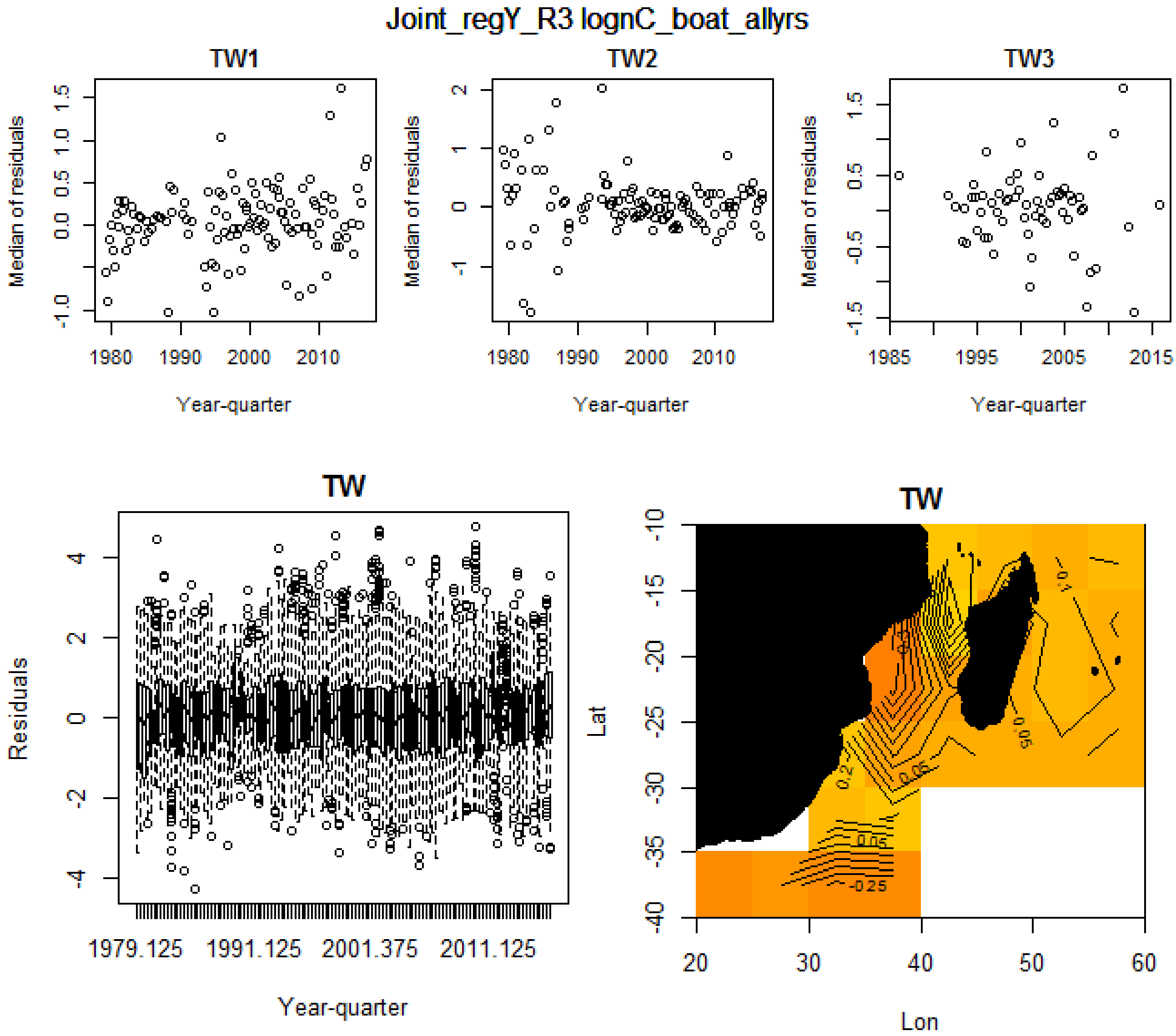

Figure 45. (Top) Median residuals from the lognormal constant model per year-quarter (x-axis), by cluster (subplots), for yellowfin in region 3. (Bottom) Bigeye tuna residuals for regions 3, median residuals are mapped by 5 cell (left) and plotted by year-quarter (right).

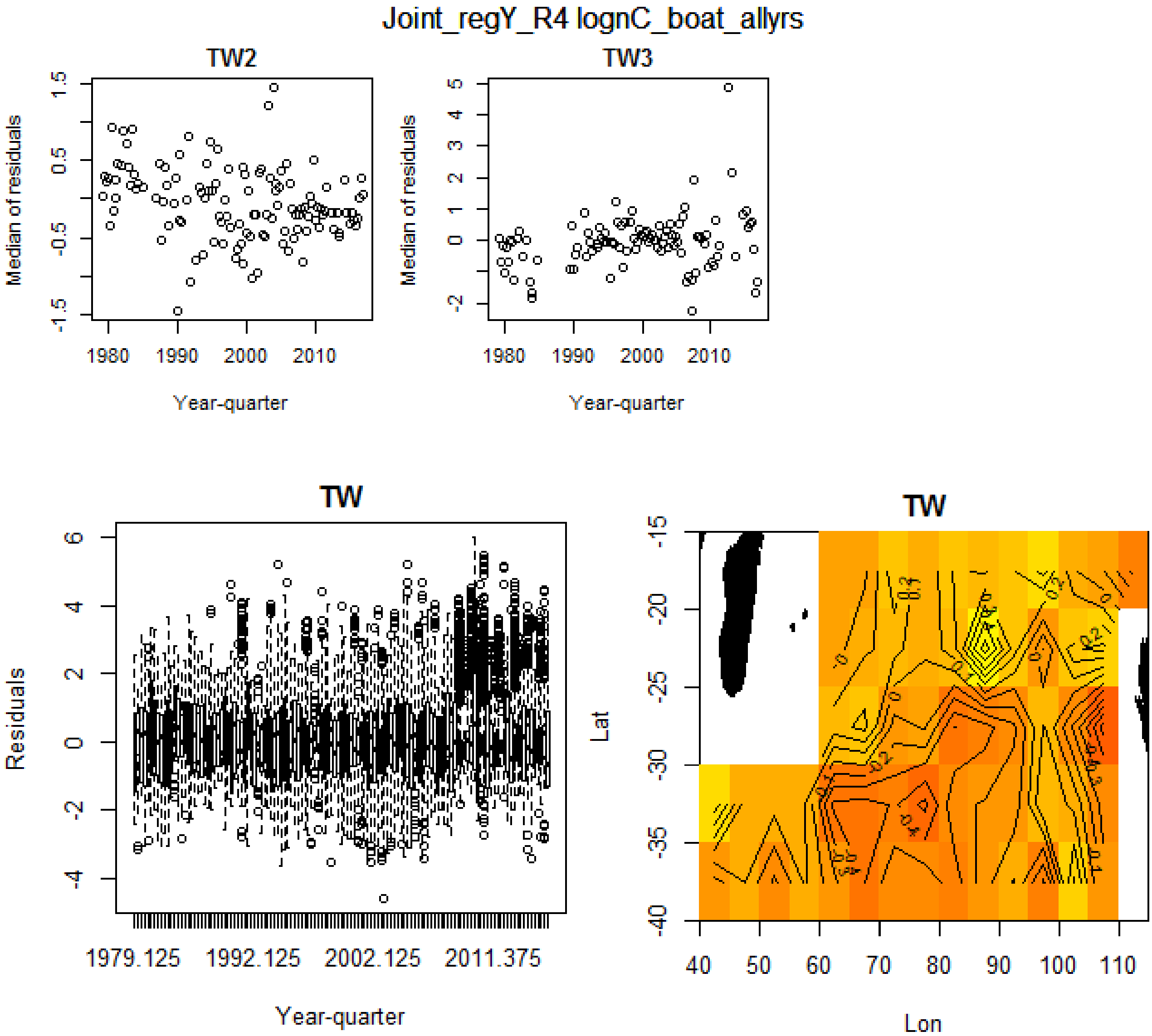

Figure 46. (Top) Median residuals from the lognormal constant model per year-quarter (x-axis), by cluster (subplots), for yellowfin in region 4. (Bottom) Bigeye tuna residuals for regions 4, median residuals are mapped by 5 cell (left) and plotted by year-quarter (right).

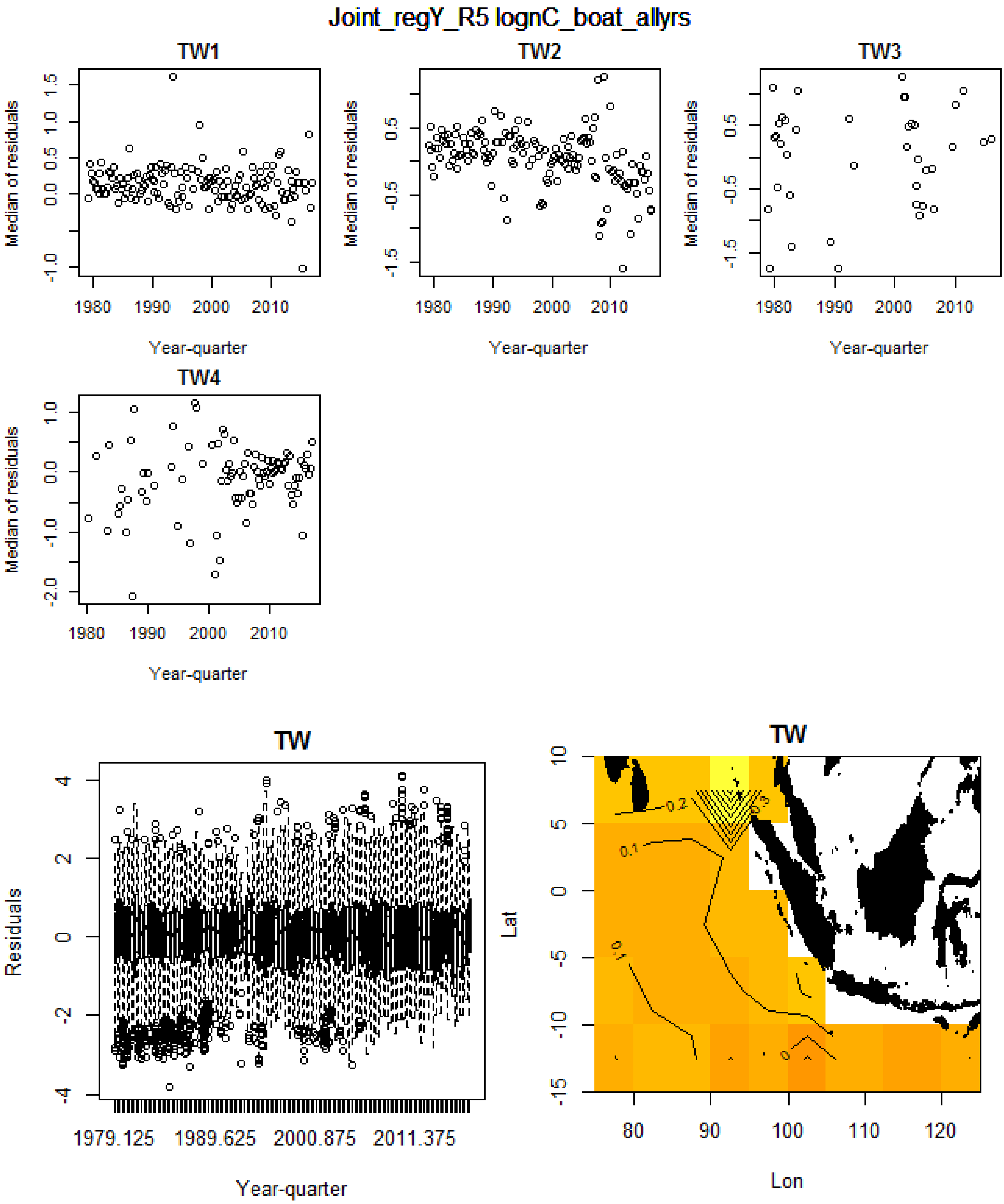

Figure 47. (Top) Median residuals from the lognormal constant model per year-quarter (x-axis), by cluster (subplots), for yellowfin in region 5. (Bottom) Bigeye tuna residuals for regions 5, median residuals are mapped by 5 cell (left) and plotted by year-quarter (right).